Constraining spatial variability in groundwater recharge in an arid environment using carbon-14

Cameron Wood

BSc. (Honours)

Thesis submitted as a requirement in full for the degree of Doctor of Philosophy in the School of the Environment, Faculty of Science and Engineering, Flinders University, South Australia

Declaration

I certify that this thesis does not incorporate without acknowledgment any material previously submitted for a degree or diploma in any other university; and that to the best of my knowledge and belief it does not contain any material previously published or written by another person except where due reference is made in the text.

Cameron Wood

April 2015

Co-authorship

Cameron Wood is the primary author on all chapters in this thesis. Co-authors listed on published chapters provided intellectual supervision and editorial support.

Acknowledgments

Completion of this thesis would not have been possible without the help of many excellent people and institutions.

Firstly, a big thank you to my supervisors Peter G. Cook and Glenn A. Harrington for their encouragement, enthusiasm and expertise in all aspects of this work. It's been great working with you both. I'd like to thank my other co-authors on various parts of this work: Karina Meredith (and the staff at the Institute for Environmental Research at ANSTO) for help setting up the unsaturated zone gas analysis for this study; Rolf Kipfer for sharing his knowledge and passion for environmental tracer interpretation; Anthony Knapton for helping with logistics in Alice Springs and with modelling the Ti Tree Basin (and coming to grips with PEST).

I'd like to thank Craig Simmons and the National Centre for Groundwater Research and Training at Flinders University for scholarship funding, project funding (through the Australian Research Council and the National Water Commission) and administrative support during my candidature. I'd especially like to thank Anna Bonnes for helping organise countless trips to Ti Tree. Thanks to the Australian Government National Collaborative Research Infrastructure Scheme (NCRIS) Groundwater Infrastructure Program for funding to install piezometers, and to the Australian Institute of Nuclear Science and Engineering (AINSE) for grant funding (ALNGRA12042) to analyse ^{14}C in soil gas, in collaboration with ANSTO through their Isotopes for Water project.

Thanks to Bob Read, John Wischusen and the Northern Territory Drilling Department for help organising things in the field, and the Aboriginal Areas Protection Authority for approving drill sites. Thanks to Greg Rinder for help drafting site maps and figures which appear in this thesis.

Staff and students from Flinders University are thanked for assistance in the field, especially Nicholas White, Lawrence Burk and Margaret Shanafield who came on nearly every field trip to Ti Tree, and Eddie Banks for help sorting out field equipment. Also thanks to my colleagues at Flinders University, in particular my office mates Michelle Irvine (for sharing the PhD experience from day one, go Salty Dolls!), Megan Sebben and Matt Knowling. I'd like to say a special thanks to the occupants of office 224 - Dr. Jim McCallum, Dr. Dylan Irvine and Dr. Saskia Noorduijn. In addition to being a great source of technical knowledge, you've been great friends and I feel lucky to have been at Flinders at the same time as you.

Outside of university I'd like to thank my friends and family for their support, patience and humour over the past four years. I'd especially like to thank my parents Philip and Anne for being a constant source of support and encouragement.

Summary

Carbon-14 (^{14}C) dating of groundwater has been widely used over the past 50 years to estimate apparent groundwater ages and investigate groundwater recharge. With a half-life of approximately 5730 years, ^{14}C has proven particularly useful in arid environments, where low rainfall and low recharge rates can result in long residence times. However knowledge gaps relating to ^{14}C interpretation still exist.

The first part of this thesis investigates the ^{14}C activity of unsaturated zone gas. Unsaturated zone $^{14}CO_2$ is typically assumed to be in equilibrium with atmospheric $^{14}CO_2$ (ie. modern). A number of researchers have shown that this may not be the case, with significant implications for groundwater ^{14}C interpretation. However little is known about how unsaturated zone ^{14}C activities may vary spatially. Measurements of ^{14}C in unsaturated zone gas were made at five sites across the arid Ti Tree Basin in central Australia. At all sites, a trend of decreasing ^{14}C activity with depth in the unsaturated zone was observed. Variation in unsaturated zone thickness related to variation in the ^{14}C activity above the watertable at each site (generally lower ^{14}C for deeper unsaturated zones). Modelling of unsaturated zone CO_2 production and transport showed that the dilution of unsaturated zone ^{14}C related to production of 'old' CO_2 in the unsaturated zone, most likely from mineral dissolution-precipitation fluxes. Where these processes are homogeneous, spatial variation in unsaturated zone thickness leads to spatial variation in the ^{14}C activity of unsaturated zone gas above the watertable.

The second part of this thesis explores the influence of spatially variable ^{14}C inputs and recharge on ^{14}C activities in an aquifer. This was investigated through theoretical 2D groundwater flow and solute transport modelling, with a focus on low recharge environments (where diffusive transport is significant). Results show that recharge estimated from discrete point measurements of ^{14}C may be wrong when recharge and ^{14}C inputs vary spatially, and that vertical profiles of ^{14}C in groundwater are needed to overcome this problem. Vertical profiles of ^{14}C in groundwater in the Ti Tree Basin were then interpreted using 2D flow and transport models, with a spatially variable boundary condition for ^{14}C. This revealed mountain front recharge, as well as recharge from ephemeral surface water to be important mechanisms.

The final part of this thesis synthesizes these findings into a 3D regional groundwater flow and solute transport model of the Ti Tree Basin. Carbon-14 activities were modelled directly, accounting for advection, diffusion and dispersion. The ^{14}C boundary condition at the watertable was based on measurements of ^{14}C near the watertable and unsaturated zone thickness (ie. lower ^{14}C activities where unsaturated zones are thicker). Recharge rates were determined by calibrating to groundwater head and ^{14}C activities. The results demonstrate the value of a distributed tracer data set (and understanding of its boundary condition) in resolving spatial variability in recharge. These findings will be relevant to other arid environments, and to other tracers which are transported to groundwater through the unsaturated zone.

Contents

Declaration i

Co-authorship ii

Acknowledgements iii

Summary iv

Contents v

List of Figures viii

List of Tables xi

1 Introduction 1

1.1 The research problem 1

1.2 Thesis aims 3

1.3 Contribution of this PhD 4

2 Factors affecting carbon-14 activity of unsaturated zone CO_2 and implications for groundwater dating 7

2.1 Introduction 7

2.2 Study area 9

2.3 Methods - field programme 9

2.4 Methods - modelling 11

2.5 Results - field data 14

2.6 Results - modelling of field data 15

2.7 Results - sensitivity analysis 19

2.8 Discussion 21

2.9 Conclusion 23

3 Vertical carbon-14 profiles for resolving spatial variability in recharge in arid environments 27

3.1 Introduction 27

3.2 Theoretical modelling 28

3.2.1 Methods 28

3.2.2 Results 30

3.3 Field demonstration 33

3.3.1 Site description 33

3.3.2 Methods 35

3.3.3 Results 35

3.3.4 Sensitivity to variations in ^{14}C input at the watertable 36

3.4 Discussion 38

3.5 Conclusion 40

4 Constraining spatial variability in recharge in an arid environment through modelling carbon-14 transport in groundwater **43**

4.1 Introduction 43

4.2 Site description 44

4.3 Methods 45

4.3.1 Data collection 45

4.3.2 Numerical modelling 46

4.4 Results 48

4.4.1 Groundwater chemistry 48

4.4.2 Numerical modelling 51

4.5 Discussion 53

4.6 Conclusion 57

5 Conclusion **61**

5.1 Summary of findings 61

5.2 Future work 61

6 Appendices **65**

6.1 Appendix 1 - Data 65

6.2 Appendix 2 - Discussion of regional groundwater chemistry in the Ti Tree Basin 76

6.2.1 Introduction 76

6.2.2 Methods 77

6.2.3 Results 77

6.2.4 Conclusion 81

6.3 Appendix 3 - Determination of equilibration times for diffusion samplers in piezometers of different depth 82

6.3.1 Background 82

6.3.2 Noble gas measurements in this study 83

6.3.3 Methods for testing equilibration times 85

6.3.4 Results for testing equilibration times 86

6.3.5 Conclusions 87

Bibliography. 88

List of Figures

2.1 Study sites in the Ti Tree Basin, Northern Territory, Australia. 10

2.2 Measured concentrations of (a) ^{14}C, (b) CFC-12, (c) CO_2 and (d) $\delta^{13}C$ in unsaturated zone gas in the Ti Tree Basin. ^{14}C activities and $\delta^{13}C$ contents in groundwater beneath these profiles are also shown. . . 16

2.3 Measured and modelled concentrations of unsaturated zone CFC-12, $^{12}CO_2$, $^{14}CO_2$ and ^{14}C activity (as pMC) for Site A. 17

2.4 Calibrated unsaturated zone ^{14}C (pMC) models for all other profiles. 19

2.5 Influence of (a) shallow and (b) deep rate of $^{12}CO_2$ production for Site A. Panel (c) shows that the thickness of the zone of deep CO_2 production is relatively unimportant so long as bulk CO_2 production is the same however panel (d) shows that the thickness of the shallow production zone is important. 20

2.6 Modelled results from HYDRUS showing the influence of (a) recharge rate, (b) shallow CO_2 production, (c) deep CO_2 production and (d) the depth of the shallow CO_2 production zone (i.e. depth of root zone) on calculated ^{14}C activity (pMC) of unsaturated zone gas directly above the watertable (for DTW 12 to 100 m). 22

3.1 Theoretical scenarios 1 to 4 showing the recharge and ^{14}C activity at the watertable, the resulting streamlines, ^{14}C activities with depth and recharge rates estimated using equation (3.2) based on simulated ^{14}C activities at observation points at 8 km, 25 km and 42 km along the transect. In Scenario 1 recharge and ^{14}C are spatially constant (at 1 mm y^{-1} and 100 pMC respectively); in Scenario 2 recharge occurs exclusively at the basin margin (at 25 mm y^{-1} between 0 and 2 km); in Scenario 3 recharge occurs exclusively at the basin margin (at 25 mm y^{-1}) and ^{14}C activities at the watertable vary spatially; in Scenario 4, recharge is 25 mm y^{-1} from 0 – 2 km, 0 mm y^{-1} from 2 – 10 km, and 1 mm y^{-1} for the rest of the transect, while ^{14}C activities at the watertable vary spatially. 31

3.2 Advective (particle tracking) ages compared with apparent ages estimated from ^{14}C profiles at the observation point 42 km from the basin margin in Scenarios 1 to 4. RCH denotes recharge. Observation points are spaced vertically 4 m apart from 0 – 60 m depth, then 1 m apart in the bottom 5 m of the aquifer. Both ^{14}C and advective ages increase with increasing depth in the aquifer. 33

3.3 Location of carbon-14 observation sites in the Ti Tree Basin, Northern Territory, Australia. Also shown are inferred groundwater flow paths (based on potentiometric surfaces) and aerial imagery (Inset) showing denser vegetation around parts of the Allungra Creek floodplain.. 34

3.4 Relationship between unsaturated zone thickness and ^{14}C activity above the watertable for different rates of 'old' CO_2 production in the unsaturated zone (after Wood et al. (2014)). Also shown are unsaturated zone ^{14}C activities above the watertable measured by Wood et al. (2014)). 36

3.5 Measured and modelled ^{14}C activities in groundwater at investigation sites A, B and C. At Site A recharge occurs at the basin margin (10 mm y^{-1}), with 0 mm y^{-1} recharge between 1 km and 13 km, then -0.5 mm y^{-1} (discharge) between 13 km and 15 km. Also shown is the profile generated by spatially constant recharge (at a rate of 0.65 mm y^{-1}, equal to the total amount of recharge in the calibrated scenario) demonstrating the need to invoke spatial variability in recharge and mountain front recharge. At Site B, recharge occurs predominantly at the basin margin (28 mm y^{-1}) with a small amount of discharge (-0.1 mm y^{-1}) across the rest of the transect. Also shown is the profile generated using spatially constant recharge (1.14 mm y^{-1}, again equal to the total amount in the calibrated scenario). At Site C there is mountain front recharge and significant recharge 10 km up gradient of the observation point. 37

3.6 Measured vs. modelled ^{14}C activities at Sites A and C for the scenarios considered in the sensitivity analysis. 38

4.1 Location of ^{14}C investigation in the Ti Tree Basin, Northern Territory (NT), Australia (groundwater discharge area Stirling Swamp is not shown, but lies ~20km north-west of the northern margin). 45

4.2 (a) Carbon-14 activities measured in the Ti Tree Basin aquifer in this study and theoretical ^{14}C profiles for recharge ranging from 0.1 mm y^{-1} to 5 mm y^{-1} (based on equation 4.2 and assuming A_0 = 100 pMC) and (b) the relationship between ^{14}C activity and $\delta^{13}C$ content. 49

4.3 Vertical profiles of $\delta^{13}C$ in unsaturated zone gas ($^{13}CO_2$) and groundwater ($^{13}C_{DIC}$) at five investigation sites in the Ti Tree Basin 50

4.4 Data used in the cokriging approach for determining the ^{14}C boundary condition at the watertable: groundwater ^{14}C activities near the watertable (primary data source, where groundwater samples are the shallowest piezometer at each site, generally <10 m below the watertable) and the relationship unsaturated zone thickness and ^{14}C activity directly above the watertable (based on earlier work in the Ti Tree Basin (Wood et al., 2014)) 50

4.5 Model domain showing geometry and ^{14}C activity boundary condition for the transport model, based on the cokriging approach. 51

4.6 Measured vs. modelled hydraulic head measurements and ^{14}C activities in the Ti Tree Basin. 52

4.7 Measured vs. modelled ^{14}C vertical profiles at investigation sites in the central Ti Tree Basin (RN refers to registration number of the drill holes in which piezometer nests were installed). 52

4.8 95% confidence intervals for recharge estimates with 18 recharge zones and 4 recharge zones. 54

6.1 Groundwater sampling in the Ti Tree Basin, February 2012 78

6.2 Piper plot for major ion chemistry of groundwater in the Ti Tree Basin 78

6.3 Schoeller plot for representative groundwater samples across the Ti Tree Basin 79

6.4 Spatial distribution of groundwater salinity as given in Read and Tickell (2007) for the main part of the Ti Tree Basin. Overlain are measurements made in this study (triangles, where colours represent the same salinity ranges as Read and Tickell (2007) values). Location of Stirling Swamp is given by red triangles, where the salinity ranges from 36,859 to 148,672 mg L^{-1}. 79

6.5 Stable isotope composition of groundwater in this study. Also shown is the LMWL for Alice Springs (150 km south of the study area), and long term amount weighted mean compositions of different monthly rainfall amounts (after Harington et al. (2002)). 80

6.6 Chloride vs. δ^2H for groundwater in the Ti Tree Basin, showing the influence of evaporation (concentration of chloride and enrichment of δ^2H) and transpiration (concentration of chloride with no significant change in δ^2H) on groundwater chemistry. 81

6.7 Helium-4 concentrations vs. carbon-14 activities of groundwater samples in the Ti Tree Basin (a) collected by Harrington (1999) and in this study on multiple field trips using conventional diffusion samplers and (b) modified versions of the diffusion samplers described by Gardner and Solomon (2009) 83

6.8 Argon-40 vs. neon-20 - the green line displays concentrations that would be observed in water in equilibrium with the atmosphere for temperatures ranging from 30ºC (lowest values) to 5ºC (highest values). Deviation from this trend demonstrates ‘addition’ of noble gases, or formation of excess air, which may be as high as 80% for some of the samples near the Allungra Creek floodout. 84

6.9 Measured gas concentrations (cm^3 STP g^{-1}) and pressures in the diffusion samplers versus equilibration time. Results in the left panel are for the shallower bore, while those in the right are for the deeper bore. 86

List of Tables

2.1 Diffusion and partition coefficients used for models shown in Figure 2.3 (*the same diffusion coefficient in water D_0^w was applied to both $^{12}CO_2$ and $^{14}CO_2$). 14

2.2 Summary of CO_2 production rates and porosity values used to calibrate each model. 18

3.1 Table 1. Model parameters used in simulations where * are based on values in Gelhar et al. (1992) for the aquifer scale modelled; ** are from Browne and Firestone (1999); *** is from Li and Gregory (1974). 29

4.1 Model parameters used in simulations where * are based on values in Gelhar et al. (1992) for the aquifer scale modelled; ** are from Browne and Firestone (1999); *** is from Li and Gregory. 47

4.2 Calibrated recharge rates and 95% confidence intervals for models with 18 recharge zones. 55

4.3 Calibrated recharge rates and 95% confidence intervals for models with 4 recharge zones. 55

4.4 Calibrated recharge rates and 95% confidence intervals for models with 18 recharge zones and ^{14}C input activities based purely on unsaturated zone thickness (Figure 4.5(b)) 55

6.1 Unsaturated zone gas data (m-bgl denotes metres below ground level). 66

6.2 Location and field parameters (during sampling) of piezometers at sites where soil gas profiles were collected. 67

6.3 Dissolved ion and isotopic content of groundwater samples from piezometers at sites where soil gas profiles were collected. 68

6.4 Location and field parameters (during sampling) of piezometers near the Woodforde River. Bore elevations are taken at the top of casing (TOC). 69

6.5 Dissolved ion and isotopic content of groundwater samples from piezometers near the Woodforde River. 70

6.6 Location and field parameters (during sampling) of piezometers in Stirling Swamp. Bore elevations are taken at the top of casing (TOC). 71

6.7 Dissolved ion and isotopic content of groundwater samples from piezometers in Stirling Swamp. . . 72

6.8 Location and field parameters (during sampling) of piezometers in the central Ti Tree Basin and Allungra floodout area. Bore elevations are taken at the top of casing (TOC). 73

6.9 Dissolved ion and isotopic content of groundwater samples from piezometers in the central Ti Tree Basin and Allungra floodout area. 74

6.10 Location and field parameters (during sampling) of piezometers in the south eastern Ti Tree Basin. Bore elevations are taken at the top of casing (TOC). 75

6.11 Dissolved ion and isotopic content of groundwater samples from piezometers in the south eastern Ti Tree Basin. 76

6.12 Details for the two bores which were sampled as part of the equilibration time experiment (m-bgl denotes metres below ground level) 85

1 Introduction

1.1 The research problem

In arid zones such as central Australia, low average rainfall and high evapotranspiration result in a scarcity of surface water supplies, making groundwater an important source of water. Appropriate management of groundwater resources in arid zones requires knowledge of their water balance and turnover times. An understanding of groundwater recharge processes is therefore crucial to understanding and managing water resources in arid zones. However groundwater recharge in arid zones can be sparse and episodic, and difficult to quantify using traditional water balance techniques (Gee and Hillel, 1988).

Methods of recharge investigation using environmental tracers have been widely used in arid and semi-arid zones (IAEA, 1980; Herczeg and Leaney, 2011). A number of different tracers have been applied in arid areas to investigate different aspects of groundwater recharge. Because of the generally low recharge rates and longer residence times, radioactive 'age' tracers such as carbon-14 (^{14}C) and chlorine-36 (^{36}Cl) have been used to asses groundwater age and whether or not 'modern' groundwater recharge occurs (Torgersen et al., 1991; Cresswell et al., 1999). In arid and semi-arid areas where unsaturated zones may be quite deep (>10 m), profiles of tracers such as chloride (Cl) and tritium (^{3}H) have proven to be useful in estimating rates of groundwater recharge (Cook et al., 1989; Dincer et al., 1974). The stable isotope ratios ($^{18}O/^{16}O$ and $^{2}H/^{1}H$) of water have been used to delineate sources of recharge, for example the importance of diffuse rainfall recharge through the unsaturated zone compared with rapid infiltration of rainfall following high intensity events or flooding (Vogel and Van Urk, 1975; Harrington et al., 2002). Atmospheric noble gases (e.g. neon-20, argon-40, helium-4 (^{4}He)) have also proven useful in identifying recharge mechanisms and the influence of paleo-recharge in arid areas (Beyerle et al., 2003). Furthermore ^{4}He, which accumulates in aquifers over time through the decay of uranium and thorium minerals, has been used in arid zones as an age indicator to provide comparative chronology with tracers such as ^{14}C and ^{36}Cl (Torgersen and Clarke, 1985; Kulongoski et al., 2008) and to constrain interpretation of regional flow processes (Bethke et al., 1999).

Carbon-14 has proven to be a useful tracer for determining subsurface residence times and recharge (Vogel, 1967). Carbon-14 is produced by cosmic ray bombardment of nitrogen atoms in the atmosphere, where it mixes with atmospheric CO_2. In this phase (i.e. $^{14}CO_2$) it may equilibrate with infiltrating rainwater and become part of the total dissolved inorganic carbon (TDIC) pool in groundwater, where 'closed' from its source it decays radioactively, with activities expressed in units of percent Modern Carbon (pMC), relative to the atmospheric activity (100 pMC). Carbon-14 has a half life of 5730 years, making it useful for dating of groundwater over time scales of ~ 10^2 - 10^4 years (Clark and Fritz, 1997), and it has hence found application in arid and semi-arid settings for estimating both rates and spatial variability in recharge (Leaney and Allison, 1986; Harrington et al., 2002). It has also proven to be a useful tracer in calibrating groundwater flow models in semi arid environments. Sanford et al. (2004) modelled advective ages (particle

tracking) in the Rio Grande Basin, New Mexico, and compared the results with apparent ages derived from ^{14}C measurements in order to constrain recharge. Zhu (2000) used a groundwater flow and solute transport model (accounting for both advection and diffusion/dispersion) to simulate ^{14}C activities in the Black Mesa Basin, Arizona, and likewise compared the results to ^{14}C measurements to help calibrate the model and constrain estimates of recharge.

Despite it's widespread use in arid and semi arid settings, there remain knowledge gaps that limit the certainty with which ^{14}C activities in groundwater are interpreted. This PhD thesis investigates three of these areas:

Firstly, the interpretation of ^{14}C activities in groundwater is complicated by a number of factors. For example, weathering of carbonate minerals in the aquifer matrix through water-rock interactions can introduce 'old' carbon into the TDIC pool in groundwater, diluting the ^{14}C activity of groundwater. Consequently a number of geochemical correction models have been developed to account for carbonate weathering and assign an initial ^{14}C value at the time of recharge (Ingerson and Pearson, 1964; Tamers, 1975; Fontes and Garnier, 1979; Harrington and Herczeg, 1999). These models typically assume the ^{14}C activity of unsaturated zone gas (which infiltrating water equilibrates with prior to recharge) is in equilibrium with atmospheric CO_2 (i.e. ~ 100 pMC). Several studies have shown that this is assumption can be invalid (Haas et al., 1983; Leaney and Allison, 1986; Thorstenson et al., 1998) due to production of 'old' CO_2 in the unsaturated zone from sources such as oxidation of organic matter (Keller and Bacon, 1998) calcite precipitation-dissolution fluxes (Walvoord et al., 2005; Gillon et al., 2009), with significant implications for interpretation of ^{14}C activities in groundwater and determination of apparent groundwater age (Bacon and Keller, 1998). However these studies have typically been limited to measurement of unsaturated zone ^{14}C at one location, and there is little understanding of how these processes may vary spatially and impact groundwater ^{14}C activities over a regional scale. Thus a better understanding of the influence of unsaturated zone processes on groundwater ^{14}C is needed (Glynn and Plummer, 2005; Herczeg and Leaney, 2011).

Secondly, the interpretation of ^{14}C activities in arid environments is further complicated by diffusion and dispersion. Groundwater age tracers such as ^{14}C are often interpreted assuming that advective flux (recharge) is the primary transport mechanism into the aquifer (Cook and Bohlke, 2000). However when recharge is low (< 1 mm y^{-1}), diffusive transport of ^{14}C in the aquifer will result in a vertical tracer profile showing higher ^{14}C activities with depth than would be observed if diffusion were not occurring (Walker and Cook, 1991). Dispersion may likewise significantly influence the transport of tracers such as ^{14}C in low flux environments (Castro and Goblet, 2005), potentially leading to underestimates of groundwater age. Spatial variability in recharge can also influence the vertical shape of tracer profiles in an aquifer (Robertson and Cherry, 1989), as well as the spatial distribution of tracer concentrations (Harrington et al., 2002). However it is unclear how these processes together (diffusion, dispersion, spatial variability in recharge), along with the influence of unsaturated zone processes, influence ^{14}C activities and vertical profiles in an aquifer.

Thirdly, studies in which ^{14}C has been used as a calibration target in 3D numerical modelling have typically taken the approach of modelling advective ages (through particle tracking) and comparing modelled groundwater ages with those estimated from ^{14}C measurements in an aquifer (Sanford and Buapeng, 1996; Sanford et al., 2002; 2004; Michael and Voss, 2009). This approach compares modelled advective age (not accounting for diffusion and dispersion) with 'modelled' ^{14}C ages (where the model is the geochemical correction scheme applied to ^{14}C measurements). Approaches in which ^{14}C transport has been modelled directly (ie. solute transport modelling accounting for advection, diffusion and dispersion) have generally been limited to 2D flow and solute transport models (Zhu, 2000; Castro and Goblet, 2005; Schwartz et al., 2010). This is because the level of model discretisation required to accurately simulate dispersion and diffusion in large regional aquifers makes accurate simulation difficult (Sanford and Pope, 2010). However, in arid zones diffusion will need to be accounted for in any regional scale model of groundwater age tracers. Also, with advances in computing power, it is becoming increasingly recognised that direct simulation of age tracer concentrations with solute transport models is a desirable to model groundwater age and thus help constrain estimates of residence time and groundwater recharge (Troldborg et al., 2007; McCallum et al., 2015; Turnadge and Smerdon, 2014).

1.2 Thesis aims

The broad aim of this thesis is to investigate groundwater recharge in an arid environment through the use of ^{14}C as a tracer, with the Ti Tree Basin in central Australia serving as the study site for these investigations. The thesis looks at some of the uncertainties surrounding the use of ^{14}C as a tracer, including the influence of CO_2 production in the unsaturated zone on the ^{14}C activity of infiltrating groundwater. The thesis further explores the implications of these processes on groundwater ^{14}C activities, and how understanding these processes can assist in constraining estimates of groundwater recharge and its spatial variability. Specifically, this thesis investigates:

i. How ^{14}C activities of unsaturated zone gas may become diluted. This study build on previous research by investigating how the ^{14}C activity of unsaturated zone gas may vary spatially by measuring vertical profiles at five sites. Through numerical modelling the factors that influence unsaturated zone ^{14}C activity are explored.

ii. The influence spatial variability in unsaturated zone ^{14}C activities and spatial variability in recharge have on ^{14}C profiles in an aquifer. Through theoretical modelling, the need to measure vertical profiles of groundwater age tracers such as ^{14}C in order to constrain recharge processes is demonstrated. This is particularly important in arid environments where diffusion of tracers from the unsaturated zone into the aquifer may be important. Through a field application it is shown that measurement of vertical ^{14}C profiles, coupled with knowledge of the spatial variability in unsaturated zone ^{14}C helps constrain understanding of spatial variability in recharge along 2D flow lines.

iii. Modelling ^{14}C activities directly using a regional scale 3D flow and solute transport model. This part of the thesis builds upon the process understanding developed in earlier chapters to determine the rate and spatial variability of groundwater recharge and discharge in the Ti Tree Basin, central Australia. Calibration to ^{14}C activities and hydraulic head is achieved with the use of parameter estimation software PEST.

These areas are the focus of three manuscripts which are presented in Chapters 2, 3 and 4. Two of these manuscripts are now published in the Journal of Hydrology, and the third has been submitted for review.

1.3 Contribution of this PhD

This thesis explores the use of ^{14}C as a tool for estimating spatial variability in groundwater recharge in an arid environment. The research is performed through a field investigation in the Ti Tree Basin, central Australia, and data interpretation and analysis is augmented with numerical modelling. The research provides new constraints on the use of ^{14}C as a tracer in arid zone recharge studies. This is achieved by specifically examining:

1. How unsaturated zone ^{14}C activities may vary spatially across a groundwater basin. Unsaturated zone ^{14}C activities are typically assumed to be in equilibrium with atmospheric CO_2 in groundwater studies, however many studies have shown this assumption to be false. Despite this, little is known about spatial variability in unsaturated zone ^{14}C activities. Measurements of unsaturated zone ^{14}C in the Ti Tree Basin, coupled with interpretation through modelling help resolve this knowledge gap, by demonstrating a relationship between unsaturated zone thickness and $^{14}CO_2$ activity (with lower $^{14}CO_2$ activities where unsaturated zones are thicker).

2. How spatial variability in unsaturated zone ^{14}C activity and spatial variability in recharge may influence vertical ^{14}C profiles in an aquifer. Many studies use single point measurements of ^{14}C in groundwater to estimate apparent groundwater age and recharge rate, however these estimates may be significantly erroneous due to the influence of unsaturated zone ^{14}C activities and spatial variability in recharge. This research demonstrates through measurement and modelling that vertical profiles of ^{14}C in an aquifer, coupled with understanding of unsaturated zone ^{14}C activities, may greatly reduce error in the estimates of recharge and its spatial variability.

3. The use of this new understanding in unsaturated zone ^{14}C activities to calibrate a 3D regional scale flow and transport model and constrain estimates of spatial variability in recharge. Tracers such as ^{14}C are increasingly being used as calibration targets in numerical models, however regional transport models for ^{14}C have typically been 2D and spatial variability in the boundary condition for ^{14}C not considered. This research demonstrates the benefit in considering a spatially variable ^{14}C input concentration, and provides further constraints by using vertical profiles of ^{14}C as calibration targets.

These findings will help improve the way ^{14}C is used and interpreted in groundwater studies, particularly in arid environments. It demonstrates the importance of considering unsaturated zone ^{14}C activities and vertical profiles of ^{14}C in groundwater. This will be useful for future researchers planning groundwater studies in other arid and semi-arid environments.

Central Ti Tree Basin at dawn, January 2014

2 Factors affecting carbon-14 activity of unsaturated zone CO_2 and implications for groundwater dating

Based on the publication: Wood, C., P.G. Cook, G.A. Harrington, K. Meredith, and R. Kipfer, 2014: Factors affecting carbon-14 activity of unsaturated zone CO_2 and implications for groundwater dating. *J. Hydrol.*, **519,** Part A, 465-475, doi: 10.1016/j.jhydrol.2014.07.034

Abstract

Unsaturated zone processes may influence the carbon-14 (^{14}C) activity of infiltrating groundwater and thus introduce error in derived groundwater residence times. However unsaturated zone ^{14}C activities are rarely measured and there is little understanding of how they may vary spatially in a groundwater basin. In this study we measured ^{14}C activity in unsaturated zone gas at five sites with different watertable depths (8.2 to 31.5 m) in the arid Ti Tree Basin, central Australia. We observed a relatively uniform decrease in ^{14}C activity of unsaturated zone gas with depth at most sites, with variation in unsaturated zone depths leading to variation in ^{14}C activities directly above the watertable at each site (ranging from 54 to 106 percent Modern Carbon (pMC)). Through modelling we show that the profiles are influenced by CO_2 production at different depths from sources with different isotopic ratios, including production of 'modern' CO_2 in the root zone and production of 'old' CO_2 above the watertable. Scenario modelling showed that these processes are independent of recharge when recharge is low (0 to 10 mm y^{-1}) but that higher recharge rates (>100 mm y^{-1}) result in more advective transport of atmospheric CO_2 to the watertable. The variation in ^{14}C above the watertable was more sensitive to watertable depth and shallow and deep CO_2 production rates. These findings offer insight into how unsaturated zone ^{14}C activities may vary spatially and provide guidance as to when ^{14}C depletion in unsaturated zone CO_2 may become important for groundwater dating, particularly in arid settings.

2.1 Introduction

Carbon-14 (^{14}C) has been widely used as a tracer in groundwater studies to investigate groundwater residence time, groundwater recharge and its spatial and temporal variability, and regional flow characteristics (Vogel, 1967; Love et al., 1993; Harrington et al., 2002). A consistent problem in interpreting ^{14}C activities in groundwater is accounting for reactions and processes other than radioactive decay that may alter the ^{14}C activity (such as dilution caused by carbonate weathering and oxidation of 'old' organic matter) and determining the ^{14}C activity at the time of recharge. Geochemical mass balance models are typically used to correct for carbonate weathering and assign an initial ^{14}C activity at the time of recharge (Ingerson and Pearson, 1964; Tamers, 1975; Fontes and Garnier, 1979). Accurate calculation of the initial ^{14}C activity also requires knowledge of the ^{14}C activity of unsaturated zone gas, however this is rarely measured and typically assumed to be in equilibrium with atmospheric CO_2 (Mazor, 2004).

Several studies have shown that ^{14}C activities in unsaturated zone CO_2 can be depleted relative to atmospheric CO_2 (Haas et al., 1983; Leaney and Allison, 1986; Yang et al., 1994; Thorstenson et al., 1998;

Keller and Bacon, 1998) and the implications for groundwater age calculation may be significant (Bacon and Keller, 1998). Bacon and Keller (1998) reported unsaturated zone ^{14}C activities of 20 pMC in a 7 m deep profile in Saskatchewan, Canada. This depletion of ^{14}C was caused by oxidation of old (low ^{14}C) organic matter near the watertable, and hence production of old CO_2. They presented a model of unsaturated zone ^{14}C transport (with diffusion in the gas phase being the dominant transport process) with two isotopically distinct zones of CO_2 production: a shallow zone of CO_2 production with an atmospheric ^{14}C activity (representing plant root respiration) and a deeper zone of CO_2 production with a depleted ^{14}C activity (from oxidation of organic matter). Walvoord et al. (2005) reported unsaturated zone ^{14}C activity of 20 pMC in a 110 m deep profile in the Amargosa Desert, USA, and likewise replicated their profile with a gas transport model that considers shallow and deep zones of CO_2 production with different isotope signatures. However Walvoord et al. (2005) considered the source of deep older CO_2 to be calcite precipitation at a slowly declining watertable. Walvoord et al. (2005) also assessed the sensitivity of ^{14}C profiles to shallow 'modern' CO_2 production (in a 1 m thick root zone) and deep 'old' CO_2 production, however the influence of other processes such as recharge rate, root zone thickness and watertable depth was not assessed.

These studies demonstrate both the importance of measuring ^{14}C in the unsaturated zone and provide a conceptual understanding of the controlling processes. However despite the wealth of studies that have used ^{14}C activities to date groundwater, there remains a paucity of measured unsaturated zone ^{14}C profiles in the literature (approximately 9 profiles to the authors knowledge that are >10 m in depth (Thorstenson et al., 1983; Haas et al., 1983, Suchomel et al., 1990; Leaney and Allison, 1986; Striegl and Healy, 1990; Yang et al., 1996; Keller and Bacon, 1998; Walvoord et al., 2005; Gillon et al., 2009). Most of the previous studies are limited to one to two profiles and are in arid settings, hence limiting their assessment of spatial variability in unsaturated zone ^{14}C, and how understanding of the controlling processes may be transferred to other locations. Consequently there is a poor understanding of when unsaturated zone processes are likely to alter the ^{14}C activity of unsaturated zone gas, and the difficulties in interpreting ^{14}C activities in groundwater persist (Herczeg and Leaney, 2011).

In this study we measured unsaturated zone ^{14}C activities at five sites with different watertable depths in the arid Ti Tree Basin, central Australia, providing insight into spatial variability in unsaturated zone ^{14}C activity. We interpret and model our data in terms of CO_2 production in the unsaturated zone from sources with different carbon isotope compositions, consistent with previous studies. Diffusive transport is constrained by measurements and modelling of chlorofluorocarbons (CFCs) in the unsaturated zone (rather than measuring porosity and assuming a value for tortuosity, which may be poorly constrained in gravelly sediments (Walvoord et al., 2005)). This enables CO_2 production rates to be much more accurately determined. We then evaluate the influence of recharge rate, and shallow and deep CO_2 production on unsaturated zone ^{14}C profiles over a range of watertable depths. This sensitivity analysis draws attention to the factors most likely to affect ^{14}C activity at the watertable, and demonstrates how spatial variability in ^{14}C activity at the watertable may arise. These findings help constrain the conditions under which dilution of the ^{14}C activity

of unsaturated zone CO_2 may occur, and act as a guide as to when these unsaturated zone processes need to be considered in groundwater dating studies.

2.2 Study area

The Ti Tree Basin covers an area of ~5500 km^2 and is located 150 km north of Alice Springs in central Australia (Figure 2.1). Mean annual rainfall is low (300 mm y^{-1}) and occurs mostly in the southern hemisphere summer (December – March). Soil types are generally either dark red massive clays that support predominantly Mulga vegetation (*Acacia* spp.) or red earthy sands that are dominated by Spinifex grass (*Trioda* spp.) under a sparse open woodland of bloodwood (*Corymbia* spp.) and coolabah trees (*Eucalyptus* spp.). The basin is comprised of Tertiary lacustrine and fluviatile sediments which make up the main unconfined aquifer (undifferentiated sandstone, limestone and silty sandstone). Depth to groundwater ranges from >60 m in the southern portion of the basin to <10 m in the north (Figure 2.1). Observation wells in shallower watertable areas near the Woodforde River have historically shown rises in response to heavy rainfall and flooding, however there is little evidence that this has occurred since the year 2000, and groundwater levels are generally static or slightly declining at rates of 0.01 to 0.05 m y^{-1} (Knapton, 2009). Total dissolved solids (TDS) of groundwater ranges from <1,500 mg L^{-1} in the southern parts of the basin, but increases to >100,000 mg L^{-1} towards the northern terminus of the basin.

Harrington et al. (2002) investigated recharge processes in the basin using environmental tracers (chloride, carbon-14 and stable isotopes). Carbon-14 activities in groundwater ranged from 4 to 70 pMC, and groundwater ages were estimated using a geochemical correction scheme that accounted for addition of HCO_3 from weathering of old silicate minerals and calcite. The ^{14}C activity of soil gas was assumed to be 100 pMC. Estimated recharge rates from corrected groundwater ages ranged from 0.1 to 50 mm y^{-1} (median 0.9 mm y^{-1}), in reasonable agreement with the mean rate provided by the chloride mass balance method (0.8 mm y^{-1}). The higher recharge rates were spatially linked to the areas overlain by the (normally dry) Woodforde River and Allungra Creek floodplain. Hence across the Basin recharge is believed to be low, although higher recharge may occur during rare flood events in areas associated with surface water features (Harrington et al., 2002).

2.3 Methods - field programme

Installation of unsaturated zone gas samplers was concurrent with piezometer installation in the Ti Tree Basin between 2011 and 2012. Conventional rotary drilling methods were used with a blade bit and air circulation. Where hard calcrete and silcrete layers were encountered, a hammer bit was used. Piezometers were completed at five sites with 50 mm diameter PVC that had slotted screens of 1 mm aperture. For all piezometers, screen length was between 1 and 2 m with a gravel pack (5 to 7 mm aggregate gravel) around the screen. Bentonite was used to seal the borehole annulus above the gravel pack and the remainder of the

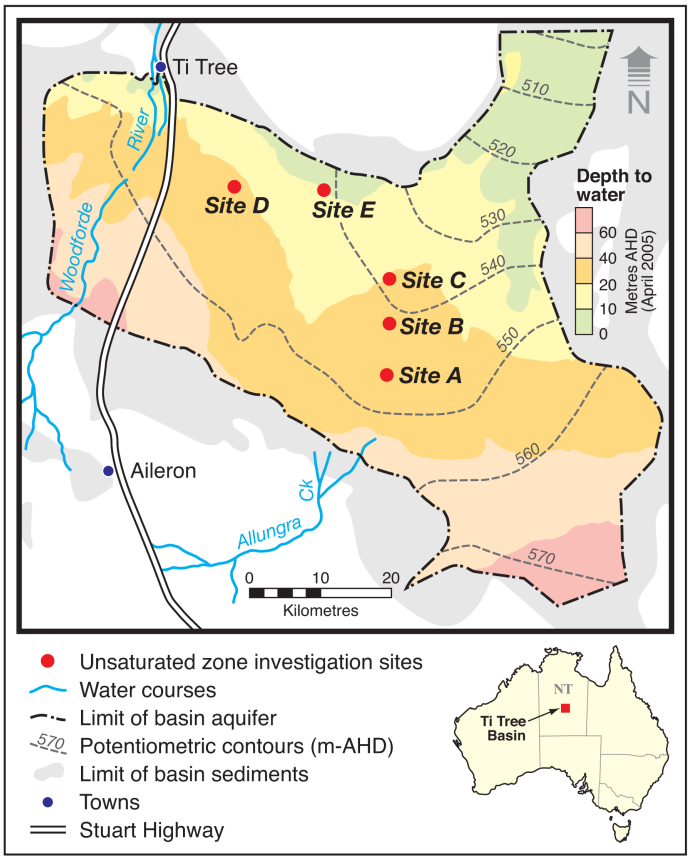

Figure 2.1: Study sites in the Ti Tree Basin, Northern Territory, Australia.

borehole was back filled to the surface with sand. Unsaturated zone gas sampling tubes consisted of ¼" nylon tubing fitted with a stainless steel filter on the end. These were taped to the outside of the piezometers during installation and a connection port was attached to the tubing at the ground surface. The filter ends of the gas sampling tubes served to prevent any soil particulate matter entering and potentially clogging the tubing, and were 'screened' in the backfill material (sand). At each site up to six gas sampling tubes of different length were attached to the outside of the piezometer, so that samples could be taken at multiple depths.

Samples of unsaturated zone gas were collected for analysis of CO_2 (percent by volume), ^{14}C (pMC), $\delta^{13}C$ (‰), CFC-11 and CFC-12 (pptv). Sampling was conducted in 2011 for sites A to E (Figure 2.1). Unsaturated zone gas samples were collected by attaching a small air pump to the sampling ports at the surface. The pump was run for five minutes at a flow rate of ~500 mL min^{-1} to flush the sampling tube then a sample was collected into either 110 mL Isotubes (^{14}C and $\delta^{13}C$ analysis) or 330 mL stainless steel canisters (CFC and CO_2 analysis). Groundwater was sampled from the piezometers to which the gas samplers were attached, using a Grundfos MP1 submersible pump. Samples were collected for carbon isotope analysis after approximately three bore volumes had been purged and field parameters (electrical conductance, pH, temperature) had stabilised, and stored in 1 L high density polyethelene plastic bottles.

Analysis of ^{14}C and $\delta^{13}C$ was performed on groundwater and unsaturated zone gas using the method described by Meredith et al. (2012), however acid evolution (to convert DIC to CO_2) was not required

in the case of unsaturated zone gas. The analysis was performed using AMS facilities at the Australian Nuclear Science and Technology Organisation (ANSTO, Fink et al., (2004)). ^{14}C activities of unsaturated zone gas and groundwater are reported as the ratio $^{14}CO_2$:$^{12}CO_2$ and $^{14}C_{DIC}$:$^{12}C_{DIC}$ (respectively) relative to the international standard (Stuiver and Pollach, 1977) in units of pMC. Stable isotope ratios (^{13}C:^{12}C) are reported in per mil (‰) relative to the international standard (Craig, 1957). CO_2 analysis was performed at Flinders University, South Australia, using a Quibit S-151 CO_2 analyser. Given the relatively low range of the CO_2 analyser (0 to 2000 ppm), samples were diluted in a closed loop of known volume using ultra high purity (UHP) nitrogen and appropriate corrections applied to give an accurate measurement of CO_2 concentration. CFCs were analysed by gas chromatography at CSIRO Land and Water in Adelaide, South Australia, using a setup similar to that described by Busenberg and Plummer (1992). Only CFC-12 data is presented in this paper, as the trends in both tracers are well correlated.

2.4 Methods - modelling

Based on previous studies, dilution of unsaturated zone ^{14}C can be linked to production of CO_2 relatively devoid of ^{14}C, hence our modelling approach is to model both $^{14}CO_2$ and $^{12}CO_2$ production and transport in the unsaturated zone. Modelling $^{12}CO_2$ and $^{14}CO_2$ separately in identical units allows us to consider the ratio ^{14}C:^{12}C in soil gas for direct comparison to our measured units of ^{14}C activity (pMC). Following the work of Thorstenson et al. (1983), we converted ^{14}C activity in pMC to concentration units of $^{14}CO_2$ in mass/volume (mmol m^{-3}), and estimated $^{12}CO_2$ concentration (mmol m^{-3}) based on measurements of CO_2 (ppm) and the calculated $^{14}CO_2$ concentrations (knowing that ^{14}C in pMC directly relates to the ratio ^{14}C:^{12}C).

Our model considers advective and diffusive transport in the liquid phase and diffusive transport in the gaseous phase. However given the arid environment transport is predominantly diffusive in the gas phase. We have constrained diffusive transport through measurement and modelling of CFCs. CFCs are trace gases of anthropogenic origin, which were introduced into the atmosphere in the 1950s. Their atmospheric concentration increased until the 1990s when they were phased out of production (owing to their ozone depleting qualities). Atmospheric concentrations have been measured in several locations, including Australia, over the past 60 years, hence input concentrations to the unsaturated zone over time are known. Therefore CFCs can be used to indicate timescales of unsaturated zone gas transport (Cook and Solomon, 1995) and help determine parameters related to the effective diffusion coefficient in a soil (e.g. porosity and tortuosity, Weeks et al. (1982)).

To reproduce our data we modelled CFC-12, $^{12}CO_2$ and $^{14}CO_2$ using HYDRUS 1-D (Simunek et al., 2013). HYDRUS uses the Richards equation to model variably saturated flow:

$$\frac{\partial \theta}{\partial t} = \frac{\partial}{\partial x}\left(K\left(\frac{\partial h}{\partial x} + cos\alpha\right)\right) - S \tag{2.1}$$

Where θ is the volumetric water content (m^3 m^{-3}), h is the water pressure head (m), t is time (y), x is the spatial coordinate (m), K is the unsaturated hydraulic conductivity (m y^{-1}) α is the angle between the flow direction and the vertical axis (0° for vertical flow in our case) and S is the sink term. Solute transport is modelled with an advection dispersion equation in which transport may occur in the liquid and gas phases. Exchange between the liquid and gas phase is assumed to be instantaneous and determined by the partition coefficient:

$$k_g = \frac{c_w}{c_g} \tag{2.2}$$

Where c_w and c_g are concentrations in the liquid and gas phase (mmol m^{-3}). We assume that sorption is negligible for both CFCs (Cook and Solomon, 1995) and CO_2, hence there is no partitioning between the solid and liquid phases. Sorption of $^{14}CO_2$ may become important as water content increases (Striegl and Armstrong, 1990), however preliminary modelling showed our results to be insensitive to sorption at the low water contents we model. Thus the solute transport equation can be written as:

$$\frac{\partial \theta c_w}{\partial t} + \frac{\partial a_v c_g}{\partial t} = \frac{\partial}{\partial x}\left(\theta D^w \frac{\partial (c_w)}{\partial x}\right) + \frac{\partial}{\partial x}\left(a_v D^g \frac{\partial c_g}{\partial x}\right) - \frac{\partial q c_w}{\partial x} - \lambda \theta c_w - \lambda a_v c_g + \gamma c_g a_v \tag{2.3}$$

where q is the volumetric flux (m y^{-1}); λ is the decay constant for ^{14}C (y^{-1}), γ represents production of CO_2 in the gas phase (mmol m^{-3} y^{-1}), a_v is the air content (m^3 m^{-3}), D^w is the dispersion coefficient in the liquid phase (m^2 y^{-1}) and D^g is the diffusion coefficient in the gas phase (m^2 y^{-1}). The dispersion and diffusion coefficients are calculated as follows:

$$D^w = D_L \frac{|q|}{\theta} + \theta D_0^w \tau_w \tag{2.4}$$

$$D^g = a_v D_0^g \tau_g \tag{2.5}$$

where D_L is longitudinal dispersivity (m), $|q|$ is the absolute value of the volumetric water flux (m y^{-1}), D_0^w is the molecular diffusion coefficient of the solute in free water (m^2 y^{-1}) and τ_w is tortuosity for the liquid phase (-); D_0^g is the molecular diffusion coefficient in free air and τ_g is tortuosity in the gas phase (-). Tortuosity is calculated within the model based on water and air content in the liquid and gas phase using the relationships derived by Millington and Quirk (1961):

$$\tau_w = \frac{\theta^{\frac{7}{3}}}{\theta_s^2} \tag{2.6}$$

$$\tau_g = \frac{a_v^{\frac{7}{3}}}{\theta_s^2} \tag{2.7}$$

where θ_s is the saturated water content (equivalent to total porosity).

The models are 1D columns which represent the full extent of both the unsaturated and saturated zones at each site, however only transport in the unsaturated zone is of interest here (as ^{14}C activities in groundwater will be influenced by up-gradient processes, and cannot be accurately considered in 1D). The Van Genuchten (1980) model for soil hydraulic properties was used. However as the models are run with steady state flow and water content does not vary with time, the model results are insensitive to the hydraulic model used. The models were finely discretised at the surface (cells of 0.05 m thickness), with increasing cell thickness with depth to a maximum of 0.5 m.

The upper boundary condition for flow was a second type boundary which allows for a specified recharge flux into the model. The upper boundary condition for solutes was a specified concentration boundary. A transient upper concentration boundary condition for CFC-12 was based on atmospheric measurements in the southern hemisphere from 1952-2012 (CSIRO, 2013). A constant upper concentration boundary for the $^{12}CO_2$ and $^{14}CO_2$ models was based on concentrations for a ^{14}C activity of ~108 pMC and a ^{14}C:^{12}C ratio of 1.39×10^{-12} estimated from data in Hua et al. (2013). The activity of 108 pMC was chosen as it appears to be consistent with the uppermost values in the unsaturated zone at our sites (from plant respired CO_2). Although the ^{14}C activity of atmospheric CO_2 has changed over the timescale of our model we do not model this, as Thorstenson et al. (1983) have previously shown that such a transient ^{14}C atmospheric boundary condition does not have a significant influence on the unsaturated zone profile.

The lower boundary for flow was a first type boundary, which was assigned by setting a pressure head boundary (m) at the bottom of the model domain, with an appropriate pressure head value to represent the watertable depth (this establishes the unsaturated/saturated interface). This boundary was made constant so that the position of the watertable does not change with time regardless of recharge fluxes across it. The lower boundary conditions for concentration were set at zero to represent infinite age at the bottom of the profile.

An initial model was run to steady state with zero recharge to establish initial flow conditions, then the CFC model was calibrated (to constrain gas transport parameters). The model for CFC-12 was run for 60 years representing the period over which atmospheric CFCs have been above zero. Diffusion coefficients in free air and water (D_0^w and D_0^g) were based on literature values (Table 2.1). Given that tortuosity is determined within the model and water contents are likely to be low, calibration was achieved manually by altering porosity (which informs the values for a_v and θ_s and hence the effective diffusion coefficients D_g and D_w).

The porosity values determined by the CFC modelling were then used to model $^{12}CO_2$ and $^{14}CO_2$ profiles (with appropriate free air and water diffusion coefficients D_0^w and D_0^g for both species, Table 2.1). Calibration of the CO_2 models was achieved manually by altering production rates in (a) the top 10 m for both $^{12}CO_2$ and $^{14}CO_2$ models – replicating respiration of modern CO_2 by plant roots (based on observations of atmospheric ^{14}C at this depth, and knowledge of the vegetation types in the area (O'Grady et al., 2009)) and (b) in a 2 m thick zone above the watertable for the $^{12}CO_2$ model only, replicating production of CO_2 devoid

of $^{14}CO_2$. The ratio of modelled $^{14}CO_2$:$^{12}CO_2$ was then calculated and compared to our measurements of ^{14}C activity as a final check on the model fit.

Table 2.1: Diffusion and partition coefficients used for models shown in Figure 2.3 (*the same diffusion coefficient in water D_0^w was applied to both $^{12}CO_2$ and $^{14}CO_2$).

Parameter	Value	Reference
CFC-12 diffusion coefficient in air (D_0^g), m^2 y^{-1}	287	(Montfort and Pellegatta, 1991)
CFC-12 diffusion coefficient in water (D_0^w), m^2 y^{-1}	3.41 x 10^{-2}	(Zheng et al., 1998)
CFC-12 partition coefficient (k_g)	0.0718	(Warner and Weiss, 1985)
$^{14}CO_2$ diffusion coefficient in air (D_0^g), m^2 y^{-1}	515	(Walvoord et al., 2005)
$^{12}CO_2$ diffusion coefficient in air (D_0^g), m^2 y^{-1}	520	(Walvoord et al., 2005)
*CO_2 diffusion coefficient in water (D_0^w), m^2 y^{-1}	6.03 x 10^{-2}	(Jahne et al., 1987)
CO_2 partition coefficient (k_g)	0.836	(Weiss, 1974)

A number of scenarios were run in order to further our understanding of unsaturated zone processes and their influence on ^{14}C activity. We modelled profiles with a variety of watertable depths (12 to 100 m) and varied recharge rates from 0 to 500 mm y^{-1}. We also varied the rate and thickness of shallow atmospheric CO_2 production (100 to 10000 mmol m^{-3} y^{-1}) to assess the influence of root respiration and root depth. These rates of CO_2 production correspond to rates of soil respiration of 0.3 to 32 mol m^{-2} y^{-1}, which equate to carbon fluxes of 3.6 to 384 g C m^{-2} y^{-1}. This covers the range for arid areas reported by Raich and Schlesinger (1992) of 60 to 224 g C m^{-2} y^{-1} (based on limited measurements). Rates of deep 'old' CO_2 production were also varied (0 to 500 mmol m^{-3} y^{-1}). There are few reported rates of shallow/deep CO_2 production in the literature that pertain to this problem. Keller and Bacon (1998) and Walvoord et al. (2005) give deep production rates of 47 and 100 mmol m^{-3} y^{-1} respectively, hence our scenarios cover this range.

2.5 Results - field data

Figure 2.2 shows measured concentrations of ^{14}C (pMC) CFC-12 (pptv), CO_2 (percent by volume) and $\delta^{13}C$ (‰) in unsaturated zone gas at each site. ^{14}C activities in groundwater sampled below these profiles (generally within 2 to 6 m of the watertable, however at Site D the groundwater sample is from 18 m below the watertable) are also shown in Figure 2.2. Measurement errors are not shown as they are generally very low ($\pm$ 5% for CFCs and CO_2, $\pm$ <1% for ^{14}C). ^{14}C activities are generally modern (>100 pMC) within the top 11 m of each profile and decline relatively uniformly with depth, with variable watertable depths leading to varying ^{14}C activities directly above the watertable. The exception is Site C which shows a sharp decline in ^{14}C activity to 54 pMC in a shallower profile than Site A and B. The shallowest site (E) shows modern ^{14}C throughout the profile to a depth of 8.2 m.

The modern ^{14}C activity and high CO_2 in the top 11 m of each profile suggests a modern source of CO_2 is present. The most likely source of this modern CO_2 is plant root respiration rather than the oxidation of organic matter, as a significant amount of modern organic matter is unlikely to be present at depths up to 11 m in this arid setting (Trumbore, 1993). Also the presence of tree roots to depths of 11 m in this type of environment is not unrealistic (O'Grady et al., 2009), and the $\delta^{13}C$ results fall in a relatively narrow range

of -13.5 to -16.8 ‰, which is around the values that would be expected from respiration from spinifex grass (~ -14 ‰, Cook and Dawes-Gromadzki (2005)).

The similarity in declines of ^{14}C activity with depth at Sites A, B and D suggest that the mechanisms responsible for ^{14}C dilution are relatively consistent throughout the study area. We have not investigated the mechanism for this dilution in great detail, however the presence of soft and cemented calcrete above and below the watertable at our sites suggests the source of 'old' CO_2 is similar to that identified by Walvoord et al. (2005). That is, precipitation of calcite at the watertable (in the case of Walvoord et al. (2005) promoted by a slowly declining watertable) releases old CO_2 via:

$$Ca^{2+}_{(aq)} + 2HCO^{-}_{3(aq)} \longleftrightarrow CO_{2(g)} + H_2O_{(l)} + CaCO_{3(s)} \tag{2.8}$$

At Site C, ^{14}C appears more depleted and the trend with depth is different to the other sites. Drilling logs from this site revealed significantly more calcrete in the profile, commencing at 6m depth (13 m above the watertable). This calcrete may act as a source of old CO_2 through active dissolution-precipitation reactions in this shallower part of the profile, with precipitation (and release of CO_2) possibly driven by evapotranspiration of shallow soil water (Dever et al., 1987). However understanding the physical drivers for calcite precipitation at our site would require further work and was beyond the scope of this study.

CFC-12 concentrations are close to current atmospheric concentrations (~525 pptv, CSIRO (2013)) in the upper parts of the profiles and then decrease with depth towards the watertable, consistent with existing theory on CFC transport in the unsaturated zone (Cook and Solomon, 1995). The CFC-12 concentrations at the bottom of the profiles represent apparent lag times (time taken for diffusive transport from the surface to the base of the profile) of 35 years for Site A (depth to water of 31.5 m), 25 years for Site B and D (watertable depths of 25.8 m and 20.6 m respectively) and 18 years for Site E (depth to water of 8.2 m). CO_2 concentrations are much higher (up to 60 times higher) than atmospheric concentrations (~393 ppm at the time of the study, CSIRO (2013)) and generally increase with depth. Concentrations are highest at site Site D from 10 to 15 m depth before declining towards the watertable. We cannot explain this decline in terms of any physical process and hence it is likely the low concentration near the watertable represents contamination from loss to the atmosphere either in sampling, sample transport or analysis. ^{14}C samples do not appear to show any contamination though, and the trend of declining activity is present.

2.6 Results - modelling of field data

Figure 2.3 shows modelling results from the deepest profile (Site A). Porosity, $^{12}CO_2$ and $^{14}CO_2$ production rates that provided the best model fit, as well as other model parameters are given in Table 2.2. The best fit to CFC-12 data was obtained with a porosity of 0.4 in the top 10 m of the profile, and 0.2 from 10 m to the watertable. The higher porosity (and hence higher effective diffusion coefficient) required in the

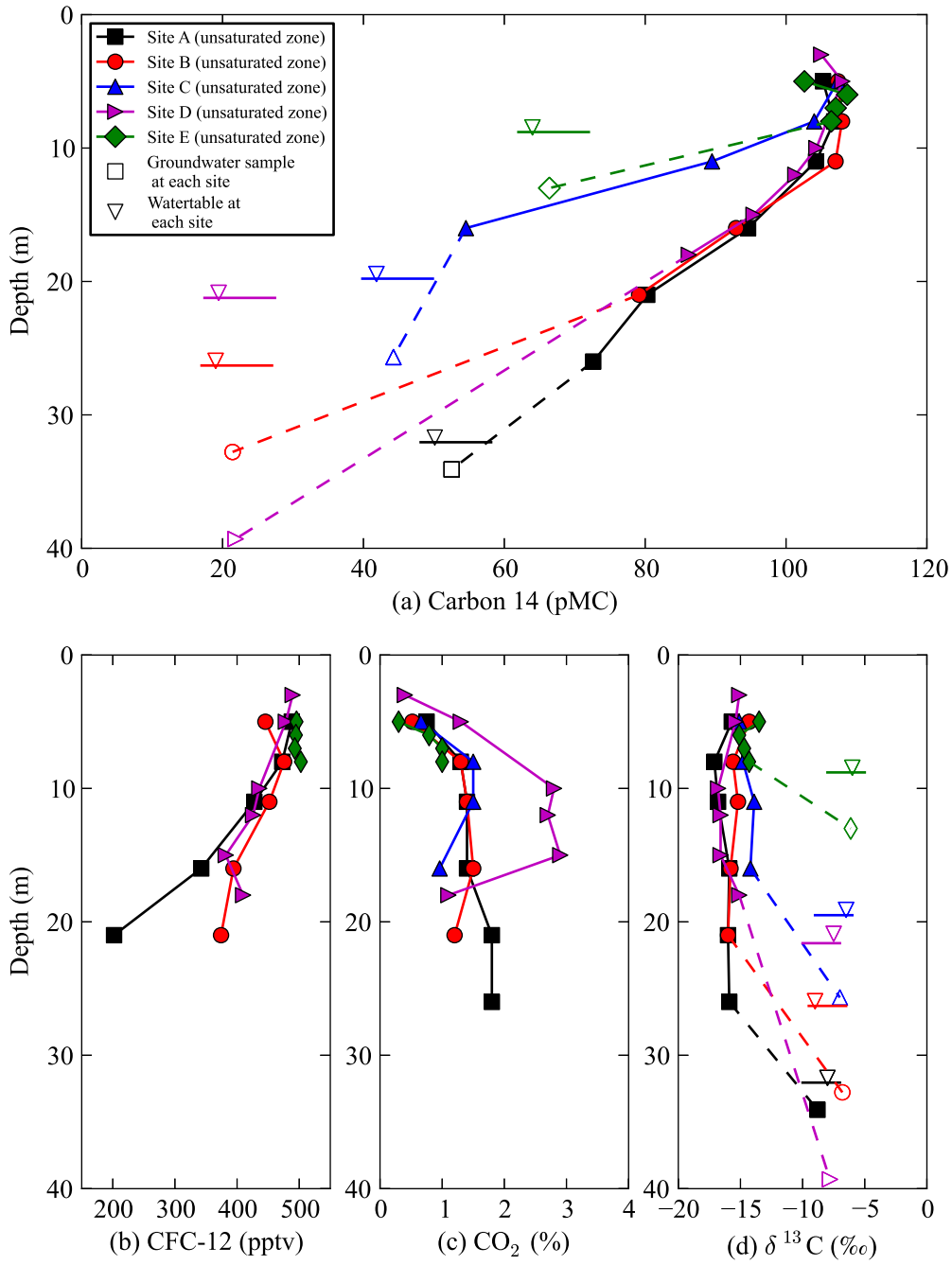

Figure 2.2: Measured concentrations of (a) ^{14}C, (b) CFC-12, (c) CO_2 and (d) δ^{13}C in unsaturated zone gas in the Ti Tree Basin. ^{14}C activities and δ^{13}C contents in groundwater beneath these profiles are also shown.

upper layers of the model may have several causes other than changes in soil texture, such as the presence of root channels and animal burrows. This also captures likely higher rates of effective gas diffusivity in the shallow unsaturated zone which may be driven by barometric pumping (Weeks et al., 1982). Since HYDRUS relates tortuosity to water and air content (equations 2.6 and 2.7), changing porosity is the only way to change the effective diffusion coefficients (equations 2.4 and 2.5) to accurately simulate the CFC

transport. The best fit to carbon isotope profiles at Site A was achieved with $^{12}CO_2$ production rates of 863 mmol m^{-3} y^{-1} in the upper 10 m (accompanied by $^{14}CO_2$ production of 1.2 x 10^{-9} mmol $m^{-3}y^{-1}$ based on the atmospheric ratio) and 290 mmol m^{-3} y^{-1} in a 2 m thick zone above the watertable (with no accompanying $^{14}CO_2$ production). $^{12}CO_2$ flux out of the top of the calibrated model (i.e. modelled soil respiration) was ~3 mol m^{-2} y^{-1}.

All other sites were likewise modelled and Figure 2.4 shows the calibrated ^{14}C (pMC) profiles. The goodness of fit varies but the profiles are mostly well matched, with the decrease in ^{14}C activity replicated in the models. Shallow production rates (0 to 10 m) varied from 600 to 1500 mmol m^{-3} y^{-1}, while deep production rates varied from 290 to 450 mmol m^{-3} y^{-1} (in a 2 m thick zone above the watertable), reflecting the range in CO_2 concentrations observed (Figure 2.2(c)). The shallowest profile (8.2 m depth) was modelled without a deep source of old CO_2 as measured $^{14}CO_2$ activity was modern for the entire profile suggesting no significant source of old CO_2. Soil respiration rates, determined from the model as the concentration flux out of the top boundary of the soil profile, ranged from 0.9 – 3.3 mol m^{-2} y^{-1} (Table 2.2 summarises this information for each profile). Our modelled soil respiration rates are relatively low compared with carbon flux values measured by eddy covariance (EC) towers in the Ti Tree Basin (up to 59 mol m^{-2} y^{-1}, Cleverly et al. (2013)). However these measurements include CO_2 flux from vegetative respiration and photodegradation of organic matter, which Cleverly et al. (2013) cite as much larger sources of CO_2 flux than soil respiration. Our values of soil respiration do however compare well with modelled values from both Keller and Bacon (1998) and Walvoord et al. (2005) of 2.9 mol m^{-2} y^{-1} and 3 mol m^{-2} y^{-1} respectively.

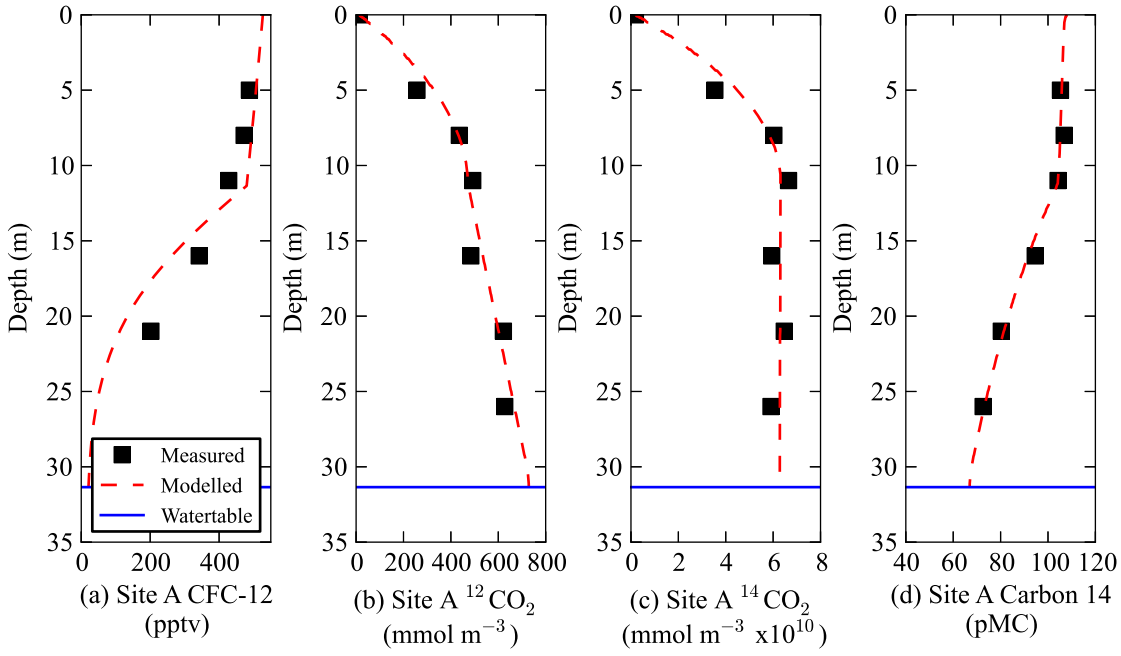

Figure 2.3: Measured and modelled concentrations of unsaturated zone CFC-12, $^{12}CO_2$, $^{14}CO_2$ and ^{14}C activity (as pMC) for Site A.

Table 2.2: Summary of CO_2 production rates and porosity values used to calibrate each model.

Site	Site A	Site B	Site C	Site D	Site E
Piezometer registration number (RN)	18611	18779	18781	18893	18897
Depth to water (m-bgl)	31.5	25.8	19.1	20.6	8.2
Shallow $^{12}CO_2$ production rate (mmol m^{-3} y^{-1})	863	1007	863	1500	600
Deep $^{12}CO_2$ production rate (mmol m^{-3} y^{-1})	290	300	400	450	-
Modelled soil respiration rate (mol m^{-2} y^{-1})	2.8	3.3	1.7	3.9	0.9
Porosity	0 to 10m: 0.4 10 to 31.5m : 0.2	0 to 10m: 0.4 10 to 23m: 0.35 23 to 25.8m: 0.2	0 to 10m: 0.35 10 to 19.1m: 0.2	0 to 10m: 0.33 10 to 15m: 0.27 15 to 20.6m: 0.38	0 to 5m: 0.28 5 to 8.2m: 0.35

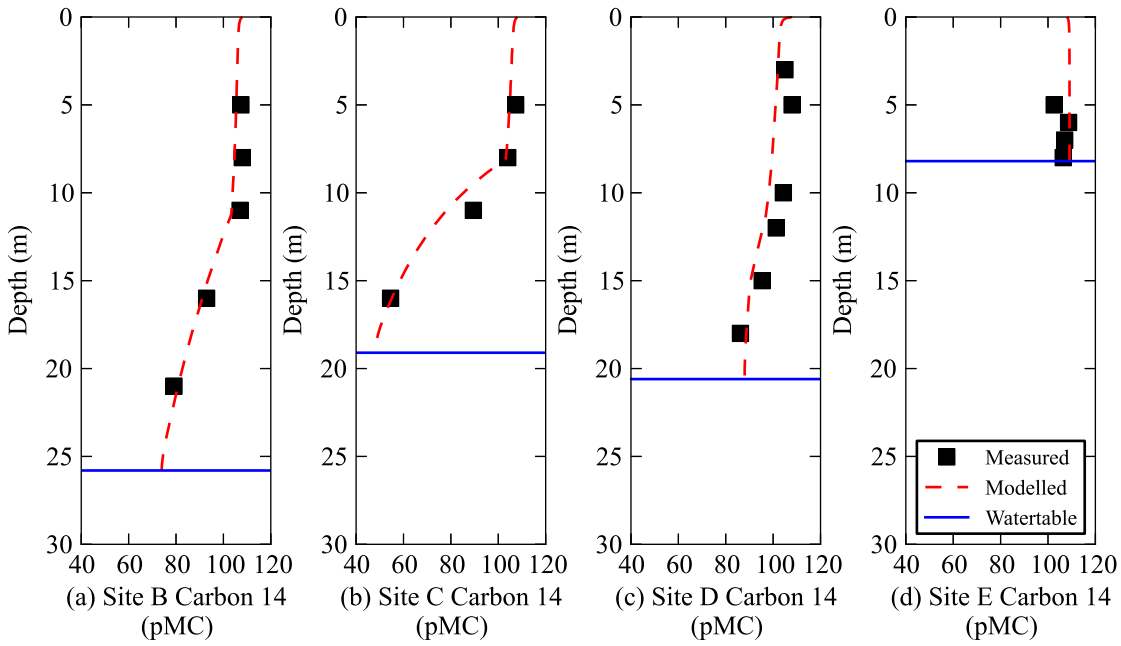

Figure 2.4: Calibrated unsaturated zone ^{14}C (pMC) models for all other profiles.

2.7 Results - sensitivity analysis

The purpose of the scenario modelling was to assess the sensitivity of ^{14}C activity in the unsaturated zone to changes in the calibrated parameters (shallow and deep production rate and thickness of production zones) as well as the influence of watertable depth and recharge rate. Figure 2.5 shows the influence of different $^{12}CO_2$ and $^{14}CO_2$ production rates and production zone thicknesses on the modelled ^{14}C (i.e. the ratio of modelled $^{14}CO_2$ to modelled $^{12}CO_2$) for Site A. Low rates of shallow atmospheric CO_2 production result in greater dilution of ^{14}C with depth (2.5(a)) as there is less 'modern' CO_2 in the profile to buffer against the production of 'old' CO_2. Similarly, lower rates of deep 'old' CO_2 production result in less dilution of ^{14}C and activities are higher with depth (2.5(b)), consistent with the sensitivity modelling performed by Walvoord et al. (2005).

The thickness of the deep production zone is relatively unimportant, so long as the total CO_2 production rate is the same. However the same cannot be said for the thickness of the shallow zone of modern CO_2 production. Panel (2.5(d)) shows that shallower zones of modern CO_2 production (with the same total amount of soil respiration) result in greater dilution of ^{14}C above the watertable. This is because with a smaller zone of modern CO_2 production there is less ^{14}C present with depth, and the profile becomes dominated by upward diffusion of the deep, older $^{12}CO_2$ (diluting the ^{14}C activity). A greater amount of modern CO_2 needs to be produced when the root zone is shallower in order to avoid this dilution. For example, modelling Site A with a 5 m thick root zone meant a $^{12}CO_2$ production rate of 10,000 mmol m^{-3} y^{-1} (i.e. ten times greater than that used in the calibrated model with a 10 m thick root zone) was needed to produce the same profile of dilution of ^{14}C. This however resulted in $^{12}CO_2$ and $^{14}CO_2$ models that show concentrations that are much higher than measured values in the top 5 m. It should be noted that in Panel

(2.5(d)), the higher porosity (0.4) is maintained in the top 10 m for all scenarios except where the root zone is extended to 15 m - here the porosity is also higher to 15 m. This explains the inflection point in the graph seen at 15 m.

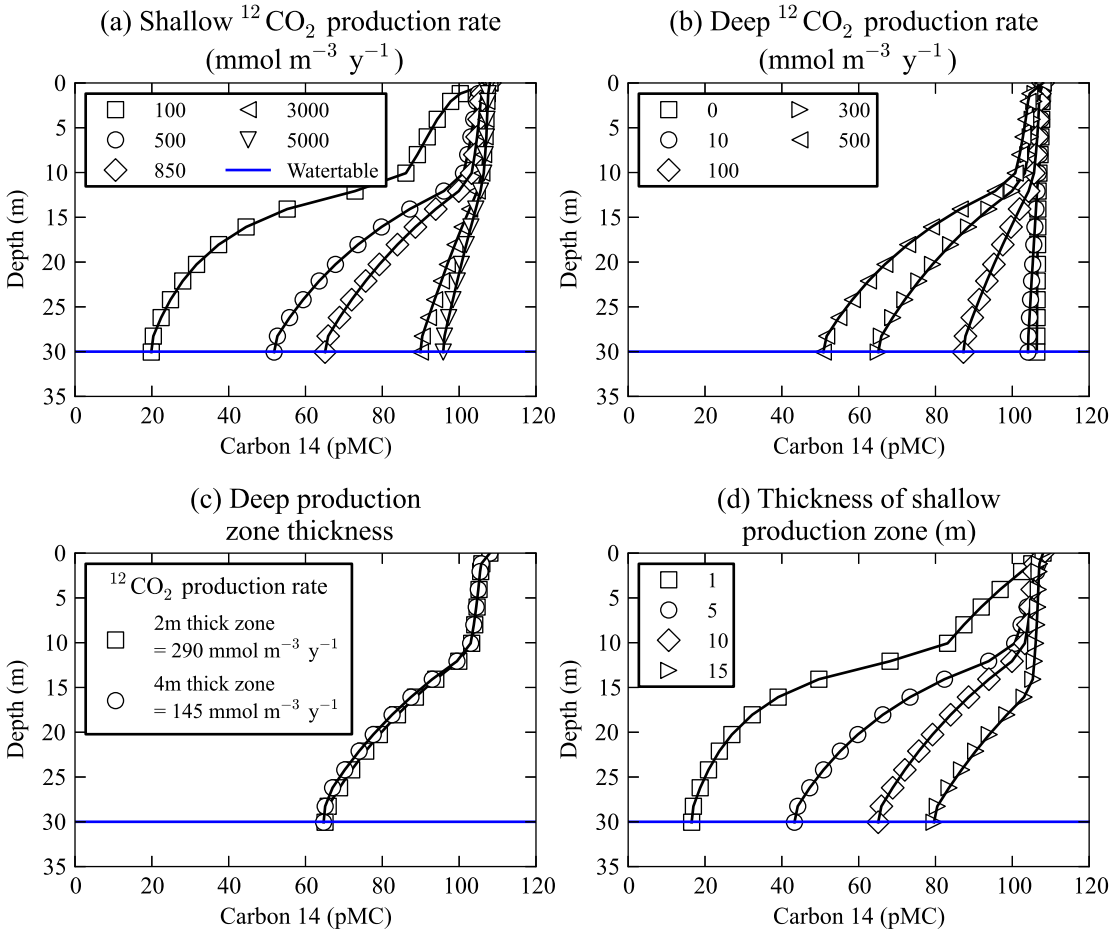

Figure 2.5: Influence of (a) shallow and (b) deep rate of $^{12}CO_2$ production for Site A. Panel (c) shows that the thickness of the zone of deep CO_2 production is relatively unimportant so long as bulk CO_2 production is the same however panel (d) shows that the thickness of the shallow production zone is important.

Figure 2.6 shows the influence of recharge (2.6(a)), shallow CO_2 production (2.6(b)), deep CO_2 production (2.6(c)) and root depth (2.6(d)) on the ^{14}C activity of unsaturated zone gas above the watertable for various watertable depths. In all these scenarios, parameters are held constant at the values used to calibrate Site A (Figure 2.3; Table 2.2) except for those parameters being tested as shown in each panel. The first apparent conclusion is that when watertables are deeper there is more depletion of ^{14}C with depth for nearly all scenarios considered. This is consistent with our field measurements which showed similar trends in ^{14}C activity with depth, but varying activities at the watertable as dictated by the variation in watertable depth.

Figure 2.6(a) shows that when recharge is low (1 to 10 mm y^{-1}), there is no significant change in ^{14}C above the watertable. As recharge increases there is less dilution of ^{14}C activity above the watertable (because there is more advective transport of $^{14}CO_2$ downwards), however this effect is most significant when the watertable is deeper. For example for recharge rates of 1 to 100 mm y^{-1}, the ^{14}C activity of gas above the watertable varies from 22 – 45 pMC when the depth to water is 100 m, but only varies from 51 to 62 pMC

when the depth to water is 40 m. When recharge is very high (>300 mm y^{-1}) there is less dilution of ^{14}C, with values generally > 80 pMC.

The influence of shallow 'modern' CO_2 production on ^{14}C activity of unsaturated zone gas above the watertable can be seen in Figure 2.6(b). As with the model for site Site A, modern CO_2 production is limited to the top 10 m of the unsaturated zone, deep production is limited to a 2 m thick zone above the watertable (with the deep production rate kept constant at 290 mmol m^{-3} y^{-1} for each scenario) and recharge is 0 mm y^{-1}.

Figure 2.6(c) shows the modelled influence of deep $^{12}CO_2$ production. Shallow $^{12}CO_2$ and $^{14}CO_2$ production is kept constant and recharge is 0 mm y^{-1}. Greater rates of deep $^{12}CO_2$ production result in greater dilution of ^{14}C. When there is no deep CO_2 production however, there is no significant dilution of ^{14}C above the watertable, even when the depth to water is 100 m. Figure 2.6(d) shows that the thickness of the zone of shallow 'modern' CO_2 production is significant in influencing the ^{14}C activity of unsaturated zone gas. As discussed earlier this is because the production of deep 'old' CO_2 starts to dominate the profile when 'modern' CO_2 is closer to the surface (and diffuses out more rapidly).

2.8 Discussion

Both our data and our model support the hypothesis that ^{14}C in unsaturated zone gas above the watertable is controlled primarily by stratified production of CO_2 from isotopically different sources. This is consistent with previous work on unsaturated zone ^{14}C measurements (Keller and Bacon, 1998; Walvoord et al., 2005). Our results extend these earlier findings to show that these processes can be relatively consistent across large areas in a groundwater basin, but that variation in watertable depth may lead to spatial variability in the ^{14}C activity of unsaturated zone gas directly above the watertable.

The scenario modelling in this study helps elucidate the conditions under which depletion of unsaturated zone ^{14}C may become significant for ^{14}C dating of groundwater. We find that depletion of ^{14}C may be more significant where watertables are deeper (>10 m). The degree to which ^{14}C is depleted above the watertable is not affected by low rates of recharge (0 to 10 mm y^{-1}). However it is sensitive to both the shallow CO_2 production rate and the thickness of this production zone (root zone thickness), with lower rates of shallow CO_2 production ($^{12}CO_2$ and $^{14}CO_2$) leading to greater depletion. This helps explain some of the different profiles seen in previous studies. For example Leaney and Allison (1986) observe high ^{14}C activity (>90 pMC) to depths of 35 m in the unsaturated zone in an area where mallee vegetation is known to be very deep rooted (roots extending to 15 to 20 m depth, (Cook et al., 1989)). However Keller and Bacon (1998) observe significant dilution of ^{14}C in a 7 m deep profile, where the root zone is only 1 m thick. Higher rates of deep 'old' CO_2 production ($^{12}CO_2$ only) likewise lead to greater depletion. Recharge is generally lower and more sporadic in arid areas (Scanlon et al., 2006), which suggests that the dilution of ^{14}C activity in unsaturated zone CO_2 may be more of a problem in arid areas, and most previous studies

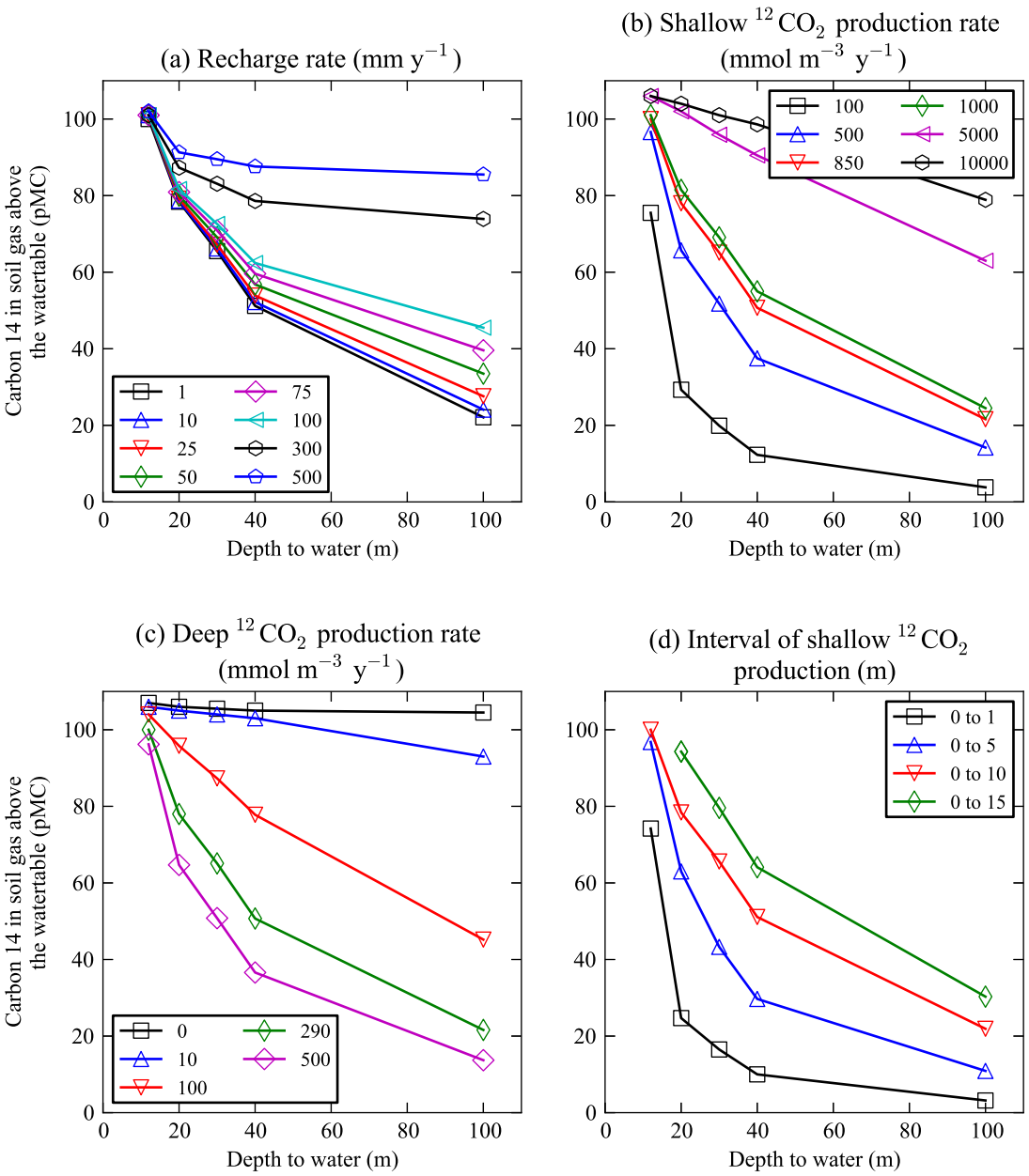

Figure 2.6: Modelled results from HYDRUS showing the influence of (a) recharge rate, (b) shallow CO_2 production, (c) deep CO_2 production and (d) the depth of the shallow CO_2 production zone (i.e. depth of root zone) on calculated ^{14}C activity (pMC) of unsaturated zone gas directly above the watertable (for DTW 12 to 100 m).

of unsaturated zone ^{14}C come from arid areas. However the root depth of vegetation in arid areas may be significant (>20 m, Canadell et al., 1996) which would potentially limit the amount of dilution as Figure 2.6(d) shows, presuming such deep roots are respiring atmospheric CO_2. Therefore determining if there is dilution of ^{14}C in unsaturated zones on a site by site basis would require a broad understanding of the local hydrogeology (recharge rates) and ecology (rooting depth). Variations in soil type will also become important, with lower porosity soils having lower diffusion coefficients, hence potentially more depletion of ^{14}C activity at depth, however we have not assessed this in our sensitivity analysis. Nevertheless, for

general purposes when watertables are deep, recharge is moderate to low and vegetation rooting does not extend to the watertable, ^{14}C in the unsaturated zone may be significantly diluted if a source of old CO_2 is present. The presence of organic matter or minerals within the aquifer such as calcite should also act as an indicator as to when unsaturated zone ^{14}C may be diluted.

Our model assumes steady state flow and production, however both recharge and root respiration will vary temporally. However previous studies have shown that transient variation in shallow unsaturated zone CO_2 does not necessarily influence variations in ^{14}C, and that ^{14}C activities of unsaturated zone CO_2 are controlled by other processes such as the ones considered in this paper (Thorstenson et al., 1983; Bacon and Keller, 1998). Episodic recharge, driven by rare and extreme rainfall events, is likely to be an important recharge mechanism in Ti Tree. Hydrographs from some bores in the Basin show sporadic sharp rises in water level, indicating episodic recharge has occurred at least five times in the last 50 years, with the last event in the year 2000 (Knapton, 2009). However this does not seem to have affected CFC profiles, with apparent gas ages of up to 35 years (i.e. equivalent of atmospheric concentrations in 1976) at depth, suggesting episodic recharge events of the magnitude observed in Ti Tree do not flush the unsaturated zone or perturb the unsaturated zone gas profiles significantly.

We did not measure the isotopic content of sedimentary organic carbon in our profiles which limits the interpretation of causes of CO_2 production in the unsaturated zone. However the assumption that production of CO_2 in the top 10 m at our site is from root respiration with a modern ^{14}C signature is likely given what is known about rooting depth of vegetation such as spinifex (Reid et al., 2008). We treat this root respiration in our model as being uniform with depth based on our CO_2 and ^{14}C measurements, however this assumption may not carry to all environments. We have not investigated organic carbon processes thoroughly as it was beyond the scope of this study, however other studies are furthering this work (Meredith et al., 2013). Likewise our understanding of the source of deep 'old' CO_2 is limited. Two mechanisms of deep CO_2 production in the unsaturated zone that have been put forward in the literature are oxidation of organic matter (Keller and Bacon, 1998), and calcite precipitation (Walvoord et al., 2005). Given the absence of any significant organic matter in the lithology in Ti Tree and the presence of calcrete layers, we postulate that calcite precipitation is a source of old CO_2 in our case. However the mechanisms behind this are poorly understand, and it is not clear whether a slowly declining watertable is a pre-condition for calcite precipitation (Walvoord et al., 2005) or whether precipitation is independent of this. More work is needed to better understand the mechanisms for deep CO_2 production in different situations and settings. Further studies and measurement of unsaturated zone ^{14}C activity in different settings would benefit not only interpretation of groundwater age, but also understanding of these CO_2 production mechanisms.

2.9 Conclusion

Depletion of ^{14}C in unsaturated zone gas is a common occurrence based on the limited amount of published measurements available worldwide. This casts doubt on the typical assumption in ^{14}C dating of groundwater

that unsaturated zone gas is in equilibrium with the atmosphere. Our measurements of unsaturated zone ^{14}C activity in the Ti Tree Basin support this finding for watertable depths >10 m. We have modelled depletion of ^{14}C in unsaturated zone gas with a shallow and deep source of CO_2 production from sources that have isotopically different signatures. We find that the processes controlling ^{14}C dilution in the unsaturated zone are relatively consistent over a large spatial area (distances of 35 km between sites), and that variation in watertable depth over this scale leads to spatial variation in ^{14}C activities directly above the watertable. It appears from our sensitivity analysis that the problem of ^{14}C dilution in the unsaturated zone may be more pronounced in arid settings (where recharge rates are lower), however further work is required to better understand the mechanisms of deep, old CO_2 production.

These findings improve our understanding of how unsaturated zone processes affect the spatial variation in ^{14}C activities directly above the watertable, with unsaturated zone depth being a key influence. This gives improved guidance as to when depletion of unsaturated zone ^{14}C becomes significant, which will be of great benefit for future researches looking to accurately determine groundwater ages from ^{14}C measurements.

Acknowledgments

Funding for carbon isotope analysis of unsaturated zone gas was provided by AINSE (Grant 12/042) under the Isotopes for Water project. Additional funding was provided by the Australian Research Council and the National Water Commission. The authors wish to thank the staff at the Institute for Environmental Research at ANSTO for their help (and their patience) in preparing the soil gas samples for analysis. Dr. Vladimir Levchenko (ANSTO) is also thanked for helpful discussions on atmospheric ^{14}C activities and ^{14}C:^{12}C ratios. The Northern Territory Government and Bob Read are thanked for drilling and piezometer and soil gas sampler installation. Dr. Brian Smerdon and Stan Smith from CSIRO are thanked for early reviews of the manuscript. We additionally thank Assistant Professor Christophe Darnault, Dr. Michelle Walvoord, and five anonymous reviewers for providing helpful comments on the manuscript.

Monitoring bore RN18611 (Site A)

3 Vertical carbon-14 profiles for resolving spatial variability in recharge in arid environments

Based on the publication: Wood, C., P.G. Cook, G. A. Harrington, 2015: Vertical carbon-14 profiles for resolving spatial variability in recharge in arid environments. *J. Hydrol.*, **520**, 134-142, doi:10.1016/j.jhydrol.2014.11.044

Abstract

Groundwater age tracers are often measured to help constrain estimates of groundwater recharge, especially in arid environments where other methods are unsuitable. However multiple processes can influence the shape of vertical tracer profiles in an aquifer including (1) variation in tracer input concentrations from the unsaturated zone, (2) the role of diffusion in transporting tracer into the aquifer when fluxes are low and (3) spatial variability in recharge. This study demonstrates the influence of spatially variable recharge and spatially variable carbon-14 (^{14}C) activities in the unsaturated zone on vertical ^{14}C profiles in groundwater. Through groundwater flow and solute transport modelling, we demonstrate that recharge estimated from single point measurements of ^{14}C may be wrong more than an order of magnitude when unsaturated zone ^{14}C activities and recharge vary spatially. We then present a case study from the Ti Tree Basin in arid central Australia, where detailed profiles of ^{14}C activity in unsaturated zone gas and groundwater have been measured, and spatial variability in unsaturated zone ^{14}C is observed (ranging from 54 to 106 pMC above the watertable). Through modelling our data, we show that when unsaturated zone ^{14}C activities are known, measurement of the ^{14}C profile can help constrain estimates of recharge and its spatial variability. This approach improves our understanding of groundwater flow in the Ti Tree Basin, by showing mountain front recharge to be an important mechanism.

3.1 Introduction

Environmental tracers have been widely used to estimate groundwater age and residence time, and can potentially provide more accurate estimates of recharge and flow velocity than traditional hydraulic methods (Cook and Bohlke, 2000). Vertical profiles of groundwater age can be especially useful as indicators of spatial variability in groundwater recharge. For example, Robertson and Cherry (1989) measured vertical profiles of groundwater age using tritium in an aquifer in Ontario. They found that the depth at which 'bomb-peak' tritium was measured in the aquifer varied spatially, and used this to infer spatial variability in groundwater recharge.

In arid environments low recharge rates lead to longer residence times and tracers that can provide estimates of age over longer time scales are needed. Carbon-14 (^{14}C) dating of total dissolved inorganic carbon (TDIC) in groundwater can provide estimates of age over time scales of ~10^2 to 10^4 years, making ^{14}C useful for estimating recharge in arid zones (Herczeg and Leaney, 2011). For example Harrington et al. (2002) measured ^{14}C activities in groundwater in the Ti Tree Basin in arid central Australia. Harrington

et al. (2002) used an analytical approach to demonstrate that recharge varied spatially, with many of the higher recharge rates lying on flow lines originating near ephemeral surface water features that are subject to flooding after rare, high intensity rainfall events. Carbon-14 may additionally be used to help calibrate groundwater flow models in arid and semi-arid environments (Sanford, 2011).

Many factors can complicate the interpretation of ^{14}C in aquifers. For example, carbonate mineral weathering can dilute the ^{14}C activity of groundwater compared to that of the atmosphere (Fontes and Garnier, 1979). In low recharge environments, diffusion and dispersion can significantly enhance transport of ^{14}C in the aquifer, and this may influence the assessment of groundwater fluxes (Walker and Cook, 1991; Castro and Goblet, 2005). Production of 'old' (low ^{14}C) CO_2 from oxidation of organic matter or calcite precipitation in the unsaturated zone may significantly reduce the ^{14}C activity of soil CO_2 (Keller and Bacon, 1998; Walvoord et al., 2005; Gillon et al., 2009), which influences the ^{14}C activity of infiltrating groundwater. This may lead to misinterpretation of ^{14}C activities when estimating groundwater age (Bacon and Keller, 1998). Wood et al. (2014) showed how variation in watertable depth may lead to spatial variation in ^{14}C activities above the watertable (i.e. ^{14}C activity that recharging water would equilibrate with) when a source of old CO_2 is present in the unsaturated zone. In this regard estimates of groundwater age from ^{14}C may differ significantly from estimates provided by other methods (e.g. estimates of age provided by other environmental tracers or advective ages determined by groundwater modelling).

While previous studies have considered these processes (diffusion, dispersion, production of old CO_2 in the unsaturated zone) and their influence on ^{14}C activities in groundwater separately (Walker and Cook, 1991; Castro and Goblet, 2005; Bacon and Keller, 1998), their potential combined effects, along with spatial variability in recharge on groundwater age profiles have not been assessed. The aim of this study is to investigate the influence of spatially variable ^{14}C activities at the watertable and spatially variable recharge on vertical ^{14}C profiles in an unconfined aquifer, firstly in a theoretical study, then secondly using a field example. We focus on low recharge environments where diffusion and dispersion are also significant. Through theoretical modelling we show how estimated ^{14}C age profiles under different recharge and ^{14}C input (^{14}C activity at the watertable) scenarios compare with those determined from particle tracking (i.e. advective ages, which are not influenced by diffusion and dispersion). We then use measured ^{14}C profiles from an unconfined aquifer in arid central Australia (Ti Tree Basin), and measurements of unsaturated zone ^{14}C activity, along with groundwater flow and solute transport modelling to inform the likely magnitude and spatial variability of recharge along three inferred flow lines.

3.2 Theoretical modelling

3.2.1 Methods

To evaluate the influence of spatial variability in recharge and ^{14}C input on ^{14}C derived age profiles, we present four scenarios using a 2D transect model constructed using the MODFLOW-2005 code. MOD-

FLOW is a widely used code which solves the partial differential groundwater flow equation using a finite differencing approach (Harbaugh, 2005). The model represents an unconfined aquifer 50 km long and 65 m deep based approximately upon the length and thickness of the unconfined aquifer in the Ti Tree Basin, Northern Territory, Australia. The domain is discretised into cells approximately 250 m long and 0.5 m thick. The left hand boundary and bottom boundary are no-flow boundaries, while the right-hand boundary is a constant head boundary set to maintain saturated thickness at 65 m. Relevant model parameters (hydraulic conductivity, porosity) are listed in Table 3.1. Recharge rates used for individual scenarios are discussed later.

Table 3.1: Model parameters used in simulations where * are based on values in Gelhar et al. (1992) for the aquifer scale modelled; ** are from Browne and Firestone (1999); *** is from Li and Gregory (1974).

Parameter	Value
Horizontal hydraulic conductivity ($K_{x,y}$)	100 m d^{-1}
Vertical hydraulic conductivity (K_z)	10 m d^{-1}
Porosity	0.2
Longitudinal dispersivity*	100 m
Transverse dispersivity*	10 m
^{14}C decay constant**	1.21 x 10^{-4} y^{-1}
^{14}C diffusion coefficient in water***	3.15 x 10^{-2} m^2 y^{-1}

Carbon-14 transport was simulated using MT3D, which couples the groundwater flow model with the advection-dispersion/diffusion equation to simulate solute transport (Zheng, 2010). The unsaturated zone was not modelled in this exercise. Rather diffusion of ^{14}C into the aquifer from the unsaturated zone is considered by assigning a concentration boundary at the watertable (which varies spatially in scenarios three and four). Parameters for diffusion, dispersion and radioactive decay are given in Table 3.1. We ignore the potential influence of geochemical reactions on ^{14}C dilution in order to assess the influence of ^{14}C input activity and spatial variability in recharge in isolation of any other complicating factors (eg. carbonate weathering).

Advective ages were modelled using the post processing particle tracking code MODPATH (Pollock, 2012), with particles being assigned to the cells where recharge is applied. This method of modelling groundwater age ignores the role of diffusion and dispersion which the solute transport model takes into account. The particles were 'forward tracked' so that the time taken to reach a particular cell of interest (i.e. a cell where age is calculated from ^{14}C concentrations) could be determined. These ages were compared with apparent ^{14}C ages, calculated from simulated ^{14}C activities using the equation:

$$t = \frac{1}{\lambda} ln \left(\frac{A_0}{A} \right) \tag{3.1}$$

where t represents age (time since recharge in years), A_0 is the initial activity (100 pMC for this exercise), A is the activity simulated in a particular model cell and λ is the decay constant for ^{14}C (Table 3.1).

Recharge rates are often estimated from measurements of groundwater age using simplified analytical solutions (Cook and Bohlke, 2000). Vogel (1967) presents such a solution, which describes the vertical age

profile in an unconfined aquifer of constant thickness and porosity for a given recharge rate. This method can be used to estimate recharge in unconfined aquifers via:

$$R = \frac{H\theta}{t} ln\left(\frac{H}{H-z}\right) \tag{3.2}$$

where R is the average recharge rate over the interval between where the groundwater was recharged and the sampling location, θ is porosity, H is the aquifer thickness and z is the depth at which groundwater age (t) is measured. Here we compare our modelled recharge rates with those that would be calculated based on application of equation (3.2) to individual points (discrete depths).

Four scenarios were considered in the modelling. In Scenario 1 a recharge rate of 1 mm y^{-1} was applied across the entire top of the model domain, representing low diffuse recharge in an arid environment. The ^{14}C input activity is 100 pMC (approximating the atmospheric value). Scenario 2 considers all the recharge to be focused in a small area at the start of the transect, representing preferential recharge or 'mountain front recharge' at an aquifer margin. Mountain front recharge may be a significant source of recharge in arid and semi-arid climates. It can occur if a basin has an uplifted boundary (eg. a mountain), and large rainfall events in the uplifted area generate runoff that can lead to focused recharge at the mountain front (the basin margin) (Wilson and Guan, 2004). The ^{14}C input activity was again 100 pMC across the whole model domain.

Focused recharge at the aquifer margin was applied in Scenario 3 but in this case the ^{14}C activity at the watertable varies spatially from 50 pMC to 100 pMC. Wood et al. (2014) measured unsaturated zone ^{14}C activities at multiple sites in the Ti Tree Basin in central Australia, and found consistent trends in ^{14}C dilution at most sites, with variation in unsaturated zone thickness leading to variation in ^{14}C activities at the watertable (lower ^{14}C when the unsaturated zone is thicker, data is presented later in section 3.3). The transition from low to high ^{14}C activity at the watertable across the transect thus replicates what would be observed if unsaturated zone thickness were to vary from deep to shallow (again, the unsaturated zone was not modelled in the transect models). Such variation may be observed in groundwater basins with variable surface topography and flow towards a surface discharge area.

Scenario 4 considers focused recharge at the aquifer margin, spatially variable ^{14}C input activities, but also includes a low amount of recharge further along the transect. Recharge rates and ^{14}C input activities for all scenarios are outlined in Figure 3.1.

3.2.2 Results

For Scenario 1 (Figure 3.1), recharge rate and ^{14}C input are spatially constant, which means the ^{14}C profiles are similar along the transect. Estimated recharge rates (from equation (3.2)) are nearly double the modelled recharge close to the watertable. This is because of diffusion of ^{14}C into the aquifer at this low recharge rate,

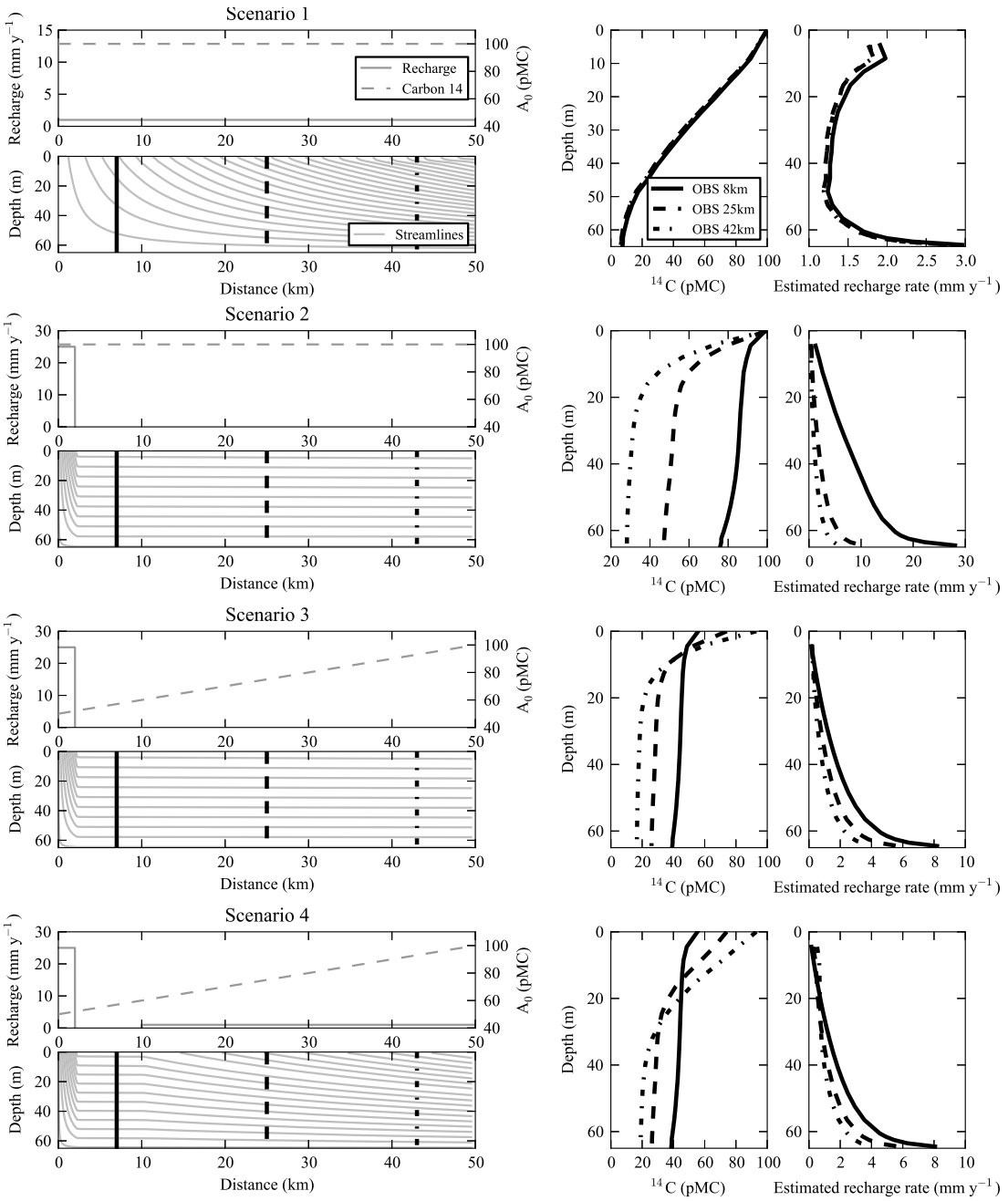

Figure 3.1: Theoretical scenarios 1 to 4 showing the recharge and ^{14}C activity at the watertable, the resulting streamlines, ^{14}C activities with depth and recharge rates estimated using equation (3.2) based on simulated ^{14}C activities at observation points at 8 km, 25 km and 42 km along the transect. In Scenario 1 recharge and ^{14}C are spatially constant (at 1mm y^{-1} and 100 pMC respectively); in Scenario 2 recharge occurs exclusively at the basin margin (at 25 mm y^{-1} between 0 and 2 km); in Scenario 3 recharge occurs exclusively at the basin margin (at 25 mm y^{-1}) and ^{14}C activities at the watertable vary spatially; in Scenario 4, recharge is 25 mm y^{-1} from 0 – 2 km, 0 mm y^{-1} from 2 – 10 km, and 1 mm y^{-1} for the rest of the transect, while ^{14}C activities at the watertable vary spatially.

which is not considered in equation (3.2). Recharge estimated from equation (3.2) is close to the modelled rate in the middle of the aquifer (~30 m depth), but increases exponentially towards the base of the aquifer, again because diffusion and dispersion transport more ^{14}C to depth in the aquifer. In the model the lower boundary is a no flow boundary. In reality however, the lower boundary of an aquifer may be an aquitard containing significantly 'older' water. In this case ^{14}C activities (and hence estimated recharge rates) at the

bottom of the aquifer would be lower, as ^{14}C would diffuse into the aquitard.

In Scenario 2 recharge occurs only at the aquifer margin, so the ^{14}C profiles become progressively 'older' further away from the recharge area. However diffusion from the unsaturated zone causes all profiles to meet the boundary condition of 100 pMC at the watertable. The result is higher ^{14}C activities at the bottom of the profile than there would be if diffusion were not occurring, consistent with previous findings (Walker and Cook, 1991). Assessment of the spatial variability in recharge cannot be captured in equation (3.2). However, for 22% of the observation points, a recharge rate of between 0.5 and 1.5 mm y^{-1} is estimated, which is close to the spatially averaged recharge rate along the transect (1 mm y^{-1}). Estimates from the remaining 78% of observation points range from 0.3 to 28 mm y^{-1}, between approximately a factor of thirty above the spatially averaged recharge rate (1 mm y^{-1}), or a factor of thirty below the recharge rate at the basin margin (25 mm y^{-1}). Deeper observation points closer to the basin margin give the best indication of the mountain front recharge rate, while shallower observations further downstream give an estimate closer to the spatially average recharge rate.

In Scenario 3 the influence of spatially variable ^{14}C activities at the watertable can be observed (Figure 1). As in Scenario 2, activities at depth become lower with increasing distance of the profile from the recharge area. However as the ^{14}C activity at the watertable is increasing further away from the recharge area, the profile shapes are different from Scenario 2. The result is that the profile furthest away from the recharge area has the lowest ^{14}C activities at depth, but the highest activities near the watertable. Conversely, the profile closest to the recharge area has the highest ^{14}C activities at depth, but the lowest activities close to the watertable. This complexity that arises from a spatially variable ^{14}C activity at the watertable is further seen in Scenario 4 (Figure 3.1) where recharge occurs at the aquifer margin, and also at a low rate across much of the transect.

Discrepancies between modelled groundwater ages using particle tracking (advective ages) and solute transport modelling (tracer ages) are expected in low flux environments, where diffusion and dispersion may have a significant influence on the distribution of tracer ages (Castro and Goblet, 2005). This discrepancy between apparent age estimated from modelled ^{14}C activities (using equation (3.1) and assuming A_0 = 100 pMC) and ages determined through particle tracking (advective ages) is shown for our theoretical scenarios in Figure 3.2. The comparison is made for each scenario at the observation points furthest from the aquifer margin. For Scenario 1 the ages agree well in the upper part of the aquifer (younger ages), however towards the bottom of the aquifer advective ages increase exponentially, while downward transport of ^{14}C by diffusion and dispersion limit the maximum ^{14}C age. In Scenario 2 advective ages are consistently >5000 years reflecting the time taken to travel from the recharge source at the aquifer margin. However the presence of a ^{14}C boundary of 100 pMC at the watertable means ^{14}C ages are younger (because of diffusion) in the upper part of the aquifer. There is some crossover where ages are in agreement in the middle of the profile, but then advective ages increase with depth while diffusion limits the increase in ^{14}C age, as is observed in Scenario 1.

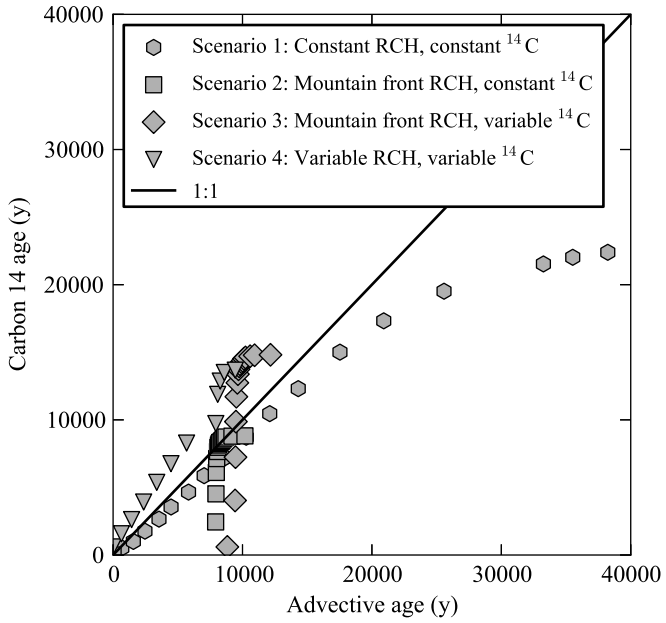

Figure 3.2: Advective (particle tracking) ages compared with apparent ages estimated from ^{14}C profiles at the observation point 42 km from the basin margin in Scenarios 1 to 4. RCH denotes recharge. Observation points are spaced vertically 4 m apart from 0 – 60 m depth, then 1 m apart in the bottom 5 m of the aquifer. Both ^{14}C and advective ages increase with increasing depth in the aquifer.

In Scenario 3 the influence of the spatially variable ^{14}C activity at the watertable has a greater effect on age disparity than that observed in Scenario 2. Apparent ages from ^{14}C become significantly older with depth than in Scenario 2 – as the ^{14}C input activity from recharge was 50 pMC (not 100 pMC as used in equation (3.1) to calculate age). In Scenario 4 both the variable ^{14}C boundary and variable recharge result in ^{14}C ages being consistently older.

3.3 Field demonstration

3.3.1 Site description

To demonstrate the benefit of considering both ^{14}C profiles in groundwater, and spatially variable ^{14}C activity at the watertable, we present data and modelling from the Ti Tree Basin in Northern Territory, Australia (Figure 3.3). The basin, which covers ~5500 km^2, is comprised of Tertiary lacustrine and fluviatile sediments that make up the main unconfined aquifer (undifferentiated sandstone, limestone and silty sandstone). Groundwater flows from deeper watertable areas in the south to shallower watertable areas in the north, where it discharges in a saline wetland.

Our focus in this study is three sites in the centre of the basin. These sites lie on the 'floodout' area of Allungra Creek – a low gradient alluvial surface that is only inundated in rare, large flood events (Tooth, 1999). Tracts of denser vegetation (predominantly mulga trees) are associated with the floodout, and clearly visible from aerial imagery (inset Figure 3.3). Harrington et al. (2002) estimated recharge rates in the Ti Tree Basin from ^{14}C activities and the chloride mass balance method, ranging from 0.1 to 50 mm y^{-1}, with

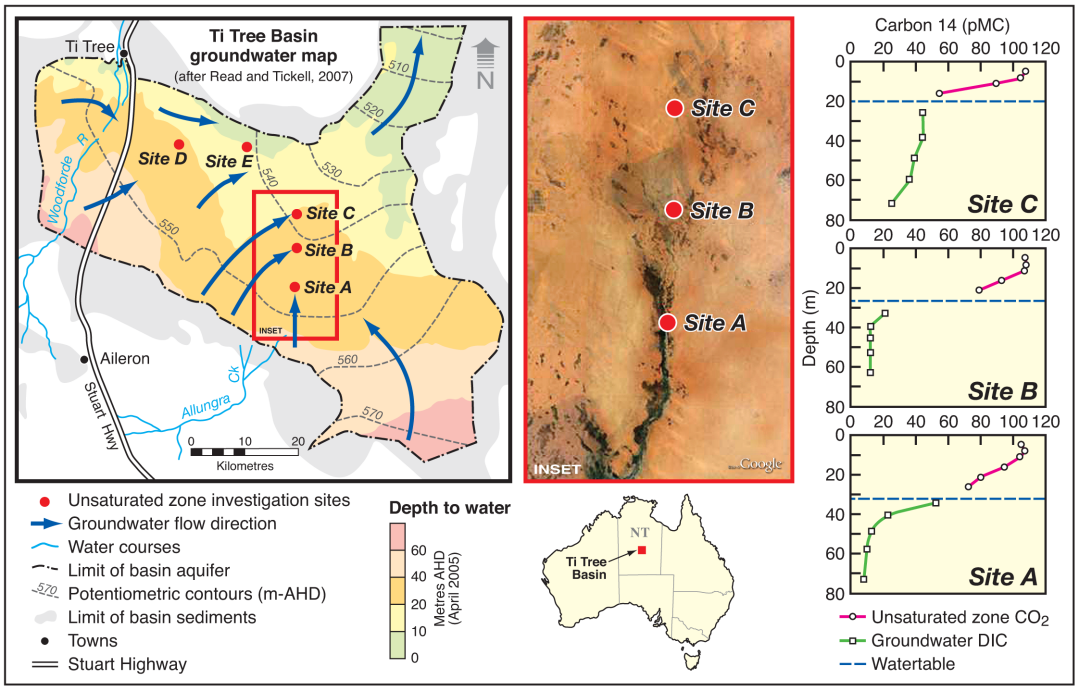

Figure 3.3: Location of carbon-14 observation sites in the Ti Tree Basin, Northern Territory, Australia. Also shown are inferred groundwater flow paths (based on potentiometric surfaces) and aerial imagery (Inset) showing denser vegetation around parts of the Allungra Creek floodplain.

a median value of 0.9 mm y^{-1}. Higher estimated recharge rates were few, and spatially associated with the floodout area of Allungra Creek and the Woodforde River. However Harrington et al. (2002) did not obtain vertical profiles of ^{14}C and did not consider diffusion and unsaturated zone processes on ^{14}C.

Detailed profiles of ^{14}C activity in unsaturated zone gas and groundwater were obtained at each site (Figure 3.3, see Wood et al. (2014) for details on sampling and analysis). Based on potentiometric contours, the three sites are assumed to lie on separate groundwater flow paths (Figure 3.3). At sites A, B and C the watertable depths are 32 m, 26 m and 19 m respectively. Along each flow line the maximum watertable depth occurs at the basin margin, and is ~50 m in the case of sites A and B, and ~40 m for site C. Wood et al. (2014) observed similarity in unsaturated zone $^{14}CO_2$ profiles with depth at five sites in the Ti Tree Basin, but noted that variations in unsaturated zone thickness led to variations in the ^{14}C activity observed above the watertable (Figure 3.4). The depletion of ^{14}C activities in soil CO_2 was attributed to production of old CO_2 deep in the unsaturated zone, most likely through dissolution-precipitation of calcite in the profile (Walvoord et al., 2005; Gillon et al., 2009). CO_2 production rates were obtained through unsaturated zone gas transport modelling and matching CO_2 and ^{14}C profiles. Sites A and B were calibrated using similar rates of deep 'old' CO_2 production (290 and 300 mmol m^{-3} y^{-1}, respectively). At Site C, ^{14}C activities were more depleted above the watertable and a higher production rate was needed to match the profile at site C (400 mmol m^{-3} y^{-1}). Wood et al. (2014) postulated this may be due to some local variation in unsaturated zone lithology, with potentially more 'old' CO_2 being produced as a result of enhanced calcite dissolution/precipitation cycles (there was significantly more calcite in the drilling cuttings from Site C). Based on a sensitivity analysis, relationships between unsaturated zone thickness and ^{14}C activity

for different rates of deep CO_2 production were developed which fit observed measurements for the majority of sites (Figure 3.4). The profile at Site C was also calibrated using lower unsaturated zone porosities than the 'base case', which explains why it does not lie on any trend line). Unsaturated zone ^{14}C data from two additional sites (D and E) are also shown on Figure 3.4, however these sites have not been modelled as part of this study.

3.3.2 Methods

For the field demonstration, the models were identical to the earlier presented theoretical models in terms of discretisation, however, hydraulic conductivity was lowered to 5 m d^{-1} based on estimates for the Ti Tree Basin given by Knapton (2007). Also the lower boundary of the aquifer at the start of the flow path was altered, with aquifer thickness increasing from 0 m at the basin margin to a maximum depth of 65 m. This is based on aquifer cross sections and borehole data presented in McDonald (1988). The aquifer depth of 65 m is an approximate yet realistic representation of saturated thickness throughout this part of the basin. The length of the transects in each case matches the length of the inferred flow lines. The ^{14}C activity at the watertable was handled in the same way, with specified concentrations being assigned in the top layer of saturated cells in the aquifer.

The relationship between unsaturated zone thickness and ^{14}C activity above the watertable shown in Figure 3.4 is used as a basis for assigning ^{14}C activities at the watertable in the field comparisons (Figure 3.5). As outlined above, the unsaturated zone ^{14}C activity at Site C was more depleted than other sites, and does not fit the same trend. Because of this, the ^{14}C boundary condition used in the field comparison in Site C is different from that of Sites A and B. Sensitivity to these concentration boundary conditions is tested in the following section.

3.3.3 Results

The profile at Site A is a similar shape to those generated in Scenarios 2 and 3 of the theoretical modelling with a steep ^{14}C gradient near the watertable, and a gentler gradient with depth. Accordingly a good fit to the ^{14}C data is found with the majority of recharge occurring at the basin margin as mountain front recharge (Figure 3.5) as recharge close to the sampling point does not produce the low ^{14}C activities (<20 pMC) at the bottom of the profile. A small amount of negative recharge (simulating groundwater discharge) is modelled immediately upgradient of the observation site in order to fit the steep ^{14}C gradient in the shallow part of the aquifer. The modelled profile is somewhat insensitive to the rate and spatial extent of mountain front recharge (e.g. twice as much recharge over half the distance would yield the same result). But importantly, the total amount of mountain front recharge and its spatial variability can be determined. The need for spatial variability in recharge along the transect can be demonstrated by comparing with a profile that would be generated by spatially constant recharge (also shown in Figure 3.5).

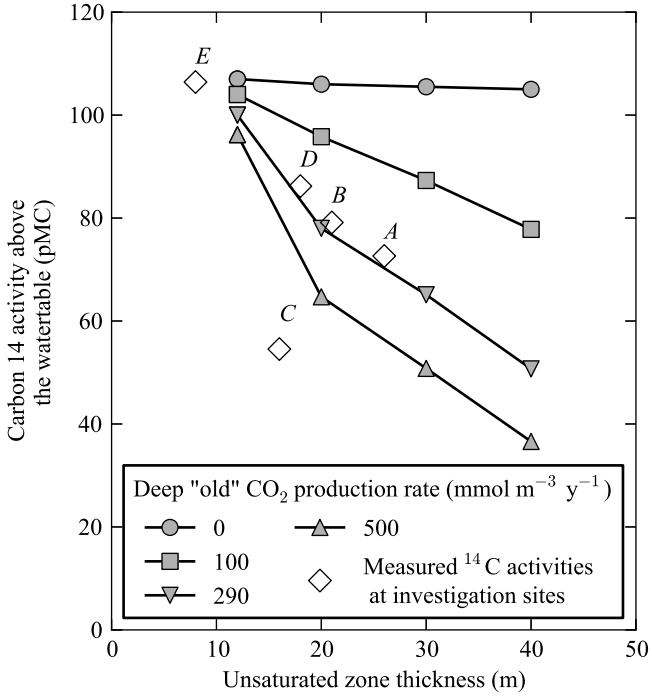

Figure 3.4: Relationship between unsaturated zone thickness and ^{14}C activity above the watertable for different rates of 'old' CO_2 production in the unsaturated zone (after Wood et al. (2014)). Also shown are unsaturated zone ^{14}C activities above the watertable measured by Wood et al. (2014)).

Site B also shows a steep ^{14}C gradient near the watertable, and a much lower gradient with depth, similar to Scenarios 2 and 3 of the theoretical modelling. A good fit is found with recharge occurring at the basin margin as mountain front recharge, then a small amount of discharge across the rest of the transect. The discharge is over a greater distance than Site A, which is required to fit the steeper profile at Site B. The ^{14}C profile at Site C is reproduced with recharge occurring at the basin margin as mountain front recharge, and also high recharge within 10 km of the observation point which is required to fit the concave shape of the profile. As discussed earlier, the ^{14}C boundary assigned at Site C is different to that of Sites A and B. At the start of the transect, ^{14}C activities are similar to those of Sites A and B, but activities are lowered closer to the site to reflect the lower unsaturated zone ^{14}C activity observed at Site C (sensitivity to this boundary condition is tested in the following section).

3.3.4 Sensitivity to variations in ^{14}C input at the watertable

To assess the sensitivity of these profiles to variations in ^{14}C input, two different scenarios were run and compared with the 'base case' scenario for sites A and C. One scenario has a ^{14}C input that varies more strongly across the transect (from 20 to 80 pMC compared to 40 to 70 pMC for Site A), and one scenario uses a constant ^{14}C input at the watertable (based on the value measured at the site). Recharge rates are then varied to fit the ^{14}C profile.

The sensitivity analysis for Site A (Figure 3.6) shows that when the ^{14}C activity at the watertable varies more steeply, a good fit to the profile can still be obtained, and recharge rates for the mountain front zone

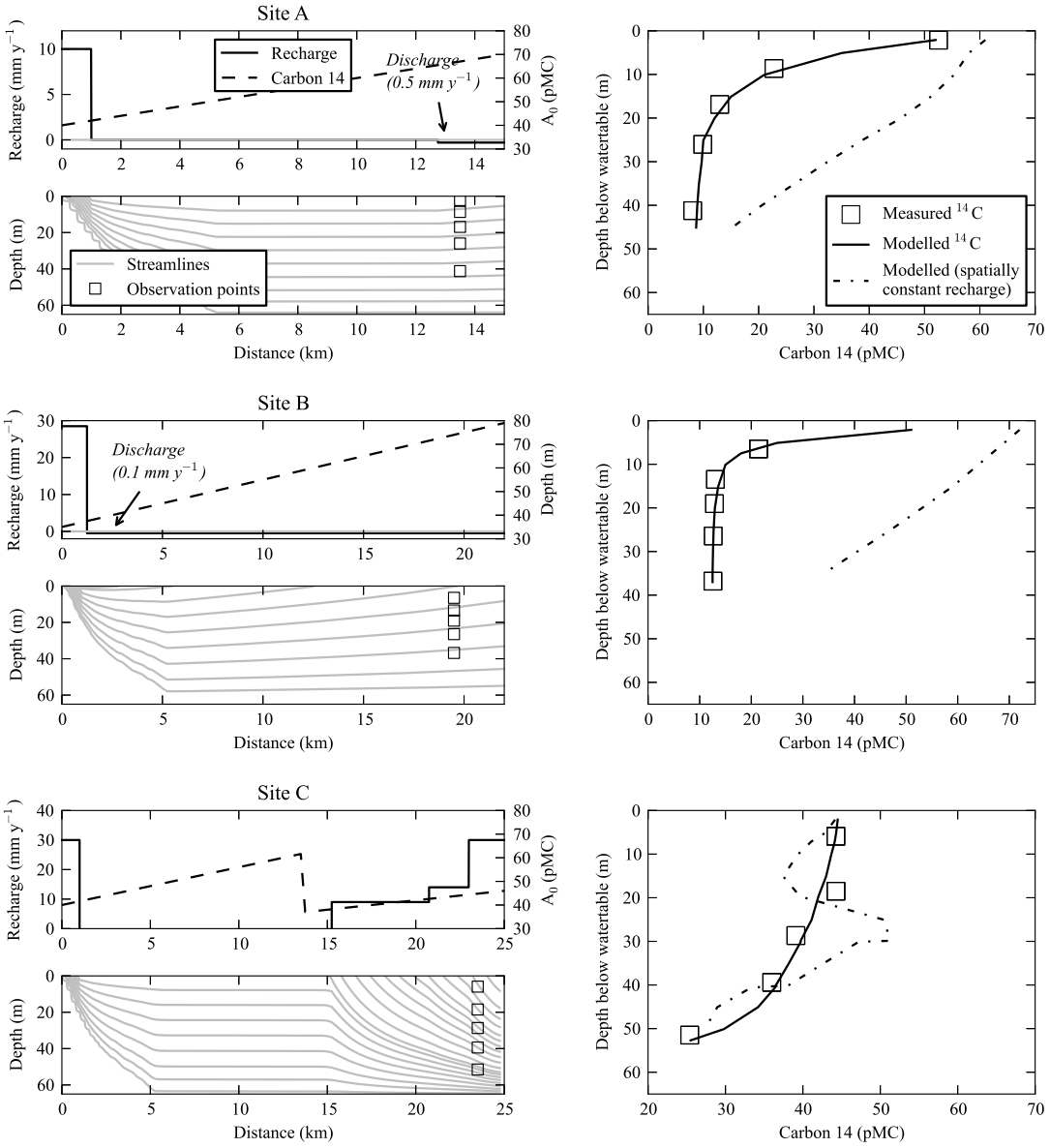

Figure 3.5: Measured and modelled ^{14}C activities in groundwater at investigation sites A, B and C. At Site A recharge occurs at the basin margin (10 mm y^{-1}), with 0 mm y^{-1} recharge between 1 km and 13 km, then -0.5 mm y^{-1} (discharge) between 13 km and 15 km. Also shown is the profile generated by spatially constant recharge (at a rate of 0.65 mm y^{-1}, equal to the total amount of recharge in the calibrated scenario) demonstrating the need to invoke spatial variability in recharge and mountain front recharge. At Site B, recharge occurs predominantly at the basin margin (28 mm y^{-1}) with a small amount of discharge (-0.1 mm y^{-1}) across the rest of the transect. Also shown is the profile generated using spatially constant recharge (1.14 mm y^{-1}, again equal to the total amount in the calibrated scenario). At Site C there is mountain front recharge and significant recharge 10 km up gradient of the observation point.

differ by only 5 mm y^{-1}. Likewise when ^{14}C activity is constant, a good fit can still be found with mountain front recharge lower by 2 mm y^{-1}. Thus with different ^{14}C boundaries upgradient of the sampling point, , the profiles can still be fit with similar patterns of spatial variability in recharge. However all models must have the same ^{14}C boundary value at the observation point in order to fit the profile. As demonstrated in Figure 3.5, the profiles cannot be fit with spatially constant recharge rate.

Sensitivity results from Site C (Figure 3.6) are more complex. A reasonable fit to the ^{14}C data is obtained

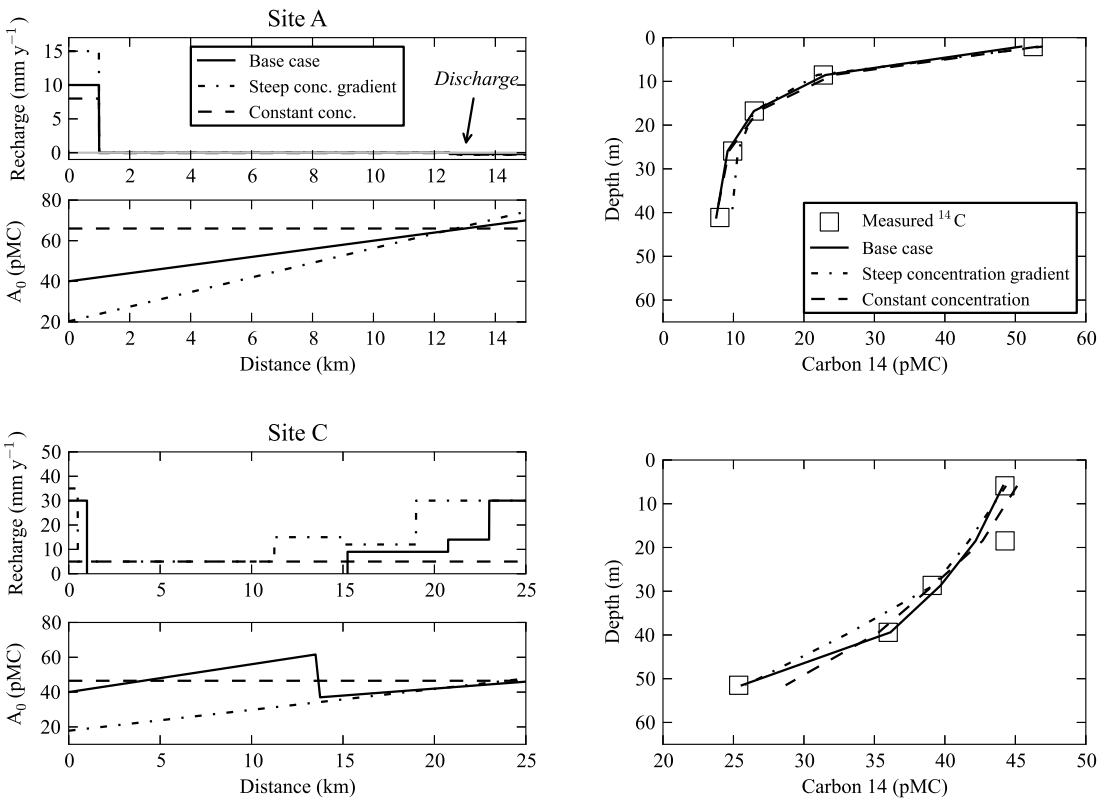

Figure 3.6: Measured vs. modelled ^{14}C activities at Sites A and C for the scenarios considered in the sensitivity analysis.

with a steeper ^{14}C boundary condition and more spatial variation in recharge. Interestingly, when ^{14}C activity at the watertable is spatially constant, a reasonable fit is achieved by modelling spatially constant recharge. Thus to determine spatial variability in recharge, an understanding of likely unsaturated zone ^{14}C activities upgradient is needed. As with Site A, ^{14}C input activity at the site is needed to model the profile accurately and determine spatial variability in recharge.

3.4 Discussion

All of the modelled recharge scenarios used to reproduce our Ti Tree Basin ^{14}C data (Figure 3.5) invoke mountain front recharge as an important mechanism. In some cases (eg. Site C), this conclusion depends upon knowing the likely ^{14}C boundary condition upgradient of the observation point. Mountain front recharge processes have been hypothesised to be important in the Ti Tree Basin, with recharge driven by surface water flow off of the uplifted basin margin in the south (Wischusen et al., 2012). Furthermore, mountain front recharge creates different depth profiles of ^{14}C than scenarios of spatially constant recharge, as both our theoretical modelling and field demonstration show. Discharge (negative recharge) is required in these models to produce some of the steep ^{14}C gradients near the watertable and is consistent with deep rooted vegetation in the basin that may induce evapotranspiration (Reid et al., 2008; O'Grady et al., 2009). The model for Site C also has mountain front recharge, as well as high amounts of recharge within 10 km of the Site. Aerial photography (Figure 3.3) shows Site C lying in an extended branch of the Allungra flood-

plain system that is not densely covered in vegetation (unlike Sites A and B). Hence, Site C is more likely to be associated with sandy soil types, rather than clays associated with denser vegetation (Harrington et al., 2002). Aerial photography also shows morphological features resembling channels (not discernible on the land surface) suggesting significant surface water flows have occurred upgradient and over Site C in the past (Figure 3.3). The higher recharge rates (up to 30 mm y^{-1}) are in the same range as the highest spatially averaged recharge estimates of Harrington et al. (2002) (25 to 50 mm y^{-1}) and estimates for other arid and semi-arid regions in the world where recharge from ephemeral streams occurs (Scanlon et al., 2006). Thus recharge from ephemeral streams and 'floodouts' is still likely to be an important mechanism in the Ti Tree Basin, in addition to mountain front recharge.

We have shown how a variable ^{14}C activity as a boundary condition for ^{14}C transport can complicate the vertical tracer profile in an aquifer. To our knowledge this has not previously been considered when ^{14}C has been incorporated into groundwater models, and may help improve such models in future studies. We also demonstrate that without measurement of vertical tracer profiles, very little can be inferred about spatial variability in recharge, and recharge estimates may be in error by more than an order of magnitude. Measurement of tracer concentrations close to the watertable help constrain the upper concentration boundary condition, while measurements from deeper in the profile help constrain upgradient recharge processes. The infrastructure required to sample unsaturated zone gas is relatively inexpensive and can easily be incorporated into a drilling program when monitoring wells are being installed (with soil gas sampling tubes being attached to the outside of a piezometer, see Wood et al. (2014) for details). Installation of piezometer nests to obtain vertical profiles can be more expensive. However, if accuracy in estimation of recharge and its spatial variability is desired, then vertical profiles of age tracers and unsaturated zone measurements are essential.

Although the main focus of this work is ^{14}C, analogous problems related to spatial variation in recharge and unsaturated zone concentrations may arise with use of other age tracers, especially in arid settings where diffusion is important. For example anthropogenic tracers with temporally varying input signals (CFCs, krypton-85, sulfur hexafluoride-6) are transported through the unsaturated zone before reaching the watertable. Where unsaturated zones are thick (>10 m), spatial variation in unsaturated zone thickness leads to spatial variation in input concentrations at the watertable (Cook and Solomon, 1995). Spatial variability in recharge is also known to generate variations in vertical tracer profiles in aquifers (Robertson and Cherry, 1989). Thus in these cases measurement of vertical profiles coupled with knowledge of unsaturated zone concentrations becomes crucial to assessing recharge. Tracers with temporally constant input signals that are not subject to unsaturated zone dilution or production will not be as problematic. Argon-39 (^{39}Ar) may be an example of one such tracer in environments where subsurface production is insignificant (Loosli et al., 2000). However discrepancies between advective age and tracer based aged will still occur for a tracer such as ^{39}Ar in arid environments, due to diffusion from the unsaturated zone into the aquifer. The discrepancy between ^{39}Ar age and advective age due to this process will be greater than that between ^{14}C

age and advective age. This is because ^{39}Ar has a shorter half-life (higher decay constant), thus the vertical gradient within the aquifer will be higher.

We have not considered the influence geochemical processes on ^{14}C. The influence of carbonate weathering has received significant attention in the past through the development of numerous correction schemes (Ingerson and Pearson, 1964; Tamers, 1975; Fontes and Garnier, 1979). Such reactions are clearly important in some settings (eg. Kroitoru et al. (1987)) and can dilute ^{14}C activities potentially leading to overestimates of groundwater age and underestimates of recharge if not accounted for. However, our work shows that fundamental problems in conceptualising and understanding the ^{14}C cycle in the unsaturated zone and groundwater exist even in geochemically simple systems. These problems can lead to significant errors in interpretation before the influence of mineral weathering on ^{14}C activities has been considered. At our site there is not a large variation in δ^{13}C values in groundwater (-6.1 to -8.8 ‰ PDB, see Wood et al. (2014)), suggesting carbonate weathering (and associated enrichment of δ^{13}C along a flowpath) does not have a significant influence on the ^{14}C profiles we observe.

Our models for the field application are both homogeneous and run in steady state. Recent studies have demonstrated the effect of increasing heterogeneity on environmental tracer data and thus groundwater age and recharge estimates (McCallum et al., 2014; Kozuskanich et al., 2014), however we do not consider aquifer heterogeneity in this study. Also, recharge in the Ti Tree Basin is likely to vary temporally in response to large infrequent rainfall events, which may be several decades or centuries apart (Harrington et al., 2002). Schwartz et al. (2010) showed how temporal variability in recharge can complicate the ^{14}C profiles in an aquifer, potentially causing larger problems for ^{14}C interpretation than carbonate dissolution alone. Temporal variability in spatial patterns of recharge could also lead to changes in the flowpath over time which we have also not considered.

3.5 Conclusion

Spatially variability in recharge and ^{14}C activity at the watertable can create complexities in apparent groundwater age profiles. Groundwater age may be significantly over or under-estimated leading to error in recharge estimation. The magnitude of this error depends upon the depth and location in the aquifer from which samples are collected and age is estimated. Measurement of vertical tracer profiles coupled with knowledge of tracer processes in the unsaturated zone may help overcome this error. Our field application shows how both measurement of vertical ^{14}C profiles in groundwater and knowledge of unsaturated zone ^{14}C activities enables us to more effectively quantify recharge and asses its spatial variability. Measurement of groundwater profiles and unsaturated zone ^{14}C activities will be particularly important in low flux (arid) environments, where diffusion from the unsaturated zone into the aquifer can be significant. Though we focus on ^{14}C in this study, analogous problems will exist with other tracers, making these findings significant for researchers concerned with tracer based estimates of groundwater age and recharge in general.

Acknowledgments

Funding for carbon isotope analysis of groundwater was provided by in part by AINSE (Grant 12/042) under the Isotopes for Water project. Additional funding was provided by the Australian Research Council and the National Water Commission. The authors wish to thank the Northern Territory Government and Bob Read for drilling and piezometer installation, and staff and students from Flinders University for assistance with field work. We thank Dr. Axel Suckow and Dr. Russell Crosbie from CSIRO for early reviews of the manuscript. Dr. Peter Birkle and two anonymous reviewers are thanked for comments which helped improve the manuscript.

Allungra Waterhole at the end of Allungra Creek in May 2011 (photo by Dr. John Wischusen)

4 Constraining spatial variability in recharge in an arid environment through modelling carbon-14 transport in groundwater

Abstract

Carbon-14 (^{14}C) has been widely used to estimate groundwater recharge in arid regions, and is increasingly being used as a tool to assist numerical model calibration. However lack of knowledge on ^{14}C inputs to groundwater potentially limits its use in solute transport modelling. In this study we use direct measurements of ^{14}C in the unsaturated zone to develop a spatially variable ^{14}C input map for a regional scale unconfined aquifer (the Ti Tree Basin in central Australia). The map is used as a boundary condition for a 3D groundwater flow and solute transport model for the basin. The model is calibrated to both groundwater ^{14}C activity and groundwater level, and calibration is achieved by varying recharge rates in 18 separate zones. We test the sensitivity of the calibration to both the ^{14}C boundary condition, and the number or recharge zones used. The calibrated recharge rates are within previously reported ranges and agree with previous studies on spatial variability in the basin (recharge is higher in the mountain front zone and near ephemeral surface water features). This approach demonstrates the importance of boundary conditions for ^{14}C transport modelling (^{14}C input activity), for improving estimates of spatial variability in recharge.

4.1 Introduction

In arid regions, understanding groundwater recharge is critical to managing groundwater resources. However quantifying recharge is complicated in such environments, as rainfall is often low and episodic (Gee and Hillel, 1988). Recharge may vary spatially and occur via different processes, such as focused recharge at the basin margin (ie. mountain front recharge (Wilson and Guan, 2004)), direct recharge beneath ephemeral rivers (Fulton et al., 2012), or aerially distributed diffuse infiltration through the unsaturated zone (Scanlon et al., 2006). Environmental tracer techniques such as groundwater dating with carbon-14 (^{14}C) have proven useful for investigating groundwater recharge (Vogel, 1967) and have been widely used in arid environments (Dincer et al., 1974; Cresswell et al., 1999; Kulongoski et al., 2008; Herczeg and Leaney, 2011).

Carbon-14 has also been used as a calibration target (in addition to groundwater level) in numerical groundwater models. Several studies have compared modelled advective groundwater ages (determined through particle tracking) with ages estimated from ^{14}C to assist in model calibration and recharge determination (Sanford and Buapeng, 1996; Sanford et al., 2002; 2004; Michael and Voss, 2009). However comparisons between modelled advective age and measured apparent age can be complicated. This is because advective ages do not account for diffusion and dispersion, which can affect the transport of a tracer such as ^{14}C (thus influencing the distribution of apparent ages). Therefore modelling of tracer concentrations directly may be more desirable (Troldborg et al., 2007; McCallum et al., 2015; Gardner et al., 2013; Turnadge and Smerdon, 2014). This is especially important in arid regions, where diffusive transport of tracers such as ^{14}C may be just as important as advective transport (Walker and Cook, 1991).

Studies that have modelled ^{14}C transport directly (ie. solute transport modelling accounting for advection, diffusion, dispersion and radioactive decay) have generally been limited to 2D transect models (Zhu, 2000; Castro and Goblet, 2005; Schwartz et al., 2010). These 2D model studies have assumed ^{14}C inputs from the unsaturated zone to be modern (90 pMC in Castro and Goblet (2005); 100 pMC in Zhu (2000) and Schwartz (2010)). However many studies have shown that unsaturated zone ^{14}C activities may be significantly diluted (Haas et al., 1983; Walvoord et al., 2005, Gillon et al., 2009) and spatially variable (Wood et al., 2014), with significant implications for the interpretation of groundwater ^{14}C activities (Bacon and Keller, 1998; Wood et al., 2015).

In this study we use measured vertical profiles of ^{14}C in groundwater in the Ti Tree Basin, central Australia, and a 3D groundwater flow and solute transport model to estimate the spatial variability of groundwater recharge. Carbon-14 activities are modelled directly, and the ^{14}C boundary condition at the watertable (^{14}C input activity) is constrained by measurements of the spatial variability of unsaturated zone ^{14}C activities (Wood et al., 2014). Parameter estimation software (PEST, (Doherty, 2010)) is used to calibrate the model to both heads and ^{14}C activities, by allowing recharge to be varied within specified zones. The recharge zones are user defined and based on physical features in the basin (e.g. ephemeral streams) as well as the conceptual understanding of recharge processes (ie. the importance of mountain front recharge in the basin, Wood et al. (2015)).

4.2 Site description

The Ti Tree Basin is located in the Northern Territory, in arid central Australia, and covers approximately 5500 km^2 (Figure 4.1). Average annual rainfall is 300 mm y^{-1} and predominantly occurs in summer months (December to March). Soil types vary from dark red massive clays that are dominated by mulga vegetation (*Acacia* spp.) to red earthy sands that are dominated by spinifex grass (*Trioda* spp.) understory and a sparse, open woodland of bloodwood (*Corymbia* spp.) and coolabah trees (*Eucalyptus* spp.). Uplifted Paleoproterozoic rocks form the boundary of the basin, with the interior being relatively topographically flat (elevation ranges from 648 m above the Australian Height Datum (m-AHD) in the south east corner to 480 m-AHD in the north). The main unconfined aquifer in the Ti Tree Basin is comprised of a 60 to 90 m deep sequence of Tertiary lacustrine and fluviatile sediments (undifferentiated sandstone, limestone and silty sandstone). Groundwater flows from deeper watertable areas (> 40 to 60 m below ground) in the southern parts of the basin to shallower watertables in the north, where it discharges in a saline wetland (approximately 20km north-west of the northern margin in Figure 4.1).

One of the main topographic features, the Woodforde River, is a predominantly dry river channel underlain by coarse, pebbly sands that reach a maximum thickness of ~6 m (the sands are underlain by a clayey sandstone). A riparian corridor of river red gums and coolabah trees (*Eucalyptus* spp.) line the river for most of its length. The coarse sands in the Woodforde River channel host a perched aquifer following flooding

events in the river, however this aquifer does not persist as water is lost via transpiration by riparian vegetation and downward leakage towards the regional aquifer (Villeneuve et al., 2015). The downstream section of the Woodforde River dissipates into a 'floodout' - a low gradient alluvial plain with dense vegetation cover (near the 550m potentiometric contour on Figure 4.1). These floodout areas only become inundated during large, rare flood events (Tooth, 1999).

Allungra Creek is an ephemeral river channel that originates in the southern basin margin, and dissipates into a floodout in the south-central part of the basin. Both Allungra Creek and the Woodforde River have previously been identified as likely locations of preferential recharge to the Ti Tree Basin (McDonald, 1988; Calf et al., 1991; Harrington et al., 2002). The margins of the basin have also been identified as areas where recharge may be higher, through mountain front recharge (Wood et al., 2015). Harrington et al. (2002) estimated recharge to the Ti Tree Basin using both ^{14}C and the chloride mass balance method, and found recharge generally ranged from 0.1 - 2 mm y^{-1}. However some higher rates (up to 50 mm y^{-1}) were estimated from ^{14}C measurements in the vicinity of the Woodforde River and Allungra Creek.

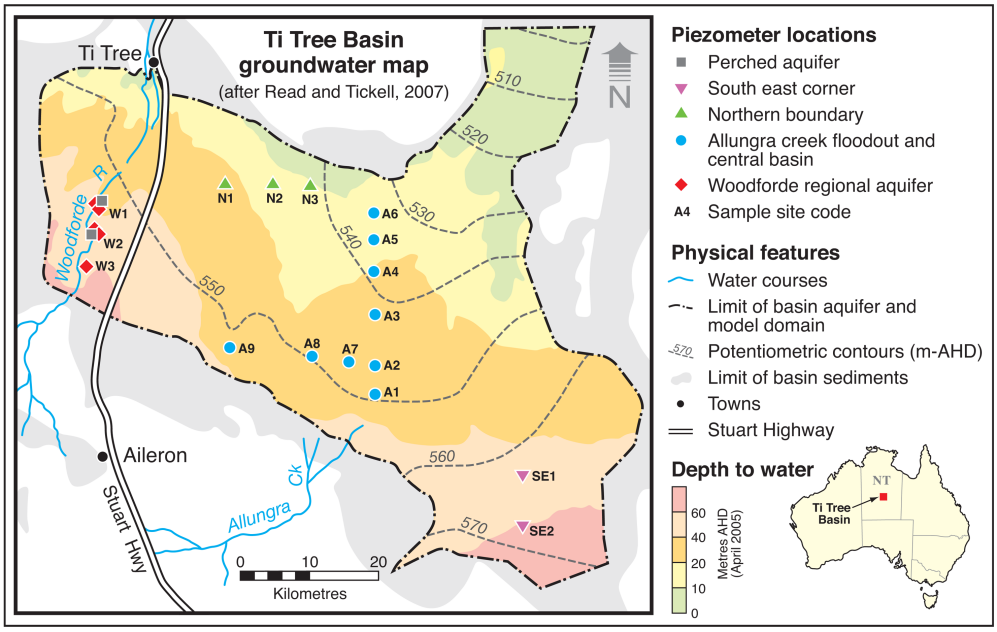

Figure 4.1: Location of ^{14}C investigation in the Ti Tree Basin, Northern Territory (NT), Australia (groundwater discharge area Stirling Swamp is not shown, but lies ~20km north-west of the northern margin).

4.3 Methods

4.3.1 Data collection

Approximately 90 piezometers were installed and sampled in this study between June 2011 and August 2012. Drilling for piezometer installation was done using conventional rotary methods and air circulation. At many locations, multiple piezometers were installed in a single borehole in 'nested' configurations, so that vertical profiles of groundwater samples could be collected. Piezometers were constructed of 50 mm diameter PVC with slotted screen apertures of 1 mm. Screen lengths were between 1 to 2 m, and a gravel

pack of 5 to 7 mm aggregate gravel was installed in the annulus around screened intervals. At each site the borehole annulus above the gravel packs was sealed with bentonite, then back-filled with drilling cuttings (to the surface in single piezometer holes, and to just below the level of the next shallowest piezometer screen for nested holes). Unsaturated zone gas sampling tubes were also installed at sites A2, A3, A4, N1 and N3 (Figure 4.1). Installation and sampling details for these may be found in Wood et al. (2014).

Groundwater was sampled using a Grundfos MP1 submersible pump, and measurements of salinity (as specific conductivity), pH and temperature were made while purging bores. Alkalinity (mg L^{-1} as $CaCO_3$) was also measured in the field by titration using a Hach AL-DT alkalinity kit. Samples for carbon isotope (^{14}C and $\delta^{13}C$) analysis of dissolved inorganic carbon (DIC) were collected after approximately three bore volumes had been purged and field parameters had stabilised. Carbon-14 isotope analysis was performed by accelerator mass spectrometry (AMS), while $\delta^{13}C$ was performed by Isotope Ratio Mass Spectrometry (IRMS). Analysis was performed predominantly at Rafter Radiocarbon (New Zealand), however 12 samples were analysed using the facilities at the Australian Nuclear Science and Technology Organisation (Fink et al., 2004). Carbon-14 activities of groundwater are reported as $^{14}C_{DIC}$:$^{12}C_{DIC}$ relative to the international standard (Stuiver and Pollach, 1977) in units of percent Modern Carbon (pMC). Stable isotope ratios ($^{13}C_{DIC}$:$^{12}C_{DIC}$) are reported in per mil (‰) relative to the international standard (Craig, 1957).

4.3.2 Numerical modelling

The use of measured ^{14}C activities in groundwater to constrain spatial variability in recharge was achieved by linking a 3D numerical flow model with a ^{14}C transport model. The numerical model in this study is based on a groundwater flow model developed by Knapton (2007) using the finite element code FEFLOW (Diersch, 2014). The model domain represents ~3700 km^2, which covers the majority of the saturated sediments in the basin, based largely on the interpretation of Read and Tickell (2007) (Figure 4.1, note the model domain does extend 10 km further north, see Figure 4.5). The domain is bounded by a no-flow boundary representing out-cropping Paleoproterozoic rocks, with the exception of the northern limit of the domain where a constant head boundary is assigned to allow discharge from the domain. This constant head boundary represents regional discharge, which in reality is thought to occur via evapotranspiration in a saline wetland further north, where the basin terminates and the watertable comes with 1 m of the ground surface. The model of Knapton (2007) consisted of two layers: an upper layer of lower horizontal conductivity (0.2 m d^{-1}) and a lower layer of higher hydraulic conductivity (5 m $d^{-1}$for the majority of the domain, then 17 m d^{-1}in the north-eastern branch of the domain). Vertical conductivities were assigned an order of magnitude lower than horizontal values. The conductivity distribution was based on information from drilling logs and aquifer tests, and the conductivity values were adjusted by Knapton (2007) during calibration. As part of this study the model was more finely discretised by increasing the number of layers (42), nodes (347,956) and elements (661,920).

Solute transport was implemented in FEFLOW to simulate ^{14}C, and relevant parameters are listed in Table

4.1. An upper concentration boundary condition was applied at the watertable by combining two spatial data sets using cokriging. Cokriging is a method of spatial interpolation that uses more than one data set (where there is a relationship between data sets) to improve interpolation. Cokriging is useful when a primary data set of interest for interpolation is sparse, and an additional data set (with some relationship to the primary data set) may provide additional spatial coverage. In our case, these data sets were:

1. ^{14}C activities measured near the watertable (generally within 0 - 10 m of the watertable, in groundwater and unsaturated zone gas) at all investigation sites in the Ti Tree Basin (Figure 4.1). These data give the best indication of spatial variability in ^{14}C inputs at the watertable (and are discussed further in the Results section (Figure 4.4)) however they provide limited spatial coverage.

2. A relationship between unsaturated zone thickness and unsaturated zone $^{14}CO_2$ activity directly above the watertable, outlined by Wood et al. (2014) (where greater unsaturated zone thickness is related to lower $^{14}CO_2$ activities above the watertable).

Table 4.1: Model parameters used in simulations where * are based on values in Gelhar et al. (1992) for the aquifer scale modelled; ** are from Browne and Firestone (1999); *** is from Li and Gregory (1974).

Parameter	Value
Porosity	0.3
Longitudinal dispersivity*	50 m
Transverse dispersivity*	5 m
^{14}C decay constant**	1.21 x 10^{-4} y^{-1}
^{14}C diffusion coefficient in water***	3.15 x 10^{-2} m^2 y^{-1}

Model calibration was performed with PEST (Doherty, 2010). PEST uses the Gauss-Levenberg-Marquardt algorithm (GLMA) to iteratively improve the fit to model calibration targets, expressed as the weighted sum of squares of the residuals between measured and modelled results:

$$\phi = \sum_i w_i (h_i^{obs} - h_i^{sim})^2 \tag{4.1}$$

where $\phi$is the objective function, $h^{obs}$is a measured value (eg. hydraulic head or ^{14}C activity), $h^{sim}$is the simulated value, and w is the weight applied to the measurement. Calibration targets were both hydraulic head measurements and ^{14}C activities. Carbon-14 activities were weighted in the calibration by applying the inverse of their assumed error (in this case ten percent of the measured value). This error accounts predominantly for sampling error (ie. possible mixing over the screened interval of the aquifer during pumping and sampling) and also analytical error (generally < 1 pMC). In this way, ^{14}C observations were normalised so that values an order of magnitude apart (eg. 6 to 81 pMC in our case) had equal contribution to the objective function. Hydraulic head values were assigned a weight of 0.2 to give them a slightly lower contribution to the objective function compared to ^{14}C. In addition to measurements made in this study, a number of hydraulic head measurements were taken from the Northern Territory Government database, where measurements may have been made up to three years prior to this study at locations where ^{14}C was not measured in this study. While groundwater levels are generally static in the Ti Tree Basin, these

measurements were nonetheless assigned a lower weight (0.1) to the head measurements made as part of this study. In total, 70 observations of both ^{14}C and head were used in the calibration.

The basin was divided into 18 zones in which recharge rates were optimised. The zones were based on physical features in the basin (such as the Woodforde River and its floodout area, and the Allungra Creek floodout) thought to be associated with recharge rates. Zones were also placed at the basin margins to represent locations where mountain front recharge may occur.

4.4 Results

4.4.1 Groundwater chemistry

Measured ^{14}C activities ranged from 104.5 pMC in the perched aquifer beneath the Woodforde River, to 6.7 pMC near the bottom of the regional aquifer in the south-central part of the basin (Figure 4.2). There is a trend of decreasing ^{14}C activity with depth below the watertable across the basin and in vertical profiles at individual sites (see later Figure 4.7 for vertical profiles). The trend of decreasing ^{14}C activity with depth can be used to infer the likely range of recharge rates, using the analytical model of Vogel (1967) that relates ^{14}C activity with depth in an aquifer to aquifer geometry, recharge and porosity:

$$A = A_0 \left(\frac{H}{H - z} \right) e^{-\lambda (H\theta / R)} \tag{4.2}$$

where A is ^{14}C activity measured at depth z, A_0 is the initial or 'input' ^{14}C activity, H is aquifer thickness, $\lambda$is the decay constant for ^{14}C, θ is porosity and R is the recharge rate. The solution to equation 4.2 assumes aquifer thickness and recharge are constant and ignores diffusive transport of ^{14}C. Assuming A_0 is 100 pMC, the decreases in ^{14}C activity with depth in this study suggest recharge ranges from 0.1 mm y^{-1} to 5 mm y^{-1} (Figure 4.2(a)). As discussed earlier, both A_0 and R are known to vary spatially in the Ti Tree Basin, thus the range of recharge rates is only a broad estimate. Nevertheless, it is consistent with generally low recharge rates estimated by previous studies (Harrington et al., 2002).

Samples collected near the Woodforde River (both in the perched aquifer and in the regional aquifer close to the river) are generally higher in ^{14}C activity (> 65 pMC, up to 23 m below the watertable) than those collected in the rest of the basin (generally < 60 pMC). As previous work has shown, depth of plant roots may play a role in determining unsaturated zone ^{14}C activities, which in turn influences ^{14}C activities in underlying groundwater (Wood et al., 2014). Close to the Woodforde River a riparian corridor of predominantly *Eucalyptus* spp. vegetation is present, and tree roots were observed in a piezometer screened 20 m below ground near the Woodforde River in November 2013. Hence these deep roots may be responsible for respiring more modern $^{14}CO_2$ at depth in the unsaturated zone.

Elsewhere in the basin, ^{14}C activities in groundwater within 0 - 10 m below the watertable generally follow a trend of being lower where unsaturated zones are thicker (Figure 4.4). This is consistent with our under-

standing of the spatial variability of ^{14}C inputs in the Ti Tree Basin (Wood et al., 2014). Figure 4.4 also shows the theoretical relationship between unsaturated zone thickness and ^{14}C activity above the watertable developed previously (Wood et al., 2014). This relationship is based unsaturated zone gas transport models of varying thickness (eg. 10 m to 50 m thick unsaturated zones) where rates of CO_2 production from root respiration (modern ^{14}C) and 'old' CO_2 production near the watertable (zero ^{14}C) are kept constant. The result is lower ^{14}C activities above the watertable where unsaturated zones are thicker. Groundwater samples lie below the line as is expected (the line represents ^{14}C activity of gas at the base of the unsaturated zine). There is some scatter, which most reflects the spatial variability in factors affecting ^{14}C dilution in the unsaturated zone and hence input activity, and the different depths at which groundwater samples were collected (0 - 10 m below the watertable). These factors include variation in lithology and unsaturated zone mineralogy (dissolution-precipitation of calcite is thought to be responsible for the ^{14}C dilution (Walvoord et al., 2005; Gillon et al., 2009; Wood et al., 2014)) and variation in root depth (which acts as a source of modern CO_2 in the unsaturated zone through respiration). As discussed earlier, deeper rooted vegetation near the Woodforde River is thought to be responsible for higher ^{14}C activities in groundwater in that area.

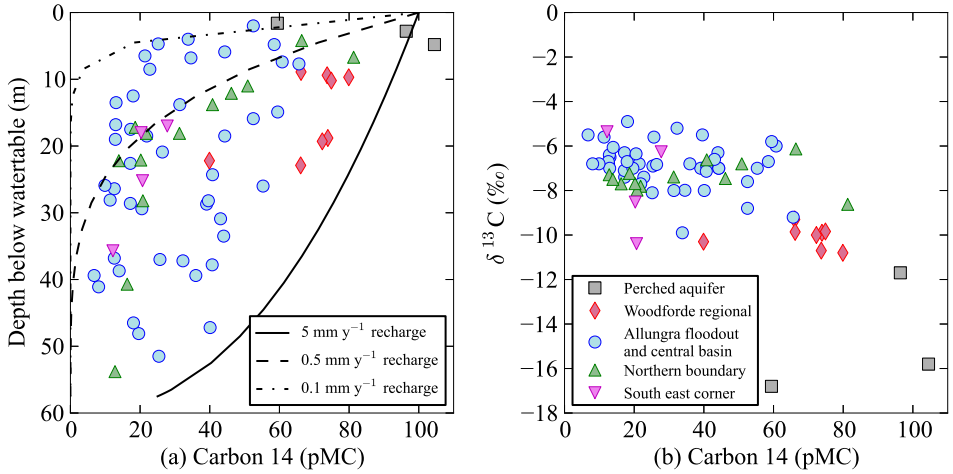

Figure 4.2: (a) Carbon-14 activities measured in the Ti Tree Basin aquifer in this study and theoretical ^{14}C profiles for recharge ranging from 0.1 mm y^{-1} to 5 mm y^{-1} (based on equation 4.2 and assuming A_0 = 100 pMC) and (b) the relationship between ^{14}C activity and $\delta^{13}C$ content.

Carbon-13 composition of DIC in groundwater ranges from -5.5 to -8.5 ‰ for most of the Ti Tree Basin, however closer to the Woodforde River and in the perched aquifer, values range from -9.3 to -16 ‰ (Figure 4.2(b)). Vertical profiles of $^{13}CO_2$ in unsaturated zone gas at five of these sites (Figure 4.3) showed values ranging from -13.5 to -16.8 ‰, consistent with respiration from C4 grasses at these sites (ie. spinifex with $\delta^{13}C$ ~-14.5 ‰ (Cook and Dawes-Gromadzki, 2005). Thus the range of $\delta^{13}C$ values in groundwater away from the river is consistent with inputs from unsaturated zone gas, given a fractionation factor of approximately 8 ‰ between $^{13}CO_2$ in unsaturated zone gas and $^{13}C_{DIC}$ in groundwater (consistent with the expected fractionation given that measured pH generally ranges from 7 to 8 and temperatures generally ~ 28 ºC (Clark and Fritz, 1997)). Vertical profiles of $\delta^{13}C$ in groundwater also show little variation spatially (Figure 4.3), suggesting that weathering of aquifer minerals, though likely to be occurring, is not a

significant source of DIC to groundwater (ie. there is no clear trend of enrichment in $\delta^{13}C$ with dilution of ^{14}C for large parts of the basin). Closer to the Woodforde River, the more depleted $\delta^{13}C$ values likely represent inputs from unsaturated zone gas where a mixture of grasses and C3 trees are present. The most depleted values are seen in the perched aquifer in the Woodforde River, where uptake of water and CO_2 respiration is likely to be dominated by riparian trees (e.g. *Eucalyptus camaldulensis* with $\delta^{13}C$ -27.7 to -29 ‰ (Thorburn and Walker, 1994)).

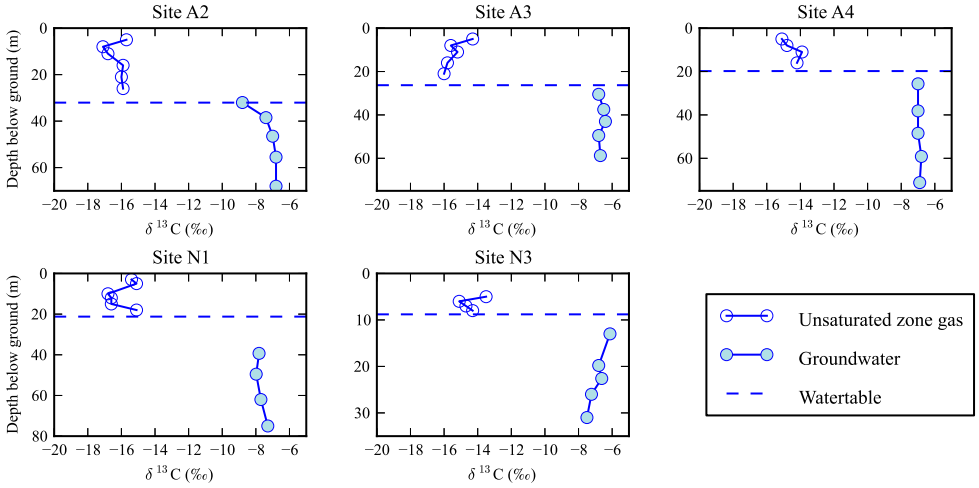

Figure 4.3: Vertical profiles of $\delta^{13}C$ in unsaturated zone gas ($^{13}CO_2$) and groundwater ($^{13}C_{DIC}$) at five investigation sites in the Ti Tree Basin

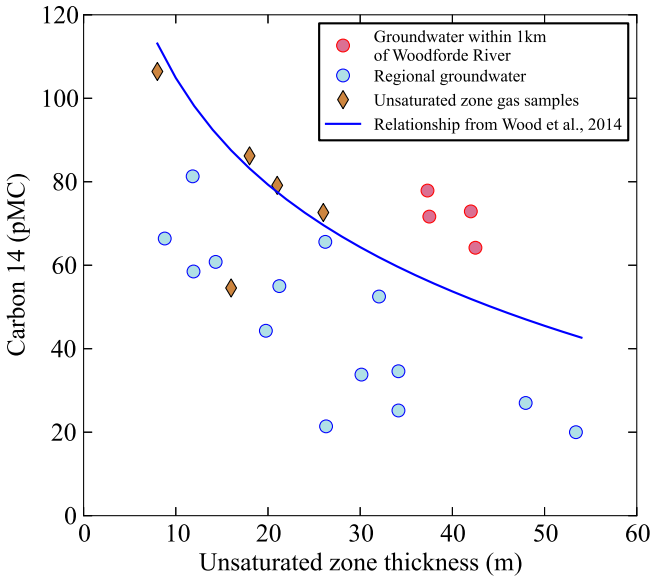

Figure 4.4: Data used in the cokriging approach for determining the ^{14}C boundary condition at the watertable: groundwater ^{14}C activities near the watertable (primary data source, where groundwater samples are the shallowest piezometer at each site, generally <10 m below the watertable) and the relationship unsaturated zone thickness and ^{14}C activity directly above the watertable (based on earlier work in the Ti Tree Basin (Wood et al., 2014) .

4.4.2 Numerical modelling

Cokriging was performed using ArcMap software (ESRI, 2014) using both measurements of ^{14}C near the watertable, and a relationship between unsaturated zone thickness and ^{14}C activity directly above the watertable (Figure 4.4). The result is a map of spatially variable ^{14}C input activities for the solute transport model (Figure 4.5(a)). Generally ^{14}C input activities are lower in the southern parts of the basin, where unsaturated zones are thicker, and become more modern in the northern parts of the basin. However higher ^{14}C activities associated with proximity to the Woodforde River can be seen near the western margin of the basin.

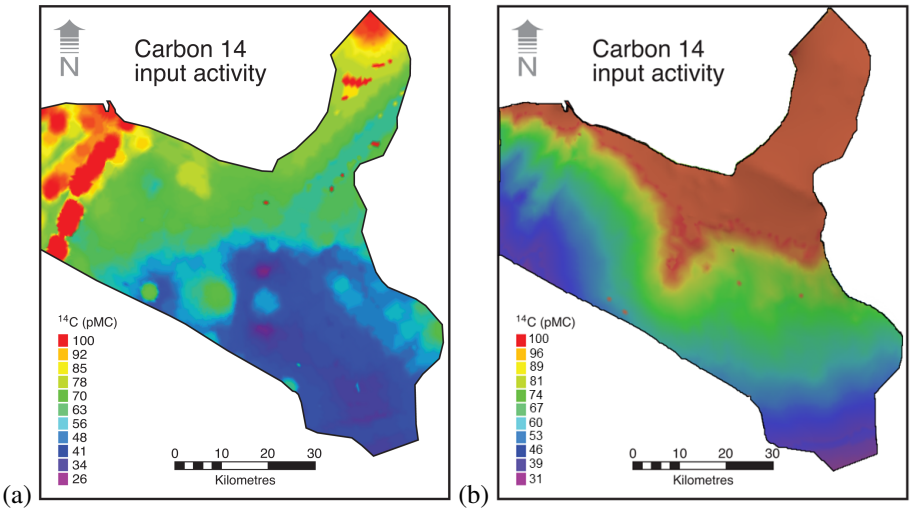

Figure 4.5: Model domain showing geometry and ^{14}C activity boundary condition for the transport model (a) based on the cokriging approach and (b) based on unsaturated zone thickness.

Prior to running PEST, a small manual refinement to the hydraulic conductivity (K) values of Knapton (2007) was made in the lower south-east portion of the model of the model domain, where lower K values were assigned ($K_{x,y}$ = 0.1 m d^{-1}). This was based on drilling and groundwater sampling conducted as part of this study, where piezometers were found to be low yielding (site SE2 in Figure 1).

The model was calibrated in steady state. Initial best-guess estimates of recharge were based on existing knowledge (higher recharge along the basin margin and the Allungra Creek floodout from Harrington et al. (2002) and Wood et al. (2015)) and then final calibration was achieved with PEST (Figure 4.6). The PEST simulations obtained recharge rates that varied spatially from -1.9 to 11.6 mm y^{-1}, with an average recharge rate across the basin of 1.11 mm y^{-1}. The root mean squared error (RMSE) for modelled groundwater level was 2.9 m. The RMSE for ^{14}C activity was 8.02 pMC, demonstrating a reasonable fit to measured ^{14}C and vertical profiles (Figure 4.7). Higher recharge rates (3.7 - 9.6 mm y^{-1}) are generally in the basin margins representing mountain front recharge (zones 2, 4, 5, 7, 8, Figure 4.8). The highest recharge rate (11.6 mm y^{-1}) is in the centre of the basin (zone 13), associated with the floodout from Allungra Creek. Negative recharge rates (ie. discharge) were found for zones 1, 9, 10, 15 and the Woodforde River vegetation area. Zones 9 and 15 are in the northern part of the basin where watertables become shallower (<10m below ground level) and higher salinity values are found (total dissolved solids > 1500 mg L^{-1}), thus discharge

may be occurring through plant transpiration.

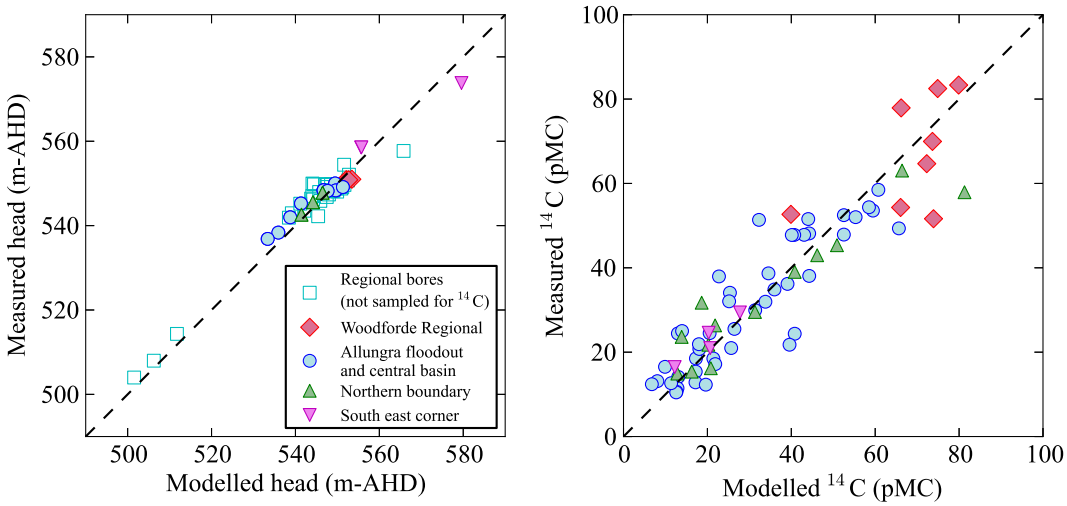

Figure 4.6: Measured vs. modelled hydraulic head measurements and ^{14}C activities in the Ti Tree Basin.

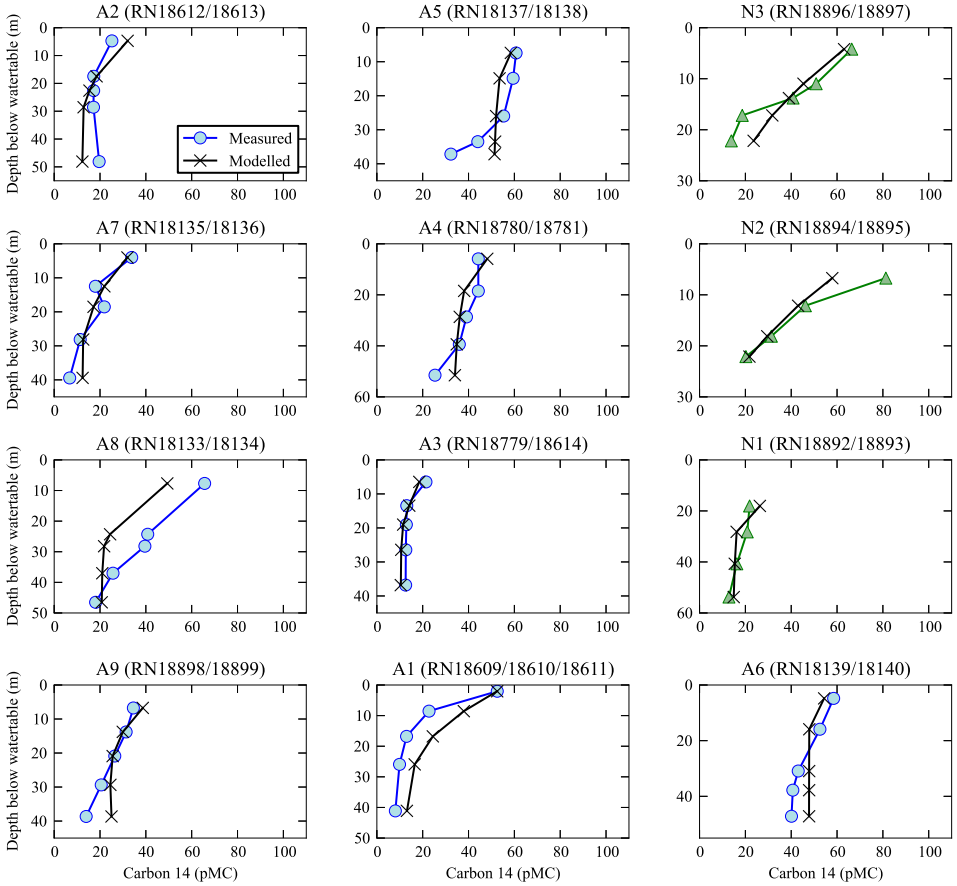

Figure 4.7: Measured vs. modelled ^{14}C vertical profiles at investigation sites in the central Ti Tree Basin (RN refers to registration number of the drill holes in which piezometer nests were installed).

PEST was used to calculate 95% confidence intervals for recharge in the 18 zones (Figure 4.8, Table 4.2). While recharge estimates in some zones appear well constrained with narrow confidence intervals (eg. zones 10 to 17), other zones have very wide confidence intervals, well outside the recharge range expected (eg. zones 7, 8, 9). This may be due to these zones being relatively small. Also the widest confidence

interval is for zone 9, which has no observation data located in it or down gradient from it (zone 8 is similar with wide confidence intervals and there is likely no influence from recharge in this zone on observations down gradient). Further sensitivity analysis was performed by reducing the number of recharge zones (amalgamating some of the 18 zones, Figure 4.8). Reducing the number of recharge zones to four resulted in narrower confidence intervals, however one zone still displays high uncertainty (zone 3 in this case - however there is little groundwater head data and no ^{14}C data in this zone (Figure 4.8, Table 4.3). Also this results in an increase in RMSE for both ^{14}C (up to 8.62 pMC) and head (up to 5.5 m). A further calibration was performed in PEST using one recharge value for the entire model domain. The calibrated recharge rate (0.36 mm y^{-1}) had narrow confidence intervals (0.07 to 0.65 mm y^{-1}), however model fit was poorer again (RMSE of 12.41 pMC for ^{14}C and 7.07 m for head). Thus while confidence in estimates for the 18 recharge zones may be low, a higher degree of spatial variability in recharge produces a better fit to measured data.

Sensitivity to the boundary condition for ^{14}C was tested by running a second model where ^{14}C input activities were based purely on the relationship between unsaturated zone thickness and ^{14}C (ie. using only the trend line in Figure 4.4 and no additional data, see Figure 4.5(a)). This model was also calibrated with PEST. Calibrated recharge rates were similar in magnitude (ranging from -1.8 to 11.7 mm y^{-1}) and spatial variability (higher recharge in the Allungra floodout and mountain front recharge zones). However the fit to ^{14}C activity and head was poorer, with a RMSE of 16.46 pMC and 5.59 m respectively, and 95% confidence intervals are generally wider for all recharge zones (see Table 4.4 for recharge rates and confidence intervals from this scenario). Also for this second model (with a simpler boundary condition), confidence intervals for nearly all zones overlap 0 mm y^{-1}, meaning there is uncertainty as to whether these are recharge or discharge zones. The exception are zones 13 (Allungra Creek floodout) and 14, where confidence intervals are positive (do not overlap 0 mm y^{-1}). However for the model with the boundary condition based on cokriging, fewer zones overlap 0 mm y^{-1}, thus an increased number of zones can be more confidently described as recharge zones (including the Allungra Creek floodout zone 13, and zones 2 and 4 representing mountain front recharge).

4.5 Discussion

The calibrated recharge rates in this study are within ranges previously reported for the Ti Tree Basin. Harrington et al. (2002) reported recharge rates (estimated from ^{14}C data) ranging generally from 0.1 to 2 mm y^{-1}, with a few estimates ranging from 5 to 50 mm y^{-1} (median 0.9 mm y^{-1}). The 'average' recharge rate from this study (ie. the total volumetric flux into the model divided by the area) is 1.11 mm y^{-1}, also in good agreement with with the average reported by Harrington et al. (2002) from the chloride mass balance method (0.8 mm y^{-1}). The highest recharge rate in this study (11.69 mm y^{-1}) is spatially associated with the Allungra Creek floodout, in the same part of the basin as Harrington et al. (2002) estimated recharge to be highest. Likewise, higher recharge rates around the basin margin (representing mountain front recharge) are in agreement with the findings of Wood et al. (2015). Recharge is estimated to be low (1.26 mm y^{-1})

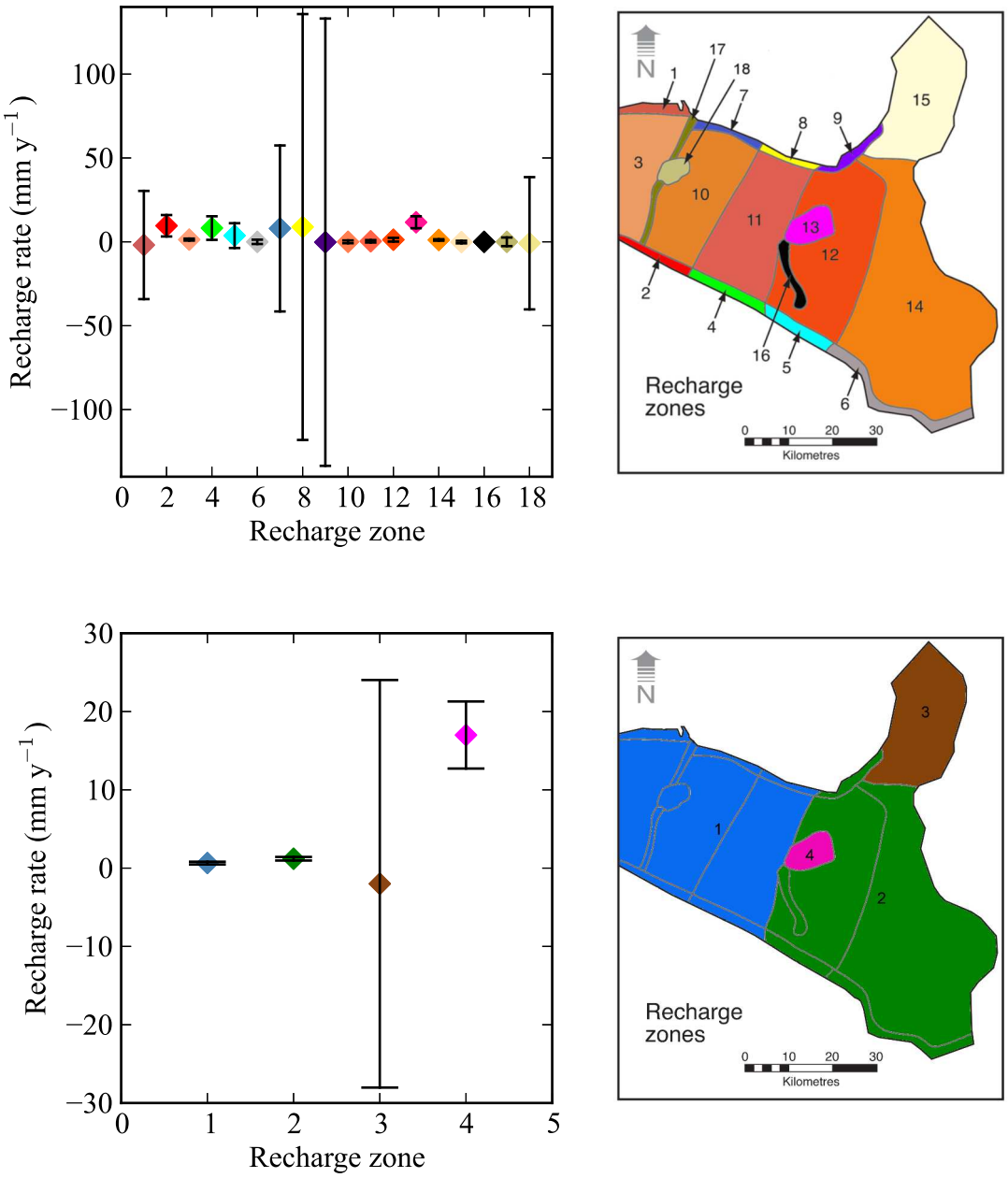

Figure 4.8: 95% confidence intervals for recharge estimates with 18 recharge zones and 4 recharge zones.

or negative (-0.85 mm y^{-1}) along the Woodforde River, despite it previously being identified as a likely recharge area. However the highest estimate of recharge near the Woodforde River from Harrington et al. (2002) of 6.86 mm y^{-1}was for a location further north of the Woodforde River floodout (recharge zone 18 in Figure 4.8) where the watertable is shallower than at our investigation sites.

The finding that recharge may be negative (ie. discharge is occurring) in parts of the basin is also consistent with recent studies showing that plant water use is a significant component of the water balance in the basin (Chen et al., 2014). Shanafield et al. (2015) investigated groundwater discharge in Stirling Swamp (thought to be the regional groundwater discharge zone, north of the model domain), and found that estimated discharge volumes were not sufficient to resolve the water balance for the basin, suggesting discharge occurs

Table 4.2: Calibrated recharge rates and 95% confidence intervals for models with 18 recharge zones

Model with eighteen recharge zones and cokriged ^{14}C boundary			
Recharge zone	**Recharge rate (mm y^{-1})**	**Upper 95% limit**	**Lower 95% limit**
1	-1.89	-34.14	30.36
2	9.59	3.19	15.98
3	1.34	0.74	1.93
4	8.21	1.19	15.23
5	3.71	-3.68	11.11
6	$3x10^{-4}$	-1.28	1.29
7	7.98	-41.49	57.46
8	8.84	-118.10	135.77
9	-0.21	-133.53	133.11
10	0.02	-0.81	0.86
11	0.33	-0.40	1.06
12	1.26	0.15	2.37
13	11.69	8.12	15.24
14	1.12	0.68	1.55
15	-0.13	-0.90	0.63
16	$7.3x10^{-4}$	-1.99	1.99
17	0.01	-2.56	2.58
18	-0.85	-40.27	38.57

Table 4.3: Calibrated recharge rates and 95% confidence intervals for models with 4 recharge zones

Model with four recharge zones and cokriged ^{14}C boundary			
Recharge zone	**Recharge rate (mm y^{-1})**	**Upper 95% limit**	**Lower 95% limit**
1	0.65	0.47	0.82
2	1.20	0.97	1.43
3	-2.00	-28.03	24.03
4	17.00	12.72	21.29

Table 4.4: Calibrated recharge rates and 95% confidence intervals for models with 18 recharge zones and 14C input activities based purely on unsaturated zone thickness (Figure 4.5(b))

Model with eighteen recharge zones and ^{14}C boundary based on unsaturated zone thickness			
Recharge zone	**Recharge rate (mm y^{-1})**	**Upper 95% limit**	**Lower 95% limit**
1	-1.37	-42.41	39.66
2	19.95	-32.01	71.91
3	3.65	-2.88	10.18
4	5.00	-3.05	13.05
5	3.79	-2.25	9.83
6	-1.00	-7.90	5.90
7	10.32	-56.33	76.97
8	13.05	-97.34	123.45
9	-0.09	-22.66	22.48
10	-0.08	-2.34	2.19
11	0.28	-0.76	1.32
12	0.01	-0.58	0.61
13	8.70	3.18	14.23
14	2.00	1.33	2.67
15	2.00	-33.05	37.05
16	2.67	-23.68	29.03
17	0.75	-22.40	23.90
18	-1.00	-31.22	29.22

elsewhere in the basin (most likely through plant transpiration). Tree roots in the study area are thought to extend to at least 10 m depth in parts of the basin (Wood et al., 2014), however work in similar environments

in central Australia has demonstrated that plant roots may extend to at least 20 m below ground level (Reid et al., 2008). Likewise profiles of soil water potential in the Ti Tree Basin and similar environments have shown that upward movement of water is likely to occur from watertables up to 20 m below ground, where soil water potentials as low as -10 mega Pascals (MP) have been observed (Cook et al., 2005).

Sensitivity analysis showed that overall confidence in estimates of spatial variability in recharge may be low, with wide confidence intervals on recharge estimates for some zones. The widest confidence intervals were for mountain front recharge zones along the northern boundary of the model. These zones were relatively small and had few or no observation data 'down gradient' of them. Reducing the number of recharge zones (amalgamating these mountain front recharge zones with larger parts of the model domain, Figure 4.8) did improve confidence in recharge estimates in these areas, however this also resulted in a poorer fit to model data, and our expert knowledge of mountain front recharge processes was not accommodated. The model fit to measured data was also sensitive to the boundary condition for transport (^{14}C input activities). A poorer fit was observed when the boundary condition was based solely on the relationship between unsaturated zone thickness and ^{14}C input activity (and not augmented with measurements of ^{14}C activity in groundwater near the watertable). Thus more accurate determination of spatial variability in ^{14}C input activities, achieved through measurement of ^{14}C activities near the watertable (in both the unsaturated zone and groundwater) can help improve model calibration.

Temporal variability in recharge has not been considered in this study, despite it being an important process in the Ti Tree Basin. The intense rainfall events and flooding that generate recharge occur approximately once every 5 - 10 years in the basin (Harrington et al., 2002). Such periodic flooding is thought to have been occurring throughout the past 20,000 years in the region (English et al., 2001). The lowest ^{14}C measurements in this study are ~6 to 8 pMC, which correspond to apparent ages of ~20,000 years, encapsulating the period over which periodic flooding has been occurring. Thus the recharge rates determined here are likely to represent long term averages for this period, and thus are useful for water resource planning and management to achieve long term sustainability.

Spatial variability in hydraulic conductivity, as well as recharge is likely to have an influence of the distribution of tracers such as ^{14}C (Sanford, 2011; McCallum et al., 2014; Kozuskanich et al., 2014). The conductivity field used in our model is based on available drilling and aquifer testing, however it is a simplification of the real hydraulic conductivity distribution. Nevertheless this study demonstrates that spatial variability in ^{14}C input activity (^{14}C activities at the watertable) is equally important in obtaining good model fit, and thus a significant constraint on modelling ^{14}C transport. Also we do not consider the influence of geochemical reactions such as carbonate weathering or oxidation of organic carbon, which may lower the activity of ^{14}C in an aquifer. Salmon et al. (2014) have developed a modelling framework for simulating the influence of such geochemistry on ^{14}C age within an aquifer, which represents an important step forward in modelling ^{14}C transport in groundwater. Though our study does not incorporate this reactive transport component, the demonstrated influence of boundary conditions for ^{14}C transport will likely

inform future studies which attempt to simulate ^{14}C transport, reactivity, and ^{14}C derived age.

We have not made a direct comparison between modelled groundwater age and ^{14}C estimated age, as previous studies have done (eg. Sanford et al. (2004)). This would be difficult in our case, as a particle tracking model would be needed to 'back track' the recharge location of ^{14}C measurement points in the model, and then determine the ^{14}C input activity (from the map of spatially variable ^{14}C inputs (Figure 4.5)) in order to provide an estimate of ^{14}C age. However the particle tracking method does not account for the influence of diffusion, which is important in defining the ^{14}C distribution where recharge is < 1 mm y^{-1} (Walker and Cook, 1991), which is the case for large parts of our model. Thus modelling tracer concentrations directly is more appropriate in this case.

Previous studies have shown the value of collecting spatially distributed tracer data and vertical profiles of age tracers for determining spatial variability in recharge (Robertson and Cherry, 1989; Solomon et al., 1992). These previous studies have considered 2D conceptual and numerical models to interpret tracer data. The present study builds upon this previous work by demonstrating the value that a spatially distributed set of age tracer data can provide in determining spatial variability in recharge across an entire basin with the use of a 3D flow and transport model. Determining regional scale variability in recharge is complex, and often involves a multidisciplinary approach where various aspects of recharge are investigated separately (eg. mountain front recharge, ephemeral river recharge, diffuse recharge (Bartolino and Cole, 2002)). Though a significant amount of previous work has been conducted in the Ti Tree Basin which has assisted our study (Calf et al., 1991; Harrington et al., 2002, Knapton, 2007), the ^{14}C data set presented here and interpretation through transport modelling has greatly improved our understanding of spatial variability in recharge and importance of different recharge processes. This would not have been possible without the measurement of unsaturated zone ^{14}C and ^{14}C activities in groundwater near the watertable. With an increase in the number of studies in which environmental tracer concentrations are interpreted with a solute transport model (Turnadge and Smerdon, 2014), these findings will be useful in the design and implementation of future environmental tracer studies.

4.6 Conclusion

Environmental tracers such as ^{14}C are finding increasing use as tools to help numerical model calibration, particularly using a solute transport modelling approach. However the suitability of such tracers to solute transport problems has not been extensively tested in 3D models, and is limited by understanding of tracer input concentrations which may vary spatially. This study demonstrates that incorporation of a spatially variable boundary condition for ^{14}C input into a regional groundwater flow and solute transport model greatly improves the use of ^{14}C as a calibration target. Recharge rates obtained from the calibrated model are in good agreement with existing estimates, helping to validate model results. Measurement of environmental tracer data near the watertable (either directly below in groundwater or above in the unsaturated

zone) provides the best way to understand the spatial variability in tracer inputs. These findings will help inform future studies of both measurement and modelling of environmental tracers such as ^{14}C.

Acknowledgements

The authors wish to thank the Northern Territory Government staff and drilling department, for technical support and field assistance throughout this project. Bob Read is thanked for field assistance, supervising drilling and logging of the bores in this study, and staff and students at Flinders University who assisted on field trips are also thanked. Bores were installed utilising funding from the Australian Government National Collaborative Research Infrastructure Scheme (NCRIS) Groundwater Infrastructure Program. Analysis of unsaturated zone ^{14}C and twelve of the groundwater samples was funded by an Australian Institute of Nuclear Science and Engineering (AINSE) grant (ALNGRA12042) under the Isotopes for Water project. Additional funding was provided by the Australian Research Council and the National Water Commission. Cameron Wood was supported with an Australian Postgraduate Award and a National Centre for Groundwater Research and Training scholarship.

Sturt's desert rose (*Gossypium sturtianum*) and an incoming storm near the Woodforde River and southern basin margin, January 2014

5 Conclusion

5.1 Summary of findings

The three studies in this thesis investigated the use of ^{14}C as a tracer in groundwater, particularly to investigate spatial variability in recharge in an arid environment. The key findings of these studies were:

1. Unsaturated zone ^{14}C activities directly above the watertable ranged from 54 to 106 pMC in the Ti Tree Basin. The reason for non-modern ^{14}C in unsaturated zone gas likely relates to mineral precipitation-dissolution fluxes in the capillary zone (release of 'old' CO_2 during calcite precipitation). Modelling showed that where these processes are homogeneous, spatial variation in unsaturated zone thickness leads to spatial variation in ^{14}C activities of unsaturated zone gas directly above the watertable (lower ^{14}C activities where unsaturated zones are thicker).

2. Spatial variability of ^{14}C in unsaturated zone gas and spatial variability in recharge both influence the distribution of ^{14}C in groundwater. In arid areas where recharge is low, diffusive transport of ^{14}C adds an additional complication to interpreting ^{14}C activities in groundwater. In these cases, vertical profiles of ^{14}C in groundwater are needed, otherwise recharge estimated from discrete points may be wrong by more than one order of magnitude. Measurement of vertical profiles of ^{14}C in groundwater and understanding of ^{14}C activities in unsaturated zone gas yields significant insight into spatial variability in recharge. Applied to the Ti Tree Basin, this revealed mountain front recharge and preferential recharge through ephemeral surface water to be important processes.

3. Synthesizing the first two studies in this thesis, spatially distributed measurements of ^{14}C in groundwater were used as calibration targets in a 3D flow and solute transport model of the Ti Tree Basin. The boundary condition for ^{14}C (^{14}C input activities) was constrained by measurement of ^{14}C in unsaturated zone gas and in groundwater close to the watertable. Calibration was achieved by altering recharge within 18 separate zones, resulting in a map of spatially variable recharge. Sensitivity analysis demonstrated the importance of understanding the boundary condition for ^{14}C in solute transport modelling.

5.2 Future work

The first study in this thesis drew conclusions relating the ^{14}C activity of unsaturated zone gas directly above the watertable to unsaturated zone thickness (where there is a source of 'old' CO_2 present). This was based on measurement of unsaturated zone gas at five sites in the Ti Tree Basin, one of which did not follow this trend. Further measurements of unsaturated zone ^{14}C in the Ti Tree Basin and other arid and semi-arid environments would greatly improve our understanding of this relationship.

Furthermore, we model dilution of unsaturated zone ^{14}C through production of 'old' CO_2 in the unsaturated zone, most likely from mineral precipitation-dissolution fluxes (eg. calcite precipitation). Our understanding of this 'production' process is limited by our measurements (eg. we did not measure the carbon

isotope composition of minerals in the unsaturated zone). Better characterisation of this process through measurement of carbon isotopes of minerals and more detailed geochemical modelling (eg. Gillon et al. (2009)) would help elucidate this process, and how it may vary with different unsaturated zone lithology/mineralogy.

The 2D and 3D models of groundwater flow and ^{14}C transport in this thesis do not consider the influence of geochemical interactions within in the aquifer on ^{14}C activities. Though this is partially supported by our $\delta^{13}C$ data, application of a reactive transport model (such as that of Salmon et al. (2014)) would help test the sensitivity of our model results to this assumption. Heterogeneity is likewise known to influence the distribution of age tracers such as ^{14}C in groundwater (McCallum et al., 2014; Kozuskanich et al., 2014), however our models are relatively simple in terms of conductivity distribution (homogeneous in Chapter 3, and only conductivity only varies with a few zones in the model in Chapter 4). Thus further work could also be done to incorporate heterogeneity into assessments of spatial variability in recharge with ^{14}C.

Chapter 4 demonstrates that better characterisation of boundary conditions for age tracers (such as ^{14}C) in solute transport models is needed, particularly for determining spatial variability in recharge. Future studies that incorporate such tracers could constrain this through measurement of tracers close to the watertable (either in groundwater or in the unsaturated zone). With an increasing number of studies using solute transport models to interpret age tracer data (Turnadge and Smerdon, 2014), these findings are timely and offer useful guidance to future researchers and practitioners.

Campsite near the Woodforde River at dusk, June 2014

6 Appendices

6.1 Appendix 1 - Data

The main focus of this thesis has been the use of carbon-14 (^{14}C) as a tracer for investigating spatial variability in groundwater recharge. While collecting samples for ^{14}C analysis in the Ti Tree Basin, additional samples for major ion chemistry, stable isotopes of water ($\delta^{2}H$ and $\delta^{18}O$) and strontium isotope ratios ($^{87}Sr/^{86}Sr$) were collected and analysed. All of this data, along with carbon isotope data (in groundwater and unsaturated zone gas) is presented here. Appendix 2 follows with a brief discussion of this data.

Noble gas (^{4}He, ^{40}Ar, ^{20}Ne) data was also collected as part of this study, and is presented and discussed in Appendix 3.

Bore ID	Site	Easting	Northing	Date sampled	Depth (m-bgl)	^{14}C (pMC)	^{14}C error (± pMC)	$\delta^{13}C$ (‰ PDB)	CO_2 (ppm)	CO_2 duplicate (ppm)	CFC-11 (pptv)	CFC-11 duplicate (pptv)	CFC-12 (pptv)	CFC-12 duplicate (pptv)
18611-5	Site A	369180	7508295	6/09/2011	5	105.26	0.44	-15.70	7476	-	206.56	197.04	504.74	471.12
18611-8	Site A	369180	7508295	6/09/2011	8	106.84	0.48	-17.10	12821	12544	205.39	194.58	474.18	471.12
18611-11	Site A	369180	7508295	6/09/2011	11	104.26	0.42	-16.80	14264	14389	189.14	-	427.81	-
18611-16	Site A	369180	7508295	6/09/2011	16	94.61	0.39	-15.90	14049	14131	136.72	-	342.32	-
18611-21	Site A	369180	7508295	6/09/2011	21	80.30	0.39	-16.00	18445	18314	84.97	-	202.07	-
18611-26	Site A	369180	7508295	6/09/2011	26	72.63	0.33	-15.90	18103	18415	-	-	-	-
18779-5	Site B	369138	7515709	7/09/2011	5	107.39	0.55	-14.30	10686	-	178.05	-	445.56	-
18779-8	Site B	369138	7515709	7/09/2011	8	107.95	0.48	-15.60	13248	13223	199.92	191.95	482.34	469.11
18779-11	Site B	369138	7515709	7/09/2011	11	107.03	0.42	-15.20	14725	-	192.82	182.35	466.01	437.88
18779-16	Site B	369138	7515709	7/09/2011	16	92.91	0.38	-15.+80	15864	15589	151.86	147.69	400.35	387.96
18779-21	Site B	369138	7515709	7/09/2011	21	79.14	0.36	-16.00	12018	12140	150.19	140.90	375.55	372.87
18781-5	Site C	369089	7522002	7/09/2011	5	107.34	0.53	-15.10	6626	-	-	-	-	-
18781-8	Site C	369089	7522002	7/09/2011	8	104.73	-	-14.80	10995	10410	-	-	-	-
18781-11	Site C	369089	7522002	7/09/2011	11	89.49	0.38	-13.90	10672	-	-	-	-	-
18781-16	Site C	369089	7522002	7/09/2011	16	54.55	0.28	-14.20	9551	9633	-	-	-	-
18893-3	Site D	347207	7535112	11/08/2012	3	108.00	0.44	-15.40	4115	-	217.56	217.22	492.72	481.81
18893-5	Site D	347207	7535112	11/08/2012	5	104.99	0.37	-15.10	13114	-	197.53	210.73	475.90	476.62
18893-10	Site D	347207	7535112	11/08/2012	10	104.31	0.33	-16.80	28174	28338	195.29	191.33	435.62	433.48
18893-12	Site D	347207	7535112	11/08/2012	12	101.32	0.31	-16.60	27071	-	181.30	184.24	441.91	402.00
18893-15	Site D	347207	7535112	11/08/2012	15	95.38	0.36	-16.60	29003	-	173.81	159.93	406.39	361.89
18893-18	Site D	347207	7535112	11/08/2012	18	86.20	0.32	-15.10	11191	11276	191.16	154.79	480.32	369.49
18897-5	Site E	359844	7534757	11/08/2012	5	102.61	0.44	-13.50	3700	3318	209.70	197.87	498.62	492.69
18897-6	Site E	359844	7534757	11/08/2012	6	108.69	0.35	-15.10	7861	7777	213.29	216.19	481.86	500.67
18897-7	Site E	359844	7534757	11/08/2012	7	107.05	0.40	-14.70	10021	9894	215.17	213.80	493.83	486.99
18897-8	Site E	359844	7534757	11/08/2012	8	106.42	0.36	-14.30	10303	-	213.80	213.46	500.63	504.66

Table 6.1: Unsaturated zone gas data (m-bgl denotes metres below ground level).

Bore ID	Easting	Northing	Date sampled	Bore elevation (m-AHD)	Watertable (m-AHD)	Depth to water (m-TOC)	Depth from watertable to midpoint of screen (m)	EC (μS cm^{-1})	pH	Temperature (ºC)	Alkalinity (mg L^{-1} as $CaCO_3$)	Notes
18611-2	369180	7508295	6/09/2011	578.746	546.70	32.05	2.05	2165	7.88	30.5	270	Site A
18611-1	369180	7508295	6/09/2011	578.749	546.70	32.05	8.54	2036	7.49	29	-	Site A
18610-2	369180	7508305	5/09/2011	578.634	546.66	31.97	16.78	1979	7.45	29.5	213	Site A
18610-1	369180	7508305	5/09/2011	578.643	546.70	31.94	25.93	2058	7.42	29.7	-	Site A
18609	369180	7508300	5/09/2011	578.601	546.71	31.90	41.13	2000	7.3	29.8	198	Site A
18779-2	369138	7515709	4/09/2011	567.608	541.31	26.30	6.48	1458	7.49	29.2	182	Site B
18779-1	369138	7515709	4/09/2011	567.479	541.31	26.17	13.46	1482	7.52	29.8	197	Site B
18614-3	369134	7515706	4/09/2011	567.671	541.32	26.36	19.03	1498	7.5	29.7	202	Site B
18614-2	369134	7515706	4/09/2011	567.589	541.32	26.27	26.45	1510	7.53	30.1	217	Site B
18614-1	369134	7515706	4/09/2011	567.532	541.34	26.19	36.80	1450	7.47	30.2	240	Site B
18781-2	369089	7522002	3/09/2011	558.525	538.76	19.77	5.90	908	6.89	28.9	270	Site C
18781-1	369089	7522002	3/09/2011	558.431	538.77	19.66	18.49	904	6.85	29.3	248	Site C
18780-3	369085	7521999	3/09/2011	558.550	538.76	19.79	28.67	933	6.79	29.8	-	Site C
18780-2	369085	7521999	3/09/2011	558.492	538.74	19.75	39.40	1009	6.8	30	214	Site C
18780-1	369085	7521999	3/09/2011	558.449	538.75	19.70	51.50	1136	6.73	30	210	Site C
18893-2	347207	7535112	8/08/2012	567.734	546.50	21.23	4.68	-	-	-	-	Site D
18893-1	347207	7535112	8/08/2012	567.728	546.49	21.24	18.07	2230	6.88	29.1	107	Site D
18892-3	347213	7535112	8/08/2012	567.765	546.47	21.30	28.22	2280	6.905	29.2	123	Site D
18892-2	347213	7535112	8/08/2012	567.721	546.45	21.27	40.73	2400	6.83	29.5	139	Site D
18892-1	347213	7535112	8/08/2012	567.717	546.47	21.25	53.75	2350	6.79	29.9	124	Site D
18897-2	359844	7534757	9/08/2012	550.257	541.46	8.80	4.20	1010	7.5	28.9	202	Site E
18897-1	359844	7534757	9/08/2012	550.276	541.46	8.82	10.98	1242	7.33	29.1	174	Site E
18896-3	359848	7534761	9/08/2012	550.243	541.42	8.82	13.78	1346	7.22	29.3	189	Site E
18896-2	359848	7534761	9/08/2012	550.263	541.45	8.82	17.19	1682	7.2	29.3	166	Site E
18896-1	359848	7534761	9/08/2012	550.271	541.45	8.82	22.18	1691	7.2	29.7	175.5	Site E

Table 6.2: Location and field parameters (during sampling) of piezometers at sites where soil gas profiles were collected.

Bore ID	TDS	Na	K	Ca	Mg	Cl	HCO3	SO4	NO3	Sr	Br	Si	$\delta^{18}O$	$\delta^{2}H$	^{14}C	$\delta^{13}C$	TDIC	$^{87}Sr/^{86}Sr$
	mg L^{-1}												‰ SMOW		pMC	‰ PDB	mmol kg^{-1}	
18611-2	1434	257	25.6	68.6	37.6	370	286.15	200	94	0.783	2.3	36.3	-7.2	-52.3	52.5	-8.80	5.96	.734224
18611-1	1349	240	27	72.9	39.8	350	246.20	180	99	0.817	2.1	37	-7.3	-53.5	22.8	-7.40	5.10	.736235
18610-2	1309	221	23.6	69.2	35.7	350	241.80	180	98	0.745	2.0	35.2	-7.4	-52.9	13.0	-7.00	4.80	.738264
18610-1	1308	222	21.3	66.9	33.7	340	246.20	200	88	0.73	2.1	33.1	-7.4	-53.1	9.9	-6.80	5.00	.740555
18609	1249	228	18.3	59.4	29.6	340	240.71	180	71	0.662	1.8	29.4	-7.4	-52.6	8.1	-6.80	4.80	.743526
18779-2	917	119	20.1	55.7	30.9	220	211.24	110	82	0.689	1.5	35.1	-6.7	-49.5	21.4	-6.80	4.40	.744879
18779-1	969	155	20.2	59	31	210	214.60	130	72	0.732	1.4	35.2	-6.7	-49.6	13.1	-6.50	4.40	.748374
18614-3	976	151	18.2	53.5	27.6	220	217.28	140	74	0.664	1.4	33.1	-6.7	-50.5	12.9	-6.40	4.50	.748179
18614-2	990	152	18.5	53.4	27.5	220	218.99	150	73	0.675	1.4	32.9	-6.8	-49.5	12.6	-6.80	4.50	.748632
18614-1	957	152	20.5	59.6	30.9	210	216.86	120	73	0.74	1.4	35.1	-6.8	-49.0	12.6	-6.70	4.50	.750130
18781-2	666	106	18.8	33.6	23.9	73	228.99	52	71	0.469	0.7	41	-7.2	-52.3	44.3	-7.00	4.70	.741221
18781-1	660	105	17.3	31.5	21.8	71	231.37	55	70	0.423	0.6	39.1	-7.1	-51.9	44.3	-7.00	4.80	.742251
18780-3	678	109	16.1	30.5	18.5	70	238.51	69	69	0.389	0.7	35.5	-7.0	-51.6	39.1	-7.00	4.90	.742513
18780-2	718	114	15.9	32.2	17	77	242.60	91	66	0.38	0.7	35.5	-6.9	-50.4	36.0	-6.80	5.00	.746271
18780-1	800	126	16.8	39	19.6	100	242.96	120	69	0.429	0.8	33.1	-6.8	-48.7	25.4	-6.90	5.00	.750380
18893-2	1238	250	43.8	121	87.8	414	-	209	8.6	1.31	2.5	23.5	-	-	-	-	-	-
18893-1	1337	165	37	97.7	73.2	478	174.8	158	68	1.14	2.1	34	-7.4	-54.2	21.8	-7.81	3.2	-
18892-3	1426	195	36.1	98.4	70.4	487	177.8	197	64	1.13	2.2	35.8	-7.4	-53.3	20.8	-7.98	3.3	-
18892-2	1587	228	33.3	108	65.8	518	185.7	277	50	1.07	2.1	34.8	-7.8	-55.5	16.3	-7.70	3.4	-
18892-1	1512	180	35.3	140	73.2	496	172.3	251	44	1.14	2.0	37.3	-7.9	-55.1	12.8	-7.29	3.1	-
18897-2	755	87.9	23.5	45.7	28.8	99	281.9	63	65	0.519	0.4	39.3	-7.4	-55.4	66.4	-6.13	4.7	-
18897-1	873	104	25.3	61.8	34.3	175	255.1	88	64	0.602	0.7	38.5	-7.4	-54.1	50.9	-6.80	4.2	-
18896-3	943	114	26	68	36.8	214	238.3	110	63	0.659	0.9	39.3	-	-	40.8	-6.62	3.9	-
18896-2	1127	151	27.2	81.4	41.1	288	220.0	170	59	0.745	1.2	36	-7.4	-53.0	18.6	-7.23	3.8	-
18896-1	1160	167	24.9	79.6	37.1	275	233.1	201	51	0.729	1.1	28.3	-7.5	-52.5	13.9	-7.50	3.9	-

Table 6.3: Dissolved ion and isotopic content of groundwater samples from piezometers at sites where soil gas profiles were collected.

Bore ID	Easting	Northing	Date sampled	Bore elevation (m-AHD)	Watertable (m-AHD)	Depth to water (m-TOC)	Depth from watertable to midpoint of screen (m)	EC (μS cm^{-1})	pH	Temperature (ºC)	Alkalinity (mg L^{-1}as $CaCO_3$)	Notes
18600	327733	7527886	30/08/2011	595.157	591.90	3.26	2.84	79.3	5.71	22.6	33.3	Woodforde River perched aquifer
18603-2	328734	7531957	31/08/2011	589.395	552.13	37.27	9.69	1347	7.44	28	572	
18603-1	328734	7531957	31/08/2011	589.413	552.11	37.30	22.92	2058	7.15	28.3	460	
18605-2	328734	7531438	31/08/2011	589.627	552.12	37.51	9.37	1642	7.47	31.3	500	
18605-1	328734	7531438	31/08/2011	589.634	552.09	37.54	18.76	1389	7.23	29.2	539	
18608-1	327045	7522693	23/11/2011	604.978	553.45	51.53	22.21	1166	6.92	32.1	291	
18889	327692	7527955	30/06/2012	596.261	591.84	4.42	3.64	50.2	5.64	25.2	21	Woodforde River perched aquifer
18888	327717	7527957	30/06/2012	595.979	591.76	4.22	4.85	88.7	5.74	26	36	Woodforde River perched aquifer
18891	329034	7532344	30/06/2012	588.640	582.67	5.97	1.58	537.2	6.29	19	-	Woodforde River perched aquifer
18337	328738	7527627	13/08/2012	595.041	552.57	42.47	8.93	1675	6.98	30.1	312	
18336-1	328254	7527873	13/08/2012	594.678	552.69	41.99	10.17	1048	7.061	29.9	337	
18336-2	328254	7527873	13/08/2012	594.578	552.61	41.97	19.29	973	7.071	29.9	276	

Table 6.4: Location and field parameters (during sampling) of piezometers near the Woodforde River. Bore elevations are taken at the top of casing (TOC).

Bore ID	TDS	Na	K	Ca	Mg	Cl	HCO_3	SO_4	NO_3	Sr	Br	Si	$\delta^{18}O$	$\delta^{2}H$	^{14}C	$\delta^{13}C$	TDIC	$^{87}Sr/^{86}Sr$
	mg L^{-1}												‰ SMOW		pMC	‰ PDB	mmol kg^{-1}	
18600	61	4.41	3.4	4.15	2.32	3.5	33.00	1.2	0.06	<0.05	0.06	8.7	-9.1	-58.7	96.4	-11.70	0.70	.750399
18603-2	1033	190	26.6	35.5	29.6	47	581.33	59	12	0.535	0.5	31.3	-9.1	-61.7	79.9	-10.80	11.60	.736941
18603-1	1363	221	20.9	66.1	49.9	300	412.12	180	30	0.852	1.5	31.5	-8.4	-56.4	66.1	-9.30	8.40	.741052
18605-2	1042	198	20.2	30.1	29.4	60	489.65	130	15	0.45	0.4	31.6	-9.6	-66.9	73.7	-10.70	9.90	.736646
18605-1	1069	196	23.2	42.2	33.8	72	534.24	82	24	0.604	0.7	33.6	-9.2	-64.2	73.9	-9.90	10.90	.738604
18608-1	842	137	11.7	43.2	26.6	150	317.20	87	10	0.509	0.95	32.1	-8.0	-55.7	39.9	-10.30	6.00	-
18889	49	4.32	3.16	3.1	1.4	2.8	25.8	1.7	<0.05	<0.05	<0.05	5.71	-11.1	-73.2	-	-	-	-
18888	82	5.83	4.81	6.55	3.1	2.8	49.7	2.3	<0.05	0.0506	<0.05	6.19	-10.4	-68.4	104.5	-15.80	1.18	-
18891	452	65.9	11.4	32.8	10.8	50	164.7	80	0.78	0.264	0.33	8.83	-11.0	-75.3	59.4	-16.80	3.40	-
18337	1228	170	20.8	73.7	51.1	272	395.0	140	32	0.788	1.2	29.5	-8.6	-58.4	66.2	-9.86	6.70	-
18336-1	857	117	17.6	46.7	31.7	90	444.1	49	14	0.506	0.4	30.5	-9.0	-59.1	74.9	-9.84	7.40	-
18336-2	784	115	13.6	40.2	26.1	83	396.1	50	13	0.41	0.4	30.5	-8.6	-58.0	72.3	-10.00	6.70	-

Table 6.5: Dissolved ion and isotopic content of groundwater samples from piezometers near the Woodforde River.

Bore ID	Easting	Northing	Date sampled	Bore elevation (m-AHD)	Watertable (m-AHD)	Depth to water (m-TOC)	Depth from watertable to midpoint of screen (m)	EC (μS cm^{-1})	pH	Temperature (ºC)	Alkalinity (mg L^{-1} as $CaCO_3$)
18830	366015	7593896	27/06/2012	475.882	472.60	3.28	2.61	93900	7.1	26.5	-
18829-3	366017	7593895	1/07/2012	475.765	472.68	3.23	4.27	105500	7.8	26.5	1000
18829-2	366017	7593895	27/06/2012	475.908	472.65	3.26	7.16	-	-	-	-
18829-1	366017	7593895	27/06/2012	475.911	472.64	3.13	9.28	99500	8.3	26.6	2600
18882	366909	7593265	27/06/2012	475.301	472.94	2.36	1.70	40025	7.99	25.5	1750
18881-1	366911	7593264	27/06/2012	475.304	472.60	2.70	4.20	105033	8.49	26.1	1320
18881-2	366911	7593264	27/06/2012	475.293	472.60	2.69	5.81	121785	8.6	26.9	1460
18881-3	366911	7593264	27/06/2012	475.243	472.54	2.70	7.25	123622	8.26	27.2	1440
18828	367430	7592891	27/06/2012	475.367	473.05	2.32	1.42	104400	7.4	23.9	2070
18827-3	367431	7592890	27/06/2012	475.304	473.12	2.27	4.03	131300	7.53	25	2100
18827-2	367431	7592890	28/06/2012	475.392	473.13	2.27	4.99	-	-	-	-
18827-1	367431	7592890	27/06/2012	475.391	473.08	2.22	8.91	123500	8	23.7	1550
18885	367840	7591685	29/06/2012	475.781	473.46	2.32	2.04	119700	7.32	23.9	2120
18884-1	367842	7591686	29/06/2012	475.733	473.51	2.22	2.61	125973	9.4	24.7	2350
18884-2	367842	7591686	29/06/2012	475.699	473.58	2.12	5.63	131411	10.14	25.5	2590
18884-3	367842	7591686	29/06/2012	475.676	473.46	2.22	9.07	128075	7.22	25.3	2190
18824-1	368372	7591169	28/06/2012	475.739	473.88	1.86	2.24	117600	7.22	24.2	2250
18824-2	368372	7591169	1/07/2012	475.756	473.86	1.90	6.19	121700	7.19	24.5	2200
18823-1	368372	7591167	30/06/2012	475.701	473.80	1.90	8.56	122989	7.84	24.1	1870
18823-2	368372	7591167	1/07/2012	475.739	473.86	1.88	9.92	122900	7.3	24.7	2310

Table 6.6: Location and field parameters (during sampling) of piezometers in Stirling Swamp. Bore elevations are taken at the top of casing (TOC).

Bore ID	TDS	Na	K	Ca	Mg	Cl	HCO_3	SO_4	NO_3	Sr	Br	Si	$\delta^{18}O$	$\delta^{2}H$	^{14}C	$\delta^{13}C$
	mg L^{-1}												‰ SMOW		pMC	‰ PDB
18830	95416	22700	3550	731	3740	36435	163.1	20896	66	15	207	<10	-4.8	-48.1	85.5	-4.50
18829-3	111852	26400	4090	693	4350	42251	194.6	25238	120	13.8	243	<10	-4.4	-46.9	70.8	-7.00
18829-2	80676	23900	4190	1410	417	40955	107.0	7098	41	40.5	192	<10	-3.5	-43.9	56.0	-19.60
18829-1	101147	24200	3790	735	3580	39848	233.1	21490	85	13.3	229	<10	-4.5	-45.8	79.5	-6.60
18882	36859	8710	1360	662	944	11488	232.3	10060	37	14	65	<5	-3.8	-24.8	104.1	-11.90
18881-1	106126	27800	3870	729	2530	42289	190.3	21526	44	11.1	238	<10	-3.9	-37.9	83.4	-8.20
18881-2	133320	34000	4670	700	3630	54832	177.7	26599	37	11.3	310	<10	-3.9	-41.8	81.4	-8.80
18881-3	136285	34200	4700	672	4410	53747	180.4	28737	46	11.9	307	<10	-4.0	-43.0	79.5	-8.30
18828	108014	26600	4170	675	2970	42215	279.0	23339	50	14.1	238	<10	-4.7	-41.9	107.5	-6.70
18827-3	148672	37300	5630	621	4190	57764	200.6	31829	674	12.8	317	<10	-3.4	-42.7	83.6	-4.40
18827-2	120776	37100	5600	1060	-	56620	1604.3	13522	578	7.65	324	<10	-3.3	-39.9	-	-
18827-1	137038	34600	5280	646	3680	53169	261.8	29192	518	11.7	309	<10	-3.8	-39.3	89.7	-5.70
18885	127495	32300	4640	691	3730	50894	189.9	25184	1542	13.5	300	<10	-1.1	-24.0	86.2	-5.30
18884-1	134798	35200	5200	808	2720	54188	322.2	26532	1212	12	321	<10	-2.0	-30.8	64.2	-8.90
18884-2	121486	37000	5510	1300	378	59063	150.2	12607	1025	12.5	342	<10	-2.5	-36.6	-	-
18884-3	145933	36500	5130	646	4700	55614	190.4	31776	854	12.5	338	<10	-3.4	-39.5	60.9	-8.00
18824-1	130103	32100	5580	590	3240	47391	290.8	26774	5308	13.5	295	<10	-3.3	-35.4	95.6	-3.80
18824-2	135242	34100	5710	637	3350	49647	270.5	27172	5373	13.9	315	<10	-3.5	-38.6	87.2	-5.00
18823-1	136152	34400	5700	663	3270	50755	250.2	26961	5243	13.2	319	<10	-3.5	-41.1	86.1	-5.70
18823-2	136714	33900	5710	661	3320	51033	323.2	27394	5278	13.8	322	<10	-3.7	-40.1	86.6	-5.60

Table 6.7: Dissolved ion and isotopic content of groundwater samples from piezometers in Stirling Swamp.

Bore ID	Easting	Northing	Date sampled	Bore elevation (m-AHD)	Watertable (m-AHD)	Depth to water (m-TOC)	Depth from watertable to midpoint of screen (m)	EC (μS cm^{-1})	pH	Temperature (ºC)	Alkalinity (mg L^{-1} as $CaCO_3$)
18134-2	359838	7509488	3/02/2012	575.898	549.68	26.22	7.69	823	7.07	30	289
18134-1	359838	7509488	3/02/2012	575.873	549.67	26.20	24.29	1051	7.01	29.9	224
18133-3	359838	7509493	3/02/2012	575.809	549.60	26.21	28.19	1086	6.95	30.1	195
18133-2	359838	7509493	3/02/2012	575.767	549.65	26.12	37.01	1308	6.94	30.3	204
18133-1	359838	7509493	3/02/2012	575.741	549.67	26.07	46.51	1265	6.87	30.4	159
18136-2	365420	7508771	4/02/2012	577.810	547.67	30.14	4.01	1734	7.17	30.5	259
18136-1	365420	7508771	4/02/2012	577.786	547.66	30.12	12.49	1565	7.14	29.7	228
18135-3	365424	7508780	4/02/2012	577.750	547.67	30.08	18.54	1565	7.03	30.2	260
18135-2	365424	7508780	4/02/2012	577.732	547.67	30.06	28.14	1494	6.93	30.3	222
18135-1	365424	7508780	4/02/2012	577.744	547.67	30.07	39.44	1400	6.93	30.3	204
18138-2	369052	7526605	5/02/2012	550.276	535.95	14.32	7.43	880	7.31	29.8	297
18138-1	369052	7526605	5/02/2012	550.272	535.95	14.32	14.87	853	7.32	29.8	243
18137-3	369048	7526601	5/02/2012	550.272	535.92	14.36	25.97	963	7.36	30	230
18137-2	369048	7526601	5/02/2012	550.288	535.91	14.38	33.50	993	7.3	30.1	233
18137-1	369048	7526601	5/02/2012	550.231	535.89	14.34	37.16	1129	7.1	30.4	226
18140-2	369028	7530582	6/02/2012	545.290	533.37	11.92	4.81	968	7.35	29.2	269
18140-1	369028	7530582	6/02/2012	545.279	533.40	11.88	15.90	1083	7.29	29.5	295
18139-3	369021	7530574	6/02/2012	545.282	533.39	11.89	30.91	1100	7.27	29.7	247
18139-2	369021	7530574	6/02/2012	545.271	533.40	11.87	37.79	1159	7.23	30	239
18139-1	369021	7530574	6/02/2012	545.236	533.40	11.84	47.16	1217	7.12	30.4	200
18899-2	347904	7510838	10/08/2012	585.481	551.33	34.15	6.75	1831	7.24	29.1	202
18899-1	347904	7510838	10/08/2012	585.510	551.31	34.20	13.80	1864	7.19	29.2	218.5
18898-3	347898	7510838	10/08/2012	585.430	551.31	34.12	20.88	1865	7.14	29.3	194
18898-2	347898	7510838	10/08/2012	585.447	551.32	34.13	29.37	1867	7.13	29.5	205
18898-1	347898	7510838	10/08/2012	585.475	551.33	34.15	38.65	1808	7.05	30.2	188
18895-2	354322	7535196	8/08/2012	556.039	544.24	11.80	3.20	-	-	-	-
18895-1	354322	7535196	8/08/2012	556.058	544.23	11.83	6.72	1293	7.28	28.8	235
18894-3	354328	7535196	9/08/2012	556.015	544.16	11.86	12.14	1625	7.16	28.3	161
18894-2	354328	7535196	9/08/2012	556.049	544.16	11.89	18.11	1880	7.1	28.6	160
18894-1	354328	7535196	9/08/2012	556.048	544.16	11.89	22.11	2220	6.96	28.7	142.5

Table 6.8: Location and field parameters (during sampling) of piezometers in the central Ti Tree Basin and Allungra floodout area. Bore elevations are taken at the top of casing (TOC).

Bore ID	TDS	Na	K	Ca	Mg	Cl	HCO3	SO4	NO3	Sr	Br	Si	$\delta^{18}O$	$\delta^{2}H$	^{14}C (pmC)	$\delta^{13}C$	TDIC	$^{87}Sr/^{86}$ Sr
	mg L^{-1}												‰ SMOW		pMC	‰ PDB	mmol kg^{-1}	
18134-2	649	79.8	21.8	33.4	20.2	51.04	328.5	41.75	30.18	0.365	0.36	28.8	-7.7	-55.6	65.6	-9.16	5.57	.732294
18134-1	764	99.5	24.4	42.5	23.7	114.19	267.2	66.51	71.06	0.428	0.85	33.9	-7.1	-52.4	40.8	-6.89	4.48	.734441
18133-3	779	107	24.2	41.1	24	124.46	250.6	70.75	79.64	0.41	0.92	34.7	-7.0	-52.1	39.6	-5.50	-	.735337
18133-2	927	124	25.3	56.6	27.9	160.24	254.4	120.89	88.38	0.504	1.15	31.8	-6.6	-49.3	25.7	-5.60	-	.739410
18133-1	872	116	25.3	51.4	28.6	172.20	229.9	92.47	91.91	0.526	1.21	35.2	-6.7	-49.0	18.1	-4.90	-	.743851
18136-2	1119	164	24.5	69.2	34.1	257.38	143.0	125.42	229.03	0.697	1.69	32.9	-6.7	-50.5	33.8	-9.91	5.5	.740547
18136-1	1053	152	24.1	63.1	30.8	233.70	162.6	102.76	214.72	0.626	1.59	37	-6.7	-50.0	18.0	-6.74	4.67	.743181
18135-3	1074	164	20.9	59.3	27.2	221.13	224.5	127.18	150.42	0.615	1.48	34.3	-6.9	-50.5	21.9	-7.68	5.24	.742500
18135-2	1057	171	21.2	57.2	28.2	205.88	286.4	147.13	66.67	0.584	1.36	33.6	-6.9	-51.3	11.4	-5.60	-	.748173
18135-1	986	152	20.2	55.6	25.5	196.39	279.9	122.63	60.09	0.606	1.21	35	-7.0	-50.4	6.8	-5.50	-	.752870
18138-2	695	93.4	18.8	30.7	20.7	54.35	304.1	45.41	72.77	0.4	0.40	38.9	-7.2	-53.0	60.8	-6.00	-	.742648
18138-1	679	85.4	19.1	31.4	21.4	55.02	304.6	37.47	72.57	0.412	0.41	39	-7.2	-53.2	59.5	-5.80	-	.743337
18137-3	749	111	17.4	29.1	20.3	59.66	303.3	73.15	73.31	0.382	0.41	37.8	-7.2	-53.0	55.3	-7.00	-	.742152
18137-2	769	107	19.2	35.7	22.6	82.37	300.5	65.85	77.62	0.45	0.56	36.8	-7.1	-51.4	44.0	-6.30	-	.744926
18137-1	836	120	19	41.3	23.5	116.32	301.6	86.34	69.54	0.468	0.74	31.7	-7.0	-50.3	32.3	-5.20	-	.748949
18140-2	747	94.8	23.1	32.8	25.6	79.69	313.7	43.88	80.41	0.464	0.49	37.6	-7.3	-53.7	58.5	-6.70	5.24	.741599
18140-1	797	109	17.4	37.6	24.1	96.29	239.1	64.55	158.95	0.445	0.69	30.3	-7.2	-52.8	52.5	-7.60	5.35	.742556
18139-3	892	111	21.4	38.4	24	107.87	388.3	67.41	79.93	0.46	0.79	32.8	-7.0	-51.7	43.1	-6.60	-	.747519
18139-2	859	118	21.8	41	24	116.41	305.9	89.85	82.75	0.468	0.86	32.4	-7.0	-51.8	40.7	-7.14	-	.751124
18139-1	869	124	19.2	41.7	23.2	127.12	245.4	92.22	143.91	0.464	0.93	25.3	-7.1	-51.1	40.1	-8.00	5.39	.753218
18899-2	1197	205	28.2	60.4	37.8	324	264.3	137	67	0.747	1.8	28.5	-7.0	-50.0	34.6	-7.99	4.3	-
18899-1	1225	200	29.6	64.7	41.7	335	275.3	146	59	0.8	1.8	27.9	-6.9	-49.8	31.4	-8.00	4.6	-
18898-3	1228	207	28.9	60.1	39.2	340	254.9	148	74	0.751	1.9	29.8	-6.7	-49.1	26.4	-6.83	4.3	-
18898-2	1224	202	26.9	67.3	37.9	337	255.7	153	68	0.776	1.8	29.4	-6.7	-49.9	20.5	-6.35	4.3	-
18898-1	1193	192	27.1	66.7	38.7	333	248.0	145	64	0.753	1.8	33.8	-6.7	-50.8	14.0	-6.06	4.4	-
18895-2	-	113	32	74.1	41	103	-	55	136	0.717	0.7	41.6	-	-	-	-	-	-
18895-1	918	114	24.7	60.2	33.2	138	292.1	80	112	0.619	0.7	37.1	-7.6	-55.9	81.3	-8.62	5.1	-
18894-3	1110	128	29.7	80.9	48	274	207.3	134	128	0.852	1.3	37.9	-7.7	-55.0	46.2	-7.46	3.7	-
18894-2	1228	141	31.5	99.2	57.1	363	206.7	158	84	0.982	1.6	36.7	-7.7	-54.8	31.3	-7.39	3.7	-
18894-1	1408	175	33.7	110	62.8	459	193.6	214	59	1.05	1.9	35.3	-7.5	-54.1	20.2	-7.69	3.3	-

Table 6.9: Dissolved ion and isotopic content of groundwater samples from piezometers in the central Ti Tree Basin and Allungra floodout area.

Bore ID	Easting	Northing	Date sampled	Bore elevation (m-AHD)	Watertable (m-AHD)	Depth to water (m-TOC)	Depth from watertable to midpoint of screen (m)	EC (μS cm^{-1})	pH	Temperature (ºC)	Alkalinity (mg L^{-1} as $CaCO_3$)
18613-2	369229	7504045	6/09/2011	583.589	549.44	34.15	4.73	2468	7.58	28.9	258
18613-1	369229	7504045	6/09/2011	583.521	549.44	34.08	17.46	2519	7.44	29.2	232
18612-3	369231	7504050	6/09/2011	583.504	549.46	34.05	22.61	2717	7.33	29.5	207
18612-2	369231	7504050	6/09/2011	583.463	549.46	34.00	28.56	2985	7.5	30.1	248
18612-1	369231	7504050	6/09/2011	583.431	549.50	33.93	48.10	2610	7.42	30.7	230
18911-3	390887	7492173	14/08/2012	609.131	555.73	53.40	4.50	-	-	-	-
18911-2	390887	7492173	5/12/2012	609.131	555.73	53.40	10.53	-	-	-	-
18900-2	390887	7492167	14/08/2012	609.053	555.65	53.40	18.00	2130	7.10	33.1	146
18911-1	390887	7492173	14/08/2012	609.150	555.73	53.42	25.22	2050	7.12	34.3	132
18900-1	390887	7492167	14/08/2012	609.133	555.78	53.35	35.73	1966	7	32.2	135
18912-2	390807	7484707	15/08/2012	627.531	579.58	47.95	16.96	1126	7.43	32.1	150
18912-1	390807	7484707	15/08/2012	627.516	579.56	47.96	26.18	-	-	-	-

Table 6.10: Location and field parameters (during sampling) of piezometers in the south eastern Ti Tree Basin. Bore elevations are taken at the top of casing (TOC).

Bore ID	TDS	Na	K	Ca	Mg	Cl	HCO3	SO4	NO3	Sr	Br	Si	δ^{18}O	δ^{2}H	^{14}C	δ^{13}C	TDIC	^{87}Sr/^{86} Sr
	(mg L^{-1})												‰ SMOW		pMC	‰ PDB	mmol kg^{-1}	
18613-2	1622	310	24.6	72.6	42.4	450	266.63	280	63	0.81	2.3	31.6	-7.0	-50.6	25.2	-8.10	5.50	.733104
18613-1	1633	297	26	79.4	46.6	500	242.41	260	76	0.891	2.4	30.6	-6.7	-49.3	17.3	-7.40	5.00	.733954
18612-3	1700	305	25.2	85.8	44.9	550	243.39	270	66	0.906	2.6	26.1	-6.7	-49.3	17.2	-6.30	4.70	.734332
18612-2	1942	398	28.4	87.3	50.1	560	240.16	360	75	1.05	2.9	29.6	-6.6	-49.4	17.2	-7.10	5.00	.731867
18612-1	1609	296	29.1	81.9	50.1	540	231.19	210	77	0.945	2.7	30.1	-6.7	-49.6	19.6	-7.00	5.00	.732950
18911-3		198	33.6	136	75.3	377		236	64	1.05	2.4	18.2	-	-	-	-	-	-
18911-2		228	31.2	123	64.3	384		251	144	0.906	2.3	22.4	-	-	-	-	-	-
18900-2	1391	187	26.5	103	51.6	400	176.1	230	128	0.778	1.9	20.7	-6.6	-50.8	20.3	-8.52	3.4	-
18911-1	1361	169	27	112	54.7	392	188.9	217	116	0.863	1.9	19.2	-6.9	-50.5	20.7	-10.39	3.3	-
18900-1	1273	152	24.8	107	49.5	382	172.3	189	109	0.706	1.7	30.2	-6.9	-49.5	12.2	-5.36	3.1	-
18912-2	815	90.8	18.9	51.8	32.9	112	216.3	49	194	0.462	0.7	33.8	-6.7	-49.8	27.8	-6.26	3.8	-
18912-1		109	21.9	74.1	35	111		61	14	0.554	0.9	29.6	-	-	-	-	-	-

Table 6.11: Dissolved ion and isotopic content of groundwater samples from piezometers in the south eastern Ti Tree Basin.

6.2 Appendix 2 - Discussion of regional groundwater chemistry in the Ti Tree Basin

The main focus of this thesis has been the use of carbon-14 (^{14}C) as a tracer for investigating spatial variability in groundwater recharge. While collecting samples for ^{14}C analysis in the Ti Tree Basin, additional groundwater samples were collected and analysed for major ion chemistry, stable isotopes of water (δ^2H and $\delta^{18}O$) and strontium isotope ratios ($^{87}Sr/^{86}Sr$). This appendix presents a brief discussion of this data. Noble gases (^4He, ^{40}Ar, ^{20}Ne) were also analysed and will be further discussed in Appendix 3.

6.2.1 Introduction

Groundwater chemistry in the Ti Tree Basin has been investigated previously (McDonald, 1988; Calf et al., 1991; Harrington, 1999), and groundwater salinity generally ranges from 500 mg L^{-1} to more than 3000 mg L^{-1}. Fresher groundwaters (total dissolved solids (TDS) < 1000 mg L^{-1}) are generally Na-HCO_3 dominated, and spatially associated with ephemeral surface water features (eg. the Woodforde River and Allungra Creek floodout, Figure 5.4). More saline groundwaters are Na-Cl dominated, and groundwater salinity generally increases towards the north of the basin. Harrington (1999) presented a geochemical mass balance model which demonstrated that the chemical evolution of fresher waters was influenced by water-rock interactions. These reactions included dissolution of gypsum (resulting in addition of Ca and SO_4 to groundwater), dissolution of Ca-Mg-HCO_3, and weathering of Na-rich silicate minerals (eg. Na-montmorillonite, albite). This was supported by mineralogical analysis of rock core samples from the Ti Tree Basin, and geochemical reactive transport modelling (using NETPATH). Harrington (1999) also reported high $^{87}Sr/^{86}Sr$ ratios in the groundwater of the Ti Tree Basin, ranging from 0.72562 to 0.76248. These high $^{87}Sr/^{86}Sr$ values further support the evolution of groundwater chemistry in the Ti Tree Basin through water rock interactions, predominantly with carbonate minerals ($^{87}Sr/^{86}Sr$ from 0.71884 to 0.73707) and silicate minerals ($^{87}Sr/^{86}Sr$ 0.74334 to 0.94883).

The higher salinity waters (dominated by Na-Cl) were interpreted by Harrington (1999) as being derived through evaporative concentration during recharge. This was supported by stable isotope ratios measured in groundwater (δ^2H and $\delta^{18}O$). Measurement of stable isotopes in groundwater, when compared to local rainfall, can yield insight into recharge processes. For example the size and intensity of rainfall events that generate recharge, and the degree of evaporation prior to recharge lead to mass based fractionation of the stable isotope compositon of water (Coplen et al., 2000). Qualitative assessments can be made by plotting δ^2H against $\delta^{18}O$ for groundwater and local rainfall. Rainfall generally follows a linear trend (referred to as a Local Meteoric Water Line (LMWL)), and groundwater may follow or deviate from this trend depending upon the recharge process. Harrington (1999) found that groundwater in the Ti Tree Basin plotted below the LMWL for Alice Springs ($\delta^2H = 6.9\ \delta^{18}O + 4.5$). The groundwater samples displayed a trend of evaporative enrichment ($\delta^2H = 4.0\ \delta^{18}O - 27.3$) from the LMWL. Extrapolating this trend showed that groundwater was likely recharged by rainfall with a depleted δ^2H and $\delta^{18}O$ signature, typical of rainfall

associated with large monsoonal storms in central Australia (where rainfall may range from 150 - 200 mm month^{-1}).

Previous studies have reported high nitrate concentrations in Ti Tree Basin groundwaters (up to 280 mg L^{-1} (McDonald, 1988; Calf et al., 1991; Harrington, 1999)), while noting there are no significant sources of anthropogenic nitrate in the basin. This is a common phenomenon in arid zone groundwaters in Australia, where nitrate fixed by bacteria in termite mounds may be flushed to the watertable following large episodic rainfall events (Barnes et al., 1992). Harrington (1999) investigated these processes in the Ti Tree Basin through analysis of nitrogen isotopes in nitrate (δ^{15}N), and found the most likely source of nitrate accession into groundwater was via termites. Bacteria within the hind gut of termites fix atmospheric nitrogen as well as ogranic nitrogen derived from the termites food source (vegetation). The excreted organic nitrogen is converted to ammonium, which is oxidised to nitrate. Thus termite mounds, which are ubiquitous in the Ti Tree Basin, act as a source of nitrate which may be mobilised and transported to the aquifer during large recharge events.

6.2.2 Methods

Groundwater samples were collected on several field trips between August 2011 and August 2012 (see Appendix 1 for dates and sample locations). Piezometers were sampled using a Grundfos MP1 submersible pump, and measurements of salinity (as specific conductivity), pH and temperature were made while purging. Alkalinity (mg L^{-1} as $CaCO_3$) was also measured in the field by titration using a Hach AL-DT alkalinity kit. Samples for major ion chemistry, stable isotopes of water (δ^2H and δ^{18}O), and ^{87}Sr/^{86}Sr analysis were collected after approximately three bore volumes had been purged and field parameters had stabilised. Major ion analysis was performed by Inductively Coupled Plasma Mass Spectrometry (ICP-MS) at CSIRO in Adelaide (Australia), and stable isotopes were analysed with a Laser Water Isotope Analyzer V2 at the University of California Davis, Stable Isotope Facility. Strontium isotope analysis was performed at Adelaide University (Australia) by Thermal Ionisation Mass Spectrometry.

6.2.3 Results

Trends in major ion chemistry in this study are similar to those reported by Harrington (1999). The freshest groundwater samples were found in the shallow perched aquifer beneath the Woodforde River (total dissolved solids (TDS) ranging from 48 - 452 mg L^{-1}). Elsewhere in the basin salinity ranged from 650 - 1942 mg L^{-1} (with the exception of Stirling Swamp, where salinity ranged from 36,859 - 148,672 mg L^{-1}). Fresher groundwater samples were generally Na-HCO_3 dominated, trending towards Na-Cl dominated with increases in salinity (Figure6.2). Spatial patterns of salinity were also similar to those reported by Harrington (1999) and Read and Tickell (2007). Salinity values were generally lower near the Woodforde River and in the centre of the Ti Tree Basin where the Allungra Creek floodout occurs (Figure 6.4). Nitrate con-

Figure 6.1: Groundwater sampling in the Ti Tree Basin, February 2012

centrations ranged from 0.06 mg L^{-1} in the perched aquifer beneath the Woodforde River to 230 mg L^{-1} in the vicinity of the Allungra Creek floodout.

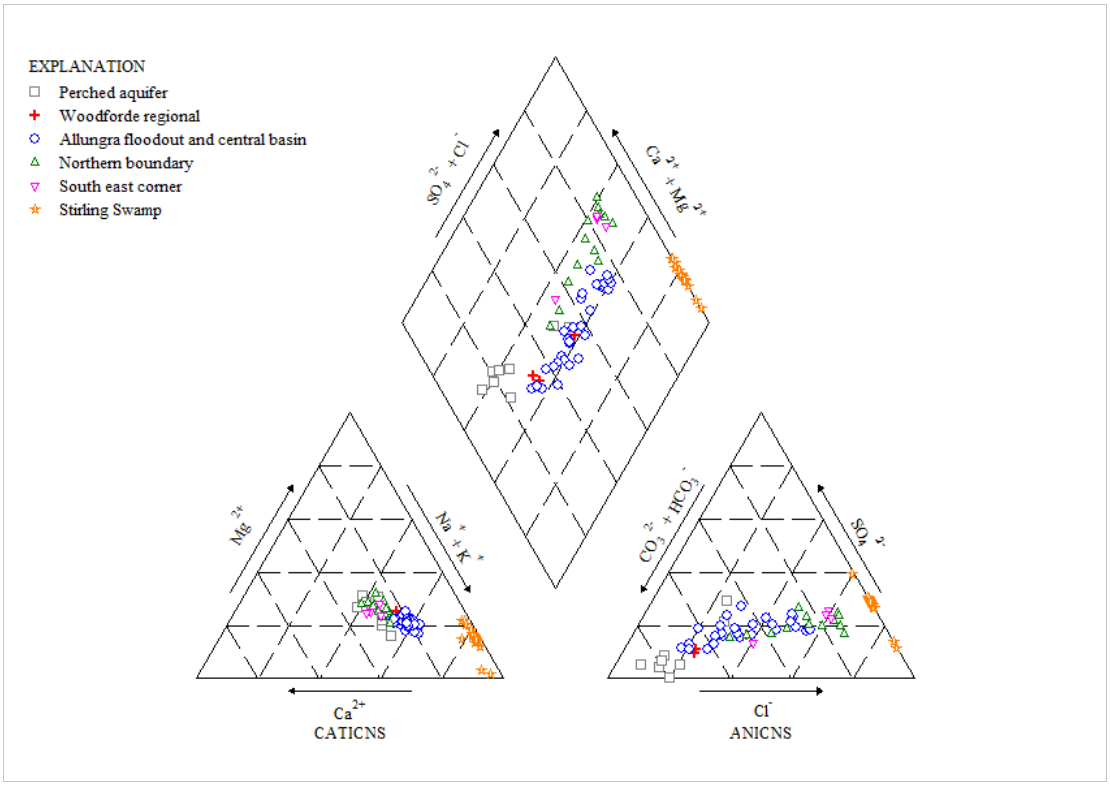

Figure 6.2: Piper plot for major ion chemistry of groundwater in the Ti Tree Basin

As with major ion chemistry - stable isotopes show very similar results to those of Harrington (1999). The low TDS samples in the perched aquifer plot on or very close to the LMWL for Alice Springs (approximately 150 km south of the study site). The rest of the samples plot below the LMWL suggesting evaporative enrichment prior to recharge (Figure 6.5). Plotting an evaporation trend line demonstrates the groundwaters are likely derived from heavy monsoonal rainfall events (where rainfall is 150 - 200 mm

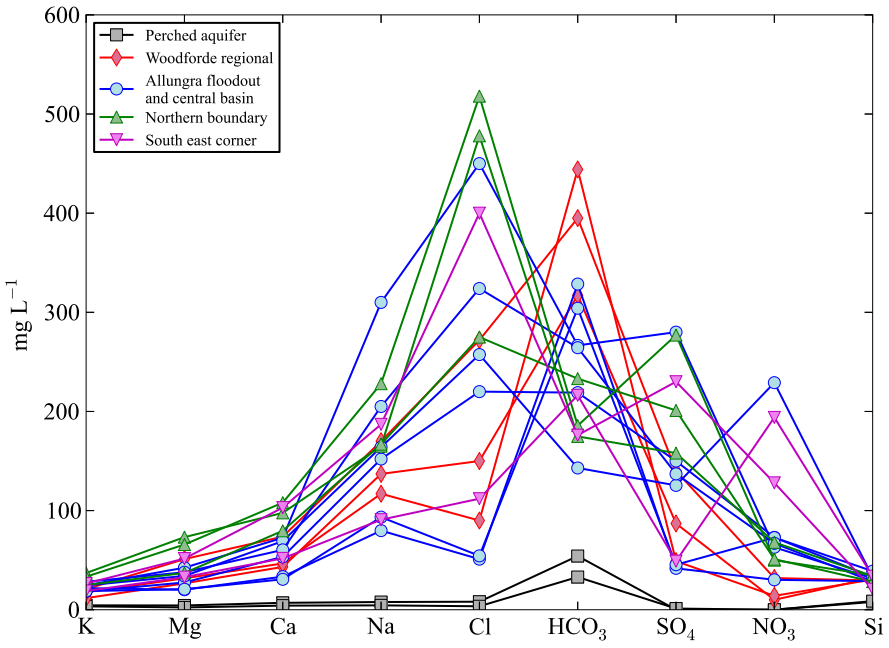

Figure 6.3: Schoeller plot for representative groundwater samples across the Ti Tree Basin

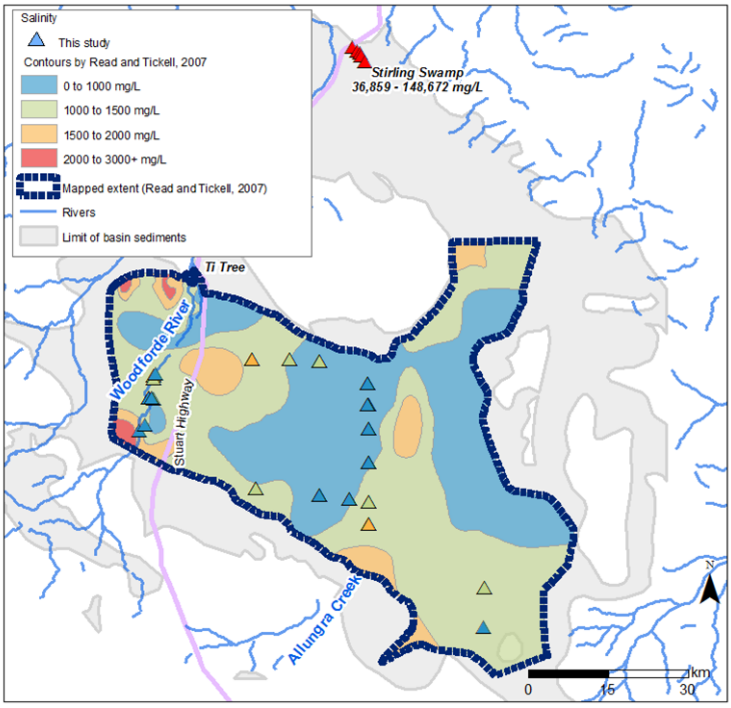

Figure 6.4: Spatial distribution of groundwater salinity as given in Read and Tickell (2007) for the main part of the Ti Tree Basin. Overlain are measurements made in this study (triangles, where colours represent the same salinity ranges as Read and Tickell (2007) values). Location of Stirling Swamp is given by red triangles, where the salinity ranges from 36,859 to 148,672 mg L^{-1}.

month^{-1}). The slope of the evaporation line in this study is only slightly different to that of Harrington (1999), and the general trend and interpretation is the same. Samples from Stirling Swamp are further enriched. There is a larger amount of scatter than with other regional samples, and one sample plots close to the LMWL. However the groundwater at Stirling Swamp is relatively shallow (1 - 3 m below ground) and

subject to seasonal recharge/discharge patterns, hence mixing of local saline groundwater with fresher (and less isotopically enriched) infiltrating water is expected.

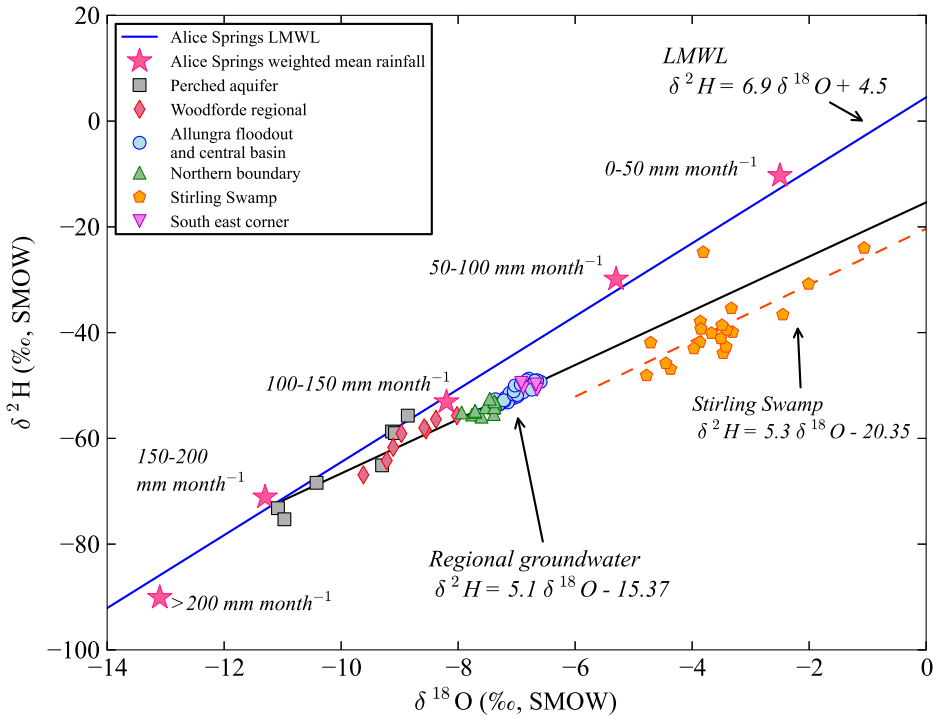

Figure 6.5: Stable isotope composition of groundwater in this study. Also shown is the LMWL for Alice Springs (150 km south of the study area), and long term amount weighted mean compositions of different monthly rainfall amounts (after Harington et al. (2002)).

The relationship between chloride and δ^2H is of interest (Figure 6.6). Samples from the shallow perched aquifer underlying the Woodforde River show δ^2H values ranging from -75 to -55 ‰ with only a small variation in chloride concentration. This suggests that rainfall events of different intensity may be responsible for recharging the perched aquifer (this can also be seen in Figure 6.5 with samples lying along the LMWL). Regional groundwater samples with low chloride concentrations (<10 to 100 mg L^{-1}) have δ^2H values ranging from -75 to -50 ‰ (higher chloride broadly correlated with more enriched δ^2H). This trend is consistent with evaporative concentration of chloride and enrichment (through fractionation) of δ^2H. However for samples with chloride ranging from 100 to 580 mg L^{-1}, there is no significant enrichment trend in δ^2H. This suggests that salinity increases over this range may be due to transpiration rather than evaporation (Simspon et al., 1987). This hypothesis is supported by earlier parts of this thesis, which showed that groundwater discharge through transpiration is likely to be occurring at various locations in the Ti Tree Basin (Chapter 3.3.3 and 4.4.2). Recent research into discharge processes in Stirling Swamp (previously thought to be the regional discharge location for the Ti Tree Basin) has also suggested that groundwater discharge may be occurring in other parts of the basin through plant water uptake (Shanafield et al., 2015).

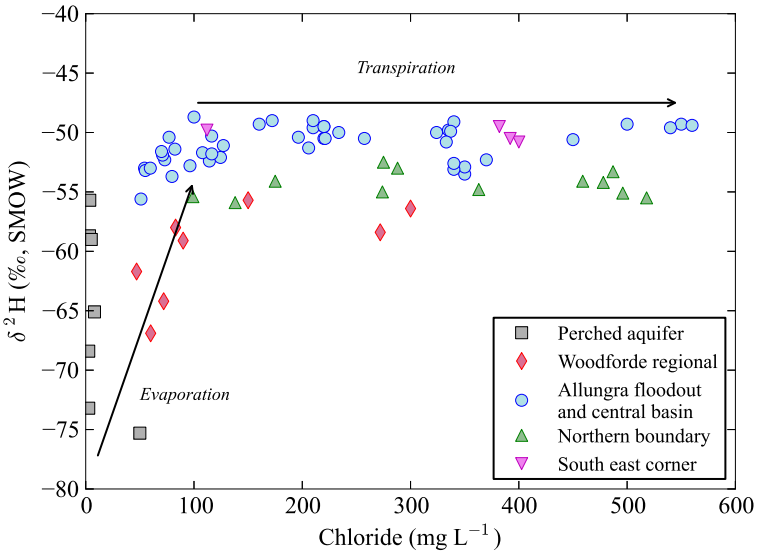

Figure 6.6: Chloride vs. δ^2H for groundwater in the Ti Tree Basin, showing the influence of evaporation (concentration of chloride and enrichment of δ^2H) and transpiration (concentration of chloride with no significant change in δ^2H) on groundwater chemistry.

6.2.4 Conclusion

Though not the primary focus of this thesis, a significant amount of major ion and isotope groundwater chemistry has been collected in the Ti Tree Basin. Qualitative analysis demonstrates that evolution of groundwater chemistry in the basin can be explained in much the same way as Harrington (1999). That is, fresher groundwaters are spatially associated with areas of likely recharge, near the Woodforde River and Allungra Creek floodout. Fresher waters are generally Na-HCO_3 dominated, with their chemistry influenced by water-rock interactions. Higher salinity samples are generally Na-Cl dominated and influenced by evaporation prior to recharge. Additionally, this thesis identifies transpiration (through groundwater uptake by vegetation) to be a likely influence on groundwater salinity on a regional scale.

6.3 Appendix 3 - Determination of equilibration times for diffusion samplers in piezometers of different depth

6.3.1 Background

An initial objective of this thesis was to obtain measurements of the dissolved noble gases helium-4 (^{4}He), argon-40 (^{40}Ar) and neon-20 (^{20}Ne) in groundwater in the Ti Tree Basin. Atmospheric noble gases are soluble in water, with their solubility being dependent upon the temperature and salinity of water, as well as elevation. Noble gas concentrations in groundwater are commonly greater than atmospheric equilibrium concentrations. This is because when rainfall infiltrates in the unsaturated zone, unsaturated zone air may be 'trapped' and forced to dissolve into the infiltrating groundwater, resulting in groundwater having higher concentrations of noble gases than expected from equilibrium with the atmosphere. This 'excess air' phenomenon may provide information on changes in groundwater recharge over time (Kipfer et al., 2002). For example - if the component of excess air can be determined and accounted for, then the noble gas concentrations can be compared to their known solubility at given temperatures yielding an indication of recharge temperatures. The amount of excess air also reflects the intensity of rainfall, and when combined with measurements of apparent groundwater age (e.g. ^{14}C measurements) can help reconstruct paleoclimate influences on groundwater recharge (Beyerle et al., 2003).

Helium-4 can provide further information on groundwater residence times. Helium-4 is produced in the Earth's crust via radioactive decay of uranium and thorium isotopes. These isotopes are present in most rock minerals, thus concentrations of ^{4}He in groundwater should accumulate with residence time in an aquifer (Solomon, 2000). Where concentrations of uranium and thorium in the aquifer matrix are known, ^{4}He can be used to calculate the apparent groundwater age via:

$$t = \left[^4He\right]_{gw} .10^7 . (\xi_{He} . (r:w) . \rho . (1.21U + 0.287Th))^{-1} \quad (6.1)$$

where t is groundwater age or residence time, $\left[^4He\right]_{gw}$ is the concentration of radiogenic ^{4}He in groundwater (cm^3 STP g^{-1}), ξ_{He} is the emanation efficiency of the minerals (assumed to be ~1), $r:w$ is the rock:water ratio in the aquifer, ρ is the rock density (g cm^{-3}), and U and Th are uranium and thorium concentrations of the aquifer matrix (g g^{-1}).

Harrington (1999) previously made measurements of ^{4}He in groundwater in the Ti Tree Basin, and found that ^{4}He concentrations in the Ti Tree Basin broadly correlated with ^{14}C estimates of groundwater age (older groundwater corresponding with higher ^{4}He). However ^{4}He derived groundwater ages were in excess of those estimated from ^{14}C based on measured uranium and thorium from aquifer mineral analysis. Harrington (1999) hypothesised that this ^{4}He excess was due to a similar mechanism reported by Solomon et al. (1996). That is diffusion of ^{4}He out of the Tertiary sediments, which themselves are comprised of weathered Precambrian rocks, in which ^{4}He would have accumulated prior to weathering (and subsequent

formation of the Tertiary aquifers).

6.3.2 Noble gas measurements in this study

Initial measurements of groundwater chemistry were made in this study in August and September 2011, in piezometers located in the vicinity of the Woodforde River and the Allungra Creek floodout. Samples for noble gas analysis were collected using diffusion samplers exactly resembling those described by Gardner and Solomon (2009), and following the recommended methodology (ie. allowing the samplers to equilibrate in the piezometer for 24 hours, and 'sealing' the equilibrated diffusion sampler below the watertable, see Gardner and Solomon (2009) for details). Bores near the Woodforde River (including one screened in the perched aquifer directly beneath the river) show higher ^{14}C activities (73 to 96 pMC) and lower ^{4}He concentrations (4.8 x10^{-8} to 1.01 x 10^{-7} cc STP g^{-1}), while bores near the Allungra Creek floodout show lower ^{14}C activities (8 to 52 pMC) and higher ^{4}He concentrations (2.23 x 10^{-7} to 2.35 x 10^{-5} cc STP g^{-1}). This trend is consistent with the results of (Harrington, 1999), suggesting that ^{4}He concentrations are broadly related to groundwater residence time (Figure 6.7(a)).

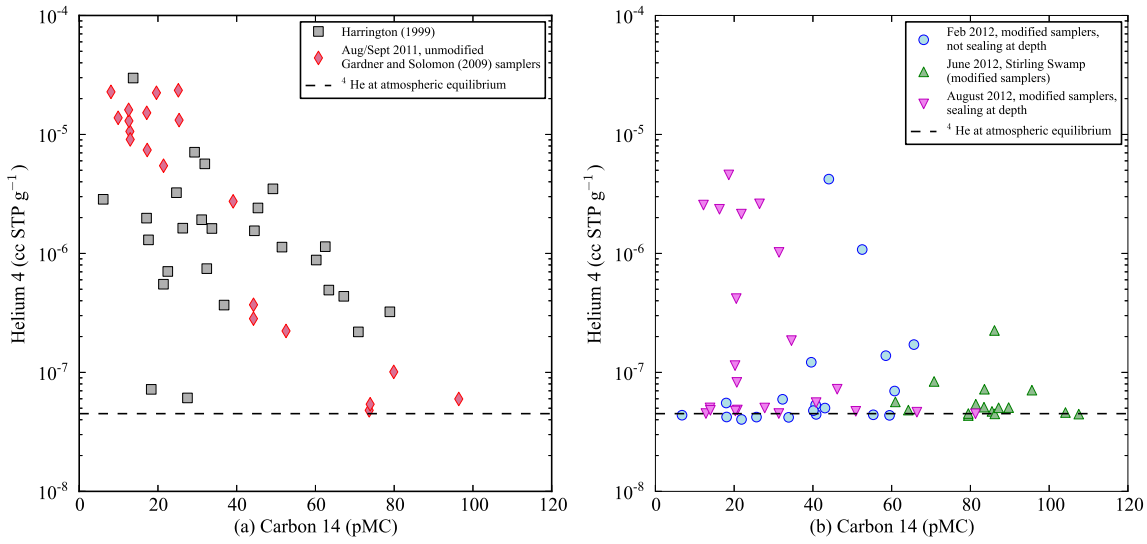

Figure 6.7: Helium-4 concentrations vs. carbon-14 activities of groundwater samples in the Ti Tree Basin (a) collected by Harrington (1999) and in this study on multiple field trips using conventional diffusion samplers and (b) modified versions of the diffusion samplers described by Gardner and Solomon (2009).

Argon-40 and neon-20 results from this first field trip (Figure 6.8) show significant amounts of excess air. The green line in Figure 6.8 shows the relationship between ^{40}Ar and ^{20}Ne for water at equilibrium with the atmosphere for temperatures ranging from 30ºC (lowest values) to 5ºC (highest values). Groundwater samples lying to the right of this line show elevated concentrations due to excess air formation during recharge. A trend line through the Allungra Creek data suggests addition of excess air (AE, up to >80 %) from recharging water with a temperature of 22ºC (mean annual temperature for this part of central Australia from 1961-1990 is between 21 to 24ºC, (BOM, 2014)). Extrapolation of individual data points would give recharge temperatures ranging from 11ºC (perched aquifer) to 28ºC, however measurement

errors are likely to be ±10%. Nevertheless, the significant amounts of excess air observed are consistent with recharge through intense monsoonal rainfall events.

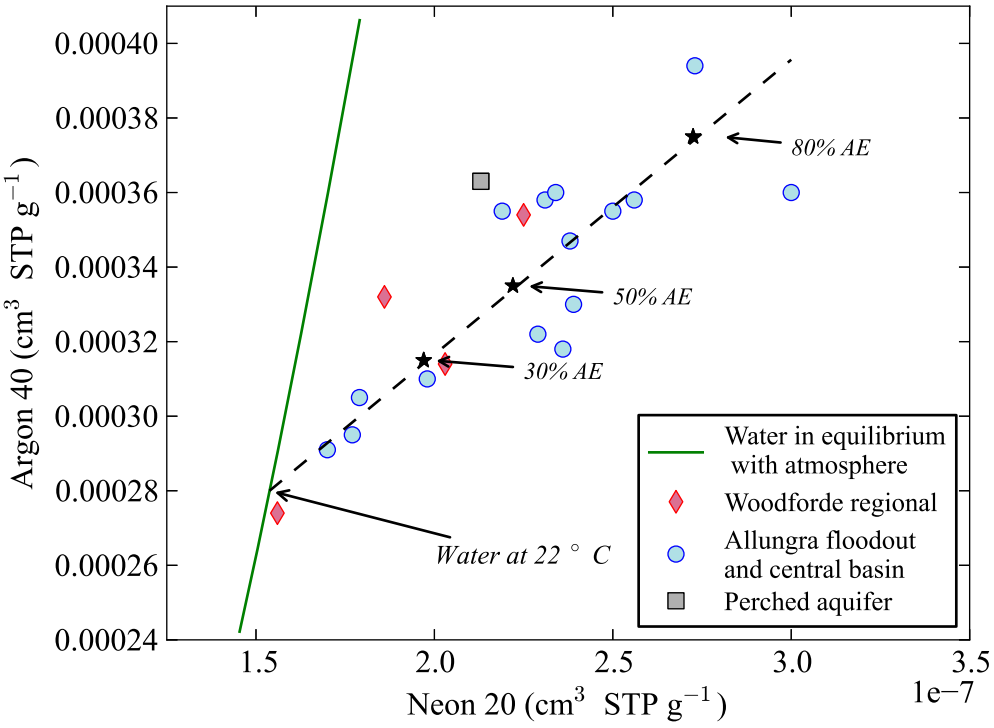

Figure 6.8: Argon-40 vs. neon-20 - the green line displays concentrations that would be observed in water in equilibrium with the atmosphere for temperatures ranging from 30ºC (lowest values) to 5ºC (highest values). Deviation from this trend demonstrates 'addition' of noble gases, or formation of excess air, which may be as high as 80% for some of the samples near the Allungra Creek floodout.

A second field trip was conducted in February 2012, in which modified versions of the diffusion samplers provided by CSIRO were used. The modifications included a perforated stainless steel sheath around the cell to protect the silicon membrane. Other changes may also have been made. However when these modified samplers were used in the field, it was found that they would not seal following the application of bike pump pressure to the deployment tube (see Gardner and Solomon (2009) and for details on the shutting mechanism of the samplers). The samplers were thus manually closed upon being brought to the surface, following instructions from the laboratory. However the majority of samples yielded atmospheric concentrations of all noble gases, even where ^{14}C activities were as low as 6 pMC (Figure 6.7(b)). Given the relatively homogeneous nature of the lithology in the Ti Tree Basin, and the close spatial proximity of piezometers with 'atmospheric' ^{4}He to high ^{4}He samples (ie. within 5 - 15 km), we do not expect such a severe departure from the trend between ^{14}C and ^{4}He. Thus we conclude that the majority of these measurements are incorrect through some fault of the diffusion samplers.

The problem associated with the shutting mechanism of the samplers was rectified for use on subsequent field trips. In June 2012 groundwater samples were collected in Stirling Swamp. Helium-4 concentrations are predominantly at or close to atmospheric equilibrium, however the groundwater in Stirling Swamp also shows high ^{14}C activities (generally >80 pMC), thus ^{4}He concentrations closer to atmospheric values are

expected. However on the final field trip upon which noble gas samples were collected using modified diffusion samplers that were sealing properly, results are mixed (Figure 6.7(b)). For example, one of the lowest ^{4}He concentrations (4.51 x 10^{-8} cc STP g^{-1}, essentially at equilibrium with atmospheric concentrations) is for a sample with a ^{14}C activity of 12.8 pMC. However a separate sample with ^{14}C activity of 12.2 pMC has a ^{4}He concentration two orders of magnitude higher than atmospheric equilibrium (2.55 x 10^{-6} STP g^{-1}). Again, given the relatively homogeneous nature of the lithology in the Ti Tree Basin, the departure from the trend between ^{14}C and ^{4}He is unexpected, thus validity of these noble gas measurements is considered questionable at best.

6.3.3 Methods for testing equilibration times

Because of these issues with the modified diffusion samplers, an experiment was designed to test equilibration times. Two piezometers in the Willunga Basin, approximately 45 km south of Adelaide, were selected for diffusion sampler testing (details in Table 6.12). The experiments were conducted from late May to early June 2013, with two additional samples collected in early August 2013. Prior to sampling the bores, diffusion samplers were placed in PVC tubes and flushed with UHP nitrogen for 30 minutes. The PVC tubes were sealed for 24 hours, then re-flushed with nitrogen for 20 - 30 minutes and re-sealed before being taken to the field for deployment.

Piezometer ID	WSS-P2-S4-5	WSS-P2-S4-2
Registration number	6627-14474	6627-14478
Total depth (m-bgl)	47	134
Screen interval (m-bgl)	44 - 47	129 – 134
Bore diameter (mm)	100	100
Depth to water (m-bgl)	7.38	12.4
Specific conductivity (μS cm^{-1})	825	3025
Temperature (°C)	19.2	19.5
Aquifer unit	Port Willunga Formation (silty sand)	North Maslin Sands (sand with minor clay)

Table 6.12: Details for the two bores which were sampled as part of the equilibration time experiment (m-bgl denotes metres below ground level)

The piezometers were purged of 50 L prior to the diffusion samplers being deployed. The diffusion samplers were deployed by attaching them to 1/4" nylon tubing and carefully lowering to the depth of the screened interval. Initially the diffusion samplers were left to equilibrate in the bores for 19 hours, then retrieved by attaching a bike pump to the nylon tubing and pumping to a pressure of 40 - 60 psi to seal the head space in the diffusion sampler (see Gardner and Solomon (2009) for a detailed description of the shutting mechanism in the samplers). The experiment was then repeated for increasing equilibration lengths (up to seven days).

6.3.4 Results for testing equilibration times

Figure 6.9 shows noble gas concentrations from samples collected in the two piezometers, all gas concentrations are in units of cm^3 STP g^{-1}. Results from the shallower piezometer (WSS-P2-S4-5, left panel) show total dissolved gas pressure (TDG, atm), nitrogen (N_2) and ^{40}Ar decreasing in concentration with increased equilibration time. The decreasing trend can be attributed to pre-flushing of the samplers with N_2 (it is possible the UHP N_2 contained some minor component of argon). Equilibrium is not reached within 24 hours, but appears to take somewhere in between 24 and 72 hours. Neon-20 concentrations show an inverse trend, increasing with time and likewise reaching equilibrium somewhere between 24 and 72 hours. Helium-4 concentrations do not change significantly with time, suggesting that equilibrium is reached within 19 hours. For the 19 hour equilibration time, two values are given for each gas, the lower concentrations are likely incorrect, however the cause for this error could not be determined.

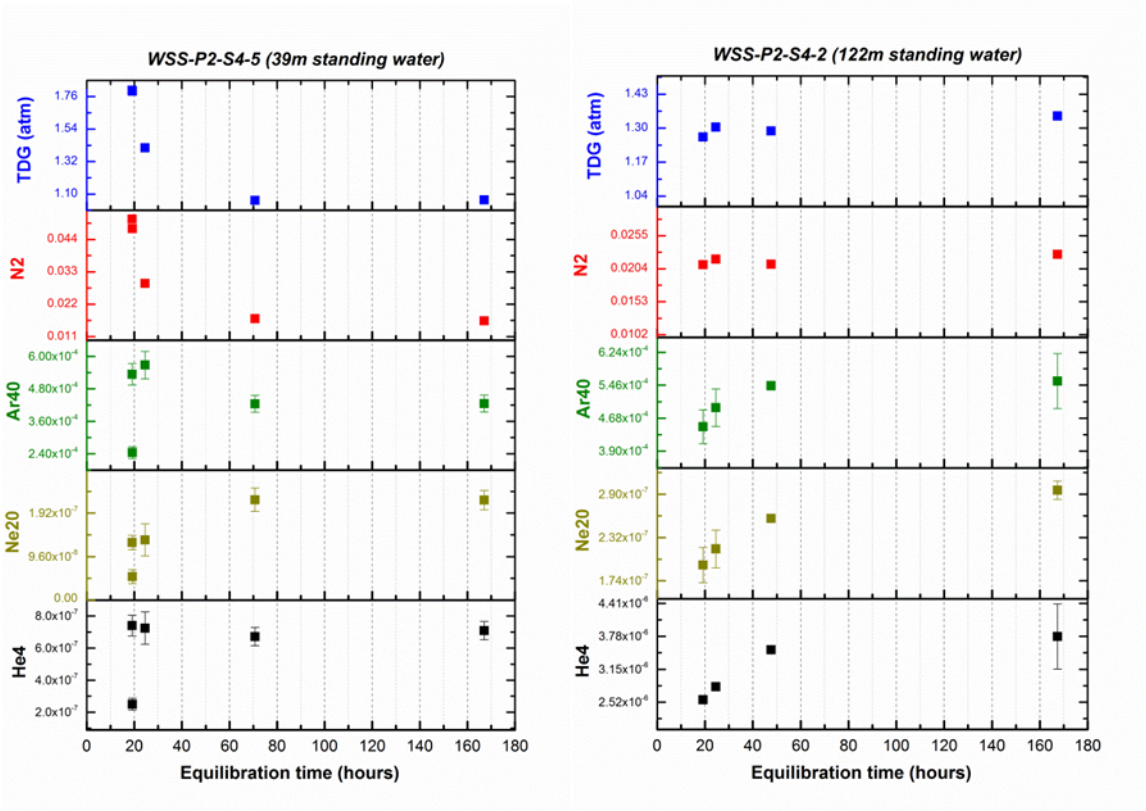

Figure 6.9: Measured gas concentrations (cm^3 STP g^{-1}) and pressures in the diffusion samplers versus equilibration time. Results in the left panel are for the shallower bore, while those in the right are for the deeper bore.

Results from the deeper piezometer with a greater water column height (WSS-P2-S4-2, right panel) are slightly different. There is no significant change in nitrogen or TDG with equilibration time. There is an increase in ^{40}Ar and ^{20}Ne concentrations with time, with equilibration being reached somewhere between 50 and 170 hours, most likely around 70 hours (approximately three days). Helium-4 also shows increasing concentrations with equilibration time, which is different to the results from the shallower piezometer which indicated equilibration occurred within 19 hours. This demonstrates that the diffusion samplers used take

longer to equilibrate when deployed in piezometers with a greater column of water above the screened interval.

6.3.5 Conclusions

This experiment has demonstrated that the diffusion samplers used in this study have equilibration times that vary for the different noble gases of interest, but also vary depending on the type of piezometer they are deployed in. Because of the modifications made to the diffusion samplers throughout the course of this study, a direct comparison with the samplers described by Gardner and Solomon (2009) cannot be made. The piezometer with a relatively shallow water column (39 m) had a short equilibration time of 19 hours for ^{4}He, and equilibration times between 24 and 72 hours for ^{20}Ne and ^{40}Ar. The piezometer with the greater water column (ie. diffusion samplers deployed further below the watertable) had equilibration times for ^{4}He, ^{20}Ne and ^{40}Ar of somewhere between 50 and 170 hours, most likely around 70 hours (i.e. three days).

These results show that care must be taken in designing sampling programs for noble gases using diffusion samplers, as equilibration times may vary depending upon the height of the water column. More thorough testing would be required to quantify this effect for piezometers with water columns depths greater than 120 m.

Bibliography

Bacon, D. H. and C. K. Keller, 1998: Carbon dioxide respiration in the deep vadose zone: Implications for groundwater age dating. *Water Resour. Res.*, **34 (11)**, 3069–3077, doi:10.1029/98WR02045.

Barnes, C. J., G. Jacobsen, and G. Smith, 1992: The origin of high-nitrate ground waters in the Australian arid zone. *J. Hydrol.*, **137 (1-4)**, 181 – 197.

Bartolino, J. R. and J. C. Cole, 2002: *Ground-water resources of the Middle Rio Grande Basin*. Technical report, USGS Circular 1222. Reston, Virginia.

Bethke, C. M., X. Zhao, and T. Torgersen, 1999: Groundwater flow and 4He distribution in the Great Artesian Basin of Australia. *J. Geophys. Res.*, **104 (B6)**, 12999–13011, doi:10.1029/1999JB90085.

Beyerle, U., J. Rueedi, M. Leuenberger, W. Aeschbach-Hertig, F. Peeters, R. Kipfer, and A. Dodo, 2003: Evidence for periods of wetter and cooler climate in the Sahel between 6 and 40 kyr BP derived from groundwater. *Geophys. Res. Lett.*, **30 (4)**, 1173, doi:10.1029/2002GL016310.

BOM, 2014: Bureau of meteorology - climate averages. http://www.bom.gov.au. Website accessed June 2014.

Browne, E. and R. B. Firestone, 1999: *Table of Isotopes*. Wiley and Sons, New York.

Busenberg, E. and L. N. Plummer, 1992: Use of chlorofluorocarbons (CCl_3F and CCl_2F_2) as hydrologic tracers and age-dating tools: The alluvium and terrace system of central Oklahoma. *Water Resour. Res.*, **28 (9)**, 2257–2283, doi:10.1029/92WR01263.

Calf, G., P. McDonal, and G. Jacobson, 1991: Recharge mechanism and groundwater age in the Ti-Tree Basin, Northern Territory. *Aust. J. Earth Sci.*, **38**, 299–306, doi:10.1080/08120099108727974.

Canadell, J., R. Jackson, J. Ehleringer, H. Mooney, O. Sala, and E. Schulze, 1996: Maximum rooting depth of vegetation types at the global scale. *Oecologia*, **108**, 583–595, doi:10.1007/BF00329030.

Castro, M. C. and P. Goblet, 2005: Calculation of ground water ages - a comparitive analysis. *Groundwater*, **43 (3)**, 368–380, doi:10.1111/j.1745-6584.2005.0046.x.

Chen, C., D. Eamus, J. Cleverly, N. Boulain, P. Cook, L. Zhang, L. Cheng, and Q. Yu, 2014: Modelling vegetation water-use and groundwater recharge as affected by climate variability in an arid-zone acacia savanna woodland. *J. Hydrol.*, **519 (Part A)**, 1084–1096, doi:10.1016/j.jhydrol.2014.08.032.

Clark, I. D. and P. Fritz, 1997: *Environmental Isotopes in Hydrogeology*. CRC Press, USA.

Cleverly, J., N. Boulain, R. Villalobos-Vega, N. Grant, R. Faux, C. Wood, P. Cook, Q. Yu, A. Leigh, and D. Eamus, 2013: Dynamics of component carbon fluxes in a semi-arid Acacia woodland, central Australia. *J. Geophys. Res.: Biogeosciences*, **118 (3)**, 1–18, doi:10.1002/jgrg.20101.

Cook, G. and T. Dawes-Gromadzki, 2005: Stable isotope signatures and landscape functioning in banded vegetation in arid-central Australia. *Landscape Ecol.*, **20 (6)**, 649–660, doi:10.1007/s10980-005-0069-1.

85

Cook, P. G. and J. K. Bohlke, 2000: Determining time frames for groundwater flow and solute transport. *Environmental tracers in subsurface hydrology*, P. G. Cook and A. L. Herczeg, eds., Kluwer, Massachusetts, 1 – 30.

Cook, P. G., A. P. O'Grady, J. D. H. Wischusen, A. Duguid, T. Fass, and D. Eamus, 2005: *Ecohydrology of sand plain woodlands in central Australia*. Natural Heritage Trust Report, 2005/147.

Cook, P. G. and D. K. Solomon, 1995: Transport of atmospheric trace gasses to the water table: Implications for groundwater dating with chlorofluorocarbons and krypton 85. *Water Resour. Res.*, **31 (2)**, 263–270, doi:10.1029/94WR02232.

Cook, P. G., G. Walker, and I. Jolly, 1989: Spatial variability of groundwater recharge in a semiarid region. *J. Hydrol.*, **111 (1)**, 195–212, doi:10.1016/0022-1694(89)90260-6.

Coplen, T. B., A. L. Herczeg, and C. Barnes, 2000: Isotope engineering - Using stable isotopes of the water molecule to solve practical problems. *Environmental tracers in subsurface hydrology*, P. G. Cook and A. L. Herczeg, eds., Kluwer, Massachusetts, 79–110.

Craig, H., 1957: Isotopic standards for carbon and oxygen correction factors for mass-spectrometric analysis of carbon dioxide. *Geochim. Cosmochim. Ac.*, **12 (1)**, 133–149, doi:10.1016/0016-7037(57)90024-8.

Cresswell, R., J. Wischusen, G. Jacobson, and K. Fifield, 1999: Assessment of recharge to groundwater systems in the arid southwestern part of Northern Territory, Australia, using chlorine-36. *Hydrogeol. J.*, **7 (4)**, 393–404.

CSIRO, 2013: Key greenhouse and ozone depleting gases. http://www.csiro.au/greenhouse-gases/. Website accessed June 2013.

Dever, L., J. Fontes, and G. Riche, 1987: Isotopic approach to calcite dissolution and precipitation in soils under semi-arid conditions. *Chem. Geol.*, **66 (3–4)**, 307–314, doi:10.1016/0168-9622(87)90050-9.

Diersch, H., 2014: *FEFLOW Finite Element Modeling of Flow, Mass and Heat Transport in Porous and Fractured Media*. Springer, Heidelberg.

Dincer, T., A. Al-Mugrin, and U. Zimmermann, 1974: Study of the infiltration and recharge through the sand dunes in arid zones with special reference to the stable isotopes and thermonuclear tritium. *J. Hydrol.*, **23 (1)**, 79–109, doi:10.1016/0022-1694(74)90025-0.

Doherty, J. E., 2010: *PEST Model-Independent Parameter Estimation User Manual*.Watermark Numerical Computing, Australia.

English, P., N. A. Spooner, J. Chappell, D. G. Questiaux, and N. G. Hill, 2001: Lake Lewis basin, central Australia: environmental evolution and OSL chronology. *Quatern. Int.*, **83–85**, 81–101.

ESRI, 2014: *ArcMap version 10.0. 86*. Environmental Systems Research Institute, Redlands CA.

Fink, D., M. Hotchkis, Q. Hua, G. Jacobsen, A. Smith, U. Zoppi, D. Child, C. Mifsud, H. van der Gaast, A. Williams, and M. Williams, 2004: The ANTARES AMS facility at ANSTO. *Nucl. Instrum. Methods Phys. Res. B*, **223–224**, 109–115, doi:10.1016/j.nimb.2004.04.025.

Fontes, J. and J. Garnier, 1979: Determination of the initial ^{14}C activity of the total dissolved carbon: A review of the existing models and a new approach. *Water Resour. Res.*, **15 (2)**, 399–413, doi:10.1029/WR015i 002p00399.

Fulton, S., D. Wohling, and A. Love, 2012: Estimating recharge through an arid zone river: a comparison of groundwater tracer and physical techniques, Great Artesian Basin, Australia. Abstract volume of the 2012 GSA Annual Meeting and Exposition, 4-7 Nov. Charlotte, North CA.

Gardner, P. and D. K. Solomon, 2009: An advanced passive diffusion sampler for the determination of dissolved gas concentrations. *Water Resour. Res.*, **45 (6)**, 1955–1974, doi:10.1029/2008WR007399.

Gardner,W. P., G. Hammond, and P. Lichtner, 2013: High performance simulation of environmental tracers in heterogeneous domains. *Groundwater*, **53 (S1)**, 71–80, doi:10.1111/gwat.12148.

Gee, G. and D. Hillel, 1988: Groundwater and recharge in arid regions: Review and critique of estimation methods. *Hydrol. Process*, **2 (3)**, 255–266, doi:10.1002/hyp.3360020306.

Gelhar, L., C. Welty, and K. Refheldt, 1992: A critical review of data on field-scale dispersion in aquifers. *Water Resour. Res.,* **28 (7)**, 1955–1974, doi:10.1029/92WR00607.

Gillon, M., F. Barbecot, E. Gibert, J. A. Corcho Alvarado, C. Marlin, and M. Massault, 2009: Open to closed system transition traced through the TDIC isotopic signature at the aquifer recharge stage, implications for groundwater ^{14}C dating. *Geochim. Cosmochim. Ac.*, **73 (21)**, 6488–6501, doi:10.1016/j.gca.2009.07.032.

Haas, H., D. Fisher, D. Thorstenson, and E. Weeks, 1983: $^{13}CO_2$ and $^{14}CO_2$ measurements on soil atmosphere sampled in the sub-surface unsaturated zone in the Western Great Plains of the US. *Radiocarbon*, **25**, 301 – 314.

Harbaugh, A., 2005: *MODFLOW-2005, The U.S. Geological Survey Modular Ground-Water Model - the Ground-Water Flow Process*. Technical report, USGS Techniques and Methods 6-A16. Reston, Virginia.

Harrington, G., C. P.G., and H. A.L., 2002: Spatial and temporal variability of ground water recharge in central Australia: A tracer approach. *Groundwater*, **40 (5)**, 518–528, doi:10.1111/j.1745-6584.2002.tb02536.x.

Harrington, G. A., 1999: *Recharge Mechanisms and Chemical Evolution in an Arid Groundwater System, Central Australia*. PhD Thesis. Flinders University, South Australia.

Herczeg, A. and F. Leaney, 2011: Review: Environmental tracers in arid-zone hydrology. *Hydrogeol. J.*, **19 (1)**, 79–29, doi:10.1007/s10040-010-0652-7. 87

Hua, Q., M. Barbetti, and A. Rakowski, 2013: Atmospheric radiocarbon for the period 1950-2010. *Radiocarbon*, **55**, 2059–2072.

Ingerson, E. and F. Pearson, 1964: Estimation of age and rate of motion of groundwater by the ^{14}C method. Recent Researches in the Fields of Atmosphere, Hydrosphere, and Nuclear Geochemistry, Sugawara Festival Volume, Maruzen Co., Tokyo.

Jahne, B., G. Heinz, and W. Dietrich, 1987: Measurement of the diffusion coefficients of sparingly soluble gases in water. *J. Geophys. Res.*, **92 (C10)**, 10767–10776, doi:10.1029/JC092iC10p10767.

Keller, C. and D. Bacon, 1998: Soil respiration and georespiration distinguished by transport analyses of vadose CO_2, $^{13}CO_2$, and $^{14}CO_2$. *Glob. Biogeochem. Cycles*, **12 (2)**, 361–372, doi:10.1029/98GB00742.

Kipfer, R.,W. Aeschbach-Hertig, F. Peeters, and M. Stute, 2002: Noble Gases in Lakes and Ground Waters. *Rev. Mineral. Geochem.*, **47**, 615–700, doi:10.2138/rmg.2002.47.14.

Knapton, A., 2007: *Development of a groundwater model for the Ti Tree Basin using the finite element modeling package FEFLOW*. Technical report, Department of Natural Resources, Environment, The Arts and Sports Report 18/2007. Northern Territory Government, Australia.

Knapton, A., 2009: *Ti Tree Basin Water Resource Report*. Technical report, Department of Natural Resources, Environment, The Arts and Sports. Northern Territory Government, Australia.

Kozuskanich, J., C. T. Simmons, and P. G. Cook, 2014: Estimating recharge rate from groundwater age using a smiplified analytical approach: Applicability and error estimation in heterogeneous porous media. *J. Hydrol.*, **511**, 290–294, doi:10.1016/j.jhydrol.2014.01.058.

Kroitoru, L., I. Carmi, and E. Mazor, 1987: Groundwater ^{14}C activity as affected by initial water-rock interactions in a carbonatic terrain with deep water tables: Judean Mountains, Israel. International Symposium on the Use of Isotope Techniques in Water Resources Development, IAEA, Vienna, 134–136.

Kulongoski, J., D. Hilton, R. Creswell, S. Hostetler, and G. Jacobsen, 2008: Helium-4 characteristics of groundwaters from Central Australia: Comparative chronology with chlorine-36 and carbon-14 dating techniques. *J. Hydrol.*, **348 (1–2)**, 176–194, doi:10.1016/j.jhydrol.2007.09.048.

Leaney, F. and G. Allison, 1986: Carbon-14 and stable isotope data for an area in the Murray Basin: its use in estimating recharge. *J. Hydrol.*, **88 (1–2)**, 129–145, doi:10.1016/0022-1694(86)90201-5.

Li, Y. and S. Gregory, 1974: Diffusion of ions in sea water and in deep sea sediments. *Geochim. Cosmochim. Ac.*, **38 (5)**, 703–714, doi:10.1016/0016-7037(74)90145-8.

Loosli, H. H., B. E. Lehman, and W. M. Smethie Jr., 2000: Noble gas radioisotopers ^{37}Ar, ^{85}Kr, ^{39}Ar and ^{81}Kr. *Environmental tracers in subsurface hydrology*, P. G. Cook and A. L. Herczeg, eds., Kluwer, Massachusetts, 379–396.

Love, A., A. Herczeg, D. Armstrong, F. Stadter, and E. Mazor, 1993: Groundwater flow regime within the Gambier Embayment of the Otway Basin, Australia: evidence from hydraulics and hydrochemistry. *J. Hydrol.*, **143 (3–4)**, 297–338, doi:10.1016/0022-1694(93)90197-H.

Mazor, E., 2004: *Chemical and Isotopic Groundwater Hydrology*. Marcel Dekker, New York.

McCallum, J. L., P. G. Cook, and C. T. Simmons, 2015: Limitations of the use of environmental tracers to infer groundwater age. *Groundwater*, **53 (S1)**, 56–70, doi:10.1111/gwat.12237.

McCallum, J. L., P. G. Cook, C. T. Simmons, and A. D. Werner, 2014: Bias of environmental tracer ages in heterogeneous environments. *Groundwater*, **52 (2)**, 239–250, doi:10.1111/gwat.12052.

McDonald, P., 1988: *Groundwater Studies, Ti Tree Basin, 1984-1988*. Technical report, Power and Water Authority Report No. 1/90, Alice Springs, Australia.

Meredith, K., D. Cendon, J. Pigois, S. Hollins, and G. Jacobsen, 2012: Using ^{14}C and ^{3}H to delineate a recharge 'window' into the Perth Basin aquifers, North Gnangara groundwater system, Western Australia. *Sci. Total Environ.*, **414**, 456–469, doi:10.1016/j.scitotenv.2011.10.016.

Meredith, K., S. Hollins, and D. Cendon, 2013: Radiocarbon dating and the challenges in revealing the age of groundwater – an example from an evaporation-dominated system in arid Australia. Abstracts Book of the IAEA/RCA Technical Meeting on Processing, Analysis, and Interpretation of Isotopic and Hydrogeochemical Data for Groundwater Dynamics, 4-8 November 2013; Beijing, China, IAEA.

Michael, H. and C. Voss, 2009: Estimation of regional-scale groundwater flow properties in the Bengal Basin of India and Bangladesh. *Hydrogeol. J.*, **17 (6)**, 1329–1346, doi:10.1007/s10040-009-0443-1.

Millington, R. J. and J. Quirk, 1961: Permeability of porous solids. Trans. Faraday Soc., **57**, 1200–1207, doi:10.1039/TF9615701200.

Montfort, J. and J. Pellegatta, 1991: Diffusion coefficients of the halocarbons CCl_2F_2 and $C_2Cl_2F_4$ with simple gases. *J. Chem. Eng. Data*, **36**, 135–137, doi:10.1021/je00002a001.

O'Grady, A., P. Cook, D. Eamus, A. Duguid, J.Wischusen, T. Fass, and D.Worldege, 2009: Convergence of tree water use within an arid-zone woodland. *Oecologia*, **160 (4)**, 643–655, doi:10.1007/s00442-009-1332-y.

Pollock, D., 2012: *User guide for MODPATH Version 6 - a particle tracking model for MODFLOW*. Technical report, USGS, Reston, Virginia.

Raich, J. and W. Schlesinger, 1992: The global carbon dioxide flux in soil respiration and its relationship to vegetation and climate. *Tellus*, **44 (2)**, 81–99, doi:10.1034/j.1600-0889.1992.t01-1-00001.x.

Read, R. and S. Tickell, 2007: *The Ti-Tree Basin Aquifer map*. Northern Territory Government, Australia.

Reid, N., S. Hill, and D. Lewis, 2008: Spinifex biogeochemical expressions of buried gold mineralisation: The great mineral exploration penetrator of transported regolith. *Appl. Geochem.*, **23 (1)**, 76 – 84, doi:10.1016/j.apgeochem.2007.09.007.

Robertson, W. and J. Cherry, 1989: Tritium as an indicator of recharge and dispersion in a groundwater system in Central Ontario. *Water Resour. Res.*, **25 (6)**, 1097–1109, doi:10.1029/WR025i006p01097.

Salmon, S. U., H. Prommer, J. Park, K. T. Meredith, J. V. Turner, and J. L. McCallum, 2015: A general reactive transport modeling framework for simulating and interpreting groundwater ^{14}C age and δ^{13}C. *Water Resour. Res.*, **51 (1)**, 359–376, doi:10.1002/2014WR015779.

Sanford, W., J. Deak, and K. Revesz, 2002: Parameter estimation using carbon-14 ages: Lessons from the Danube-Tisza interfluvial region of Hungary. *Acta U. Carol. Geol.*, 373–376.

Sanford, W. E., 2011: Calibration of models using groundwater age. *Hydrogeol. J.*, **19 (1)**, 13–16, doi:10.1007/s10040-010-0637-6.

Sanford, W. E. and S. Buapeng, 1996: Assessment of a groundwater flow model of the Bangkok Basin, Thailand using carbon-14 based ages and paleohydrology. *Hydrogeol. J.*, **4 (4)**, 26–40, doi:10.1007/s10040 0050083.

Sanford, W. E., L. N. Plummer, D. McAda, L. Bexfield, and S. Anderholm, 2004: Hydrochemical tracers in the middle Rio Grande Basin, USA: 2. Calibration of a groundwater flow model. *Hydrogeol. J.*, **12 (4)**, 389–407, doi:110.1007/s10040-004-0326-4.

Scanlon, B., K. Keese, A. Flint, L. Flint, C. Gaye, W. Edmunds, and I. Simmers, 2006: Global synthesis of groundwater recharge in semiarid and arid regions. *Hydrol. Proc.*, **20 (15)**, 3335–3370, doi:10.1002/hyp.6335.

Schwartz, F., E. Sudicky, R. McLaren, Y. Park, M. Huber, and M. Apted, 2010: Ambiguous hydraulic heads and ^{14}C activities in transient regional flow. *Groundwater*, **48 (3)**, 366–379, doi:10.1111/j.1745- 6584.2009.00655.x.

Shanafield, M., P. G. Cook, H. Gutierrez-Jurado, R. Faux, J. Cleverly, and D. Eamus, 2015: Field comparison of multiple methods of characterizing groundwater discharge by evaporation and evapotranspiration: Stirling Swamp, Ti Tree Basin, Australia. *Submitted to J. Hydrol.*

Simpson, H. J., M. S. Hamza, J. W. C. White, A. Nada, and M. A. Awad, 1987: Evaporative enrichment of deuterium and 18O in arid zone irrigation. Isotope Techniques in Water Resource Development, Proc. Symp. Vienna, IAEA, ed., 241–256.

Simunek, J., M. Sejna, H. Saito, M. Sakai, and M. T. Van Genuchten, 2013: *The HYDRUS-1D Software Package for Simulating the Movement of Water, Heat, and Multiple Solutes in Variably Saturated Media*, Version 4.16. Department of Environmental Sciences, University of California Riverside, Riverside, California, USA.

Solomon, D. K., 2000: ^{4}He in groundwater. *Environmental tracers in subsurface hydrology*, P. G. Cook and A. L. Herczeg, eds., Kluwer, Massachusetts, 425–440.

Solomon, D. K., A. Hunt, and R. J. Poreda, 1996: Source of radiogenic helium-4 in shallow aquifers: Implications for dating young groundwater. *Water Resour. Res.*, **32 (6)**, 1805–1813, doi:10.1029/96WR00600.

Solomon, D. K., R. J. Poreda, S. L. Schiff, and J. A. Cherry, 1992: Tritium and helium-3 as groundwater age tracers in the Borden aquifer. *Water Resour. Res.*, **28 (3)**, 741–755, doi:10.1029/91WR02689.

Striegl, R. and D. Armstrong, 1990: Carbon dioxide retention and carbon exchange on unsaturated Quaternary sediments. *Geochim. Cosmochim. Ac.*, **54 (8)**, 2277–2283, doi:10.1016/0016-7037(90)90051-L.

Striegl, R. and R. Healy, 1990: Transport of $^{14}CO_2$ in Unsaturated Glacial and Eolian Sediments. Chemical Modelling of Aqueous Systems II, Am. Chem. Symp. Ser. Vol 416, edited by D.C. Melchior and R.L. Bassett, Am. Chem, Soc., Washington, D.C., 202–210.

Stuiver, M. and H. Pollach, 1977: Reporting of ^{14}C data. *Radiocarbon*, **19**, 355–363.

Suchomel, K. H., D. Kreamer, and A. Long, 1990: Production and transport of carbon dioxide in a contaminated vadose zone: A stable and radioactive carbon isotope study. *Environ. Sci. Technol.*, **24 (12)**, 1824–1831, doi:10.1021/es00082a006.

Tamers, M. A., 1975: Validity of radiocarbon dates on groundwater. *Geophys. Surv.*, **2 (2)**, 217–239, doi:10.1007/BF01447909.

Thorburn, P. J. and G. R. Walker, 1994: Variations in stream water upatake by eucalyptus camaldulensis with differing access to stream water. *Oecologia*, **100 (3)**, 293–301, doi:10.1007/BF00316957.

Thorstenson, D., E. Weeks, H. Haas, E. Busenberg, L. Plummer, and C. Peters, 1998: Chemistry of unsaturated zone gases sampled in open boreholes at the crest of Yucca Mountain, Nevada: Data and basic concepts of chemical and physical processes in the mountain. *Water Resour. Res.*, **34 (6)**, 1507–1529, doi:10.1029/98WR00267.

Thorstenson, D., E. Weeks, H. Haas, and D. Fisher, 1983: Distribution of gaseous $^{12}CO_2$, $^{13}CO_2$, and $^{14}CO_2$ in the sub-soil unsaturated zone of the Western US Great Plains. *Radiocarbon*, **25**, 315–346.

Tooth, S., 1999: Floodouts in central Australia. *Varieties of Fluvial Form*, A. Miller and A. Gupta, eds., Wiley, Chichester, 219–247.

Troldborg, L., J. Refsgaard, K. Jensen, and P. Engesgaard, 2007: The importance of alternative conceptual models for simulation of concentrations in a multi-aquifer system. *Hydrogeol. J.*, **15 (5)**, 843–860, doi:10.1007/s10040-007-0192-y.

Turnadge, C. and B. D. Smerdon, 2014: A review of methods for modelling environmental tracers in groundwater: Advantages of tracer concentration simulation. *J. Hydrol.*, **519 (Part D)**, 3674–3689, doi:10.1016/j.jhydrol.2014.10.056.

Van Genuchten, M. T., 1980: A closed-form equation for predicting the hydraulic conductivity of unsaturated soils. *Soil Sci. Soc. Am. J.*, **44 (5)**, 892–898, doi:10.2136/sssaj1980.03615995004400050002x.

Villeneuve, S., P. G. Cook, M. Shanafield, C. Wood, and N. White, 2015: Arid zone recharge via infiltration through an ephemeral riverbed, central australia. *J. Arid Environ.*, **117**, 47–58, doi:10.1016/j.jaridenv.2015.02.009.

Vogel, J. C., 1967: Investigation of groundwater flow with radiocarbon. Isotopes in Hydrology, IAEA, Vienna, 355–369.

Walker, G. and P. Cook, 1991: The importance of considering diffusion when using carbon-14 to estimate groundwater recharge to an unconfined aquifer. *J. Hydrol.*, **128 (1-4)**, 41–48, doi:10.1016/0022-1694(91)90130-A.

Walvoord, M., R. Striegl, D. Prudic, and D. Stonestrom, 2005: CO_2 dynamics in the Amargosa Desert: Fluxes and isotopic speciation in a deep unsaturated zone. *Water Resour. Res.*, **41 (2)**, doi:10.1029/2004WR003599.

Warner, M. and R. Weiss, 1985: Solubilities of chlorofluorocarbons 11 and 12 in water and seawater. *Deep Sea Res.*, **32 (12)**, 1485–1497, doi:10.1016/0198-0149(85)90099-8.

Weeks, E., D. Earp, and G. Thompson, 1982: Use of atmospheric fluorocarbons F-11 and F-12 to determines diffusion parameters of the unsaturated zone in the Southern High Plains of Texas. *Water Resour. Res.*, **18 (5)**, 1365–1378, doi:10.1029/WR018i005p01365.

Weiss, R., 1974: Carbon dioxide in water and seawater: the solubility of a non-ideal gas. *Mar. Chem.*, **2 (3)**, 203–215, doi:10.1016/0304-4203(74)90015-2.

Wilson, J. L. and H. Guan, 2004: Mountain-block hydrology and mountain-front recharge. *Groundwater Recharge in a Desert Environment: The Southwestern United States*, J. Hogan, F. Phillips, and B. Scanlon, eds., American Geophysical Union, Washington DC, 113–137.

Wischusen, J., E. Bastrakov, J. Magee, S. Lewis, L. Gow, P. Kilgour, J. Bell, and T. Kelly, 2012: *Hydrogeological investigation of deep groundwater resources in the Ti-Tree Basin, Northern Territory*. Technical report, Record 2012/08. Geoscience Australia, Canberra.

Wood, C., P. G. Cook, and G. A. Harrington, 2015: Vertical carbon-14 profiles for resolving spatial variability in recharge in arid environments. *J. Hydrol.*, **520**, 134–142, doi:10.1016/j.jhydrol.2014.11.044. 92

Wood, C., P. G. Cook, G. A. Harrington, K. Meredith, and R. Kipfer, 2014: Factors affecting carbon-14 activity of unsaturated zone CO_2 and implications for groundwater dating. *J. Hydrol.*, **519 (Part A)**, 465–475, doi:10.1016/j.jhydrol.2014.07.034.

Yang, C., G. Rattray, and P. Yu, 1996: *Interpretation of Chemical and Isotopic Data from Boreholes in the Unsaturated Zone at Yucca Mountain, Nevada*. US Geological Survey Water Resources Investigation Report 96-4058. USGS, Denver, Colorado.

Yang,W., R. Amundson, and S. Trumbore, 1994: A model for soil $^{14}CO_2$ and its implication for using ^{14}C to date pedogenic carbonate. *Geochim. Cosmochim. Acta,* **58 (1)**, 393–399, doi:10.1016/0016-7037(94)90472-3.

Zheng, C., 2010: *MT3DMS v5.3 Supplemental User's Guide*. Technical Report to the U.S. Army Engineer Research and Development Center. Technical report, Department of Geological Sciences, University of Alabama.

Zheng, M.,W. Debruyn, and E. Saltzman, 1998: Measurements of the diffusion coefficients of CFC-11 and CFC-12 in pure water and seawater. *J. Geophys. Res.*, **103 (C1)**, 1375–1379, doi:10.1029/97JC02761.

Zhu, C., 2000: Estimate of recharge from radiocarbon dating of groundwater and numerical flow and transport modelling. *Water Resour. Res.,* **36 (9)**, 2607–2620, doi:10.1029/2000WR900172.